UNIVERSITY OF CALIFORNIA
RIVERSIDE

Strategies and Technologies for Improving Air Quality Around Ports

A Dissertation submitted in partial satisfaction
of the requirements for the degree of

Doctor of Philosophy

in

Chemical and Environmental Engineering

by

Mohammad Yusuf Khan

March 2013

Dissertation Committee:

Dr. David R. Cocker III
Dr. J. Wayne Miller
Dr. Akua Asa-Awuku

The Dissertation of Mohammad Yusuf Khan is approved:

_____

_____

_____

Committee Chairperson

University of California, Riverside

Acknowledgements

I am highly indebted to my graduate advisor, Dr. David Cocker. He patiently provided the vision, encouragement and advise necessary for me to proceed through doctoral program and complete my dissertation. I consider myself fortunate to have Dr. Cocker as my advisor and can never forget his endless support throughout the PhD program. I would also like to thank Dr. Cocker for inviting me to the thanksgiving dinner at his home for past four years.

My next biggest thanks go to Dr. J. Wayne Miller (My family knows him as a professor who brings jar of peanuts and fresh oranges for me). I have learned a lot from Dr. Miller through endless discussion at every corner of CE-CERT. His emphasis on planning, just like my father, will always remain in my heart. I am thankful to Dr. Miller for providing me opportunity, knowledge and resources to become a PhD and for pushing me beyond my comfort zone to broaden my perspective and develop an extensive skill set. I am also very grateful to him for making sure that I have had no funding issues. He will always be my source of inspiration for hard work and I can never forget his eternal support for me throughout my PhD.

I would like to thank Dr. Akua Asa-Awuku, one of my committee members, for taking her valuable time and sharing her knowledge. Her ideas for one of the research article that I published with her were very impressive. I would also like to thank her for forming a journal club which helped in widening my knowledge to related research fields.

Most of the studies presented in this dissertation would have not been completed without Mr. William A. Welch. A combination of Bill's expertise in field testing and his ability to

crack jokes even during tense situations at work site were the key factors behind all successful studies. Bill's presences during a field test boost my confidence of completing a job. One thing that I will take away from Bill is his never giving up attitude and finding a way around to get the job done.

Next, I would like to thank Dr. Kent C. Johnson for giving me opportunity to work on PM-PEMS project. Kent is a well-known researcher in his field. I am fortunate that I have had chance to work under Kent. I was highly impressed with his work ethics and ability to keep everything organized. While working under Kent, he has always made sure that I am always on learning curve.

I consider Dr. Varalakshmi Jayaram as my teacher for field work. Lakshmi taught me everything she could and I am very grateful to her for passing on the traits required for field testing.

Dr. Ehsan Hosseini is my big brother in lab. Every time I had any question regarding MS Office, IGOR or any other software, I always went to Ehsan for solution because I knew that he knows everything.

I also want to extend my gratitude to Mr. Charles Bufalino, Mr. Kurt Bumiller, Mr. Don Pacocha and Mr. Joe Valdez, for providing me with means and methods for the successful completion of each project. I highly appreciate their help throughout my PhD career.

I would also like to thank administrative staff at the department of Chemical and Environmental Engineering, CE-CERT and International Student Center for clarifying all of my queries and being very nice to me.

Next, I would like to thank Xiaochen, Maryam, Ping, Nick, Sindhu, Sam, Jill, Ian, Chia-Li for all the meaningless discussions and fun times.

Sandeep Dhall and Kaushik Nanda were my roommates for past four years. Video games, movie nights, pizza hut, Indian food at Punjab palace, cats, bowling, political discussions (which I stopped after sometime)and making fun of each other filled my life with hilarity when at home. I will always remember the time we had spent together and will always cherish their friendship.

My Indian buddies; Shailendra Ji, Subhash Ji, Arinder Ji, Payal, Smruti and Shruti made this journey very joyful. We shared so much of laughter and good food together.

My friend, Garima, was one of the nicest people I have ever met. She was a tremendous support in first three years of PhD and I can never forget her affection and care.

Last but not the least, I would like to thank my family who were always there for me at each and every step and helped me in dealing with any problem that I have had come across. Without moral support, encouragement, love and care from my family members, this dissertation would have not been possible at all.

The text of Chapter 2 of this dissertation, in part or in full, is reprinted from Atmospheric Environment, Volume 55; M. Yusuf Khan, Kent C. Johnson, Thomas D. Durbin, Heejung Jung, David R. Cocker, Dipak Bishnu, Robert Giannelli; Characterization of PM-PEMS for in-use measurements conducted during validation testing for the PM-PEMS measurement allowance program, Pages 311-318, Copyright (2012), with permission from Elsevier. The text of Chapter 3, in part or in full, is a reprint of the material as it appears in the Journal of

the Air and Waste Management Association, Volume 63, Issue 3, 2013, Pages 284-291. The text of Chapter 4, in part or in full, is reprinted with permission from (Impact of Algae Biofuel on In-Use Gaseous and Particulate Emissions from a Marine Vessel; M. Yusuf Khan, Robert L. Russell, William A. Welch, David R. Cocker, III, and Sujit Ghosh**;** *Energy & Fuels* 2012 *26* (10), 6137-6143) Copyright (2012) American Chemical Society. The text of Chapter 5, in part or in full, is reprinted with permission from (Benefits of Two Mitigation Strategies for Container Vessels: Cleaner Engines and Cleaner Fuels; M. Yusuf Khan, Michael Giordano, James Gutierrez, William A. Welch, A. Asa-Awuku, J. Wayne Miller, and David R. Cocker, III**;** *Environmental Science & Technology* **2012** *46* (9), 5049-5056) Copyright (2012) American Chemical Society. The text of Chapter 6, in part or in full, is reprinted with permission from (Greenhouse Gas and Criteria Emission Benefits through Reduction of Vessel Speed at Sea; M. Yusuf Khan, Harshit Agrawal, Sindhuja Ranganathan, William A. Welch, J. Wayne Miller, and David R. Cocker, III; Environmental Science & Technology 2012 46 (22), 12600-12607) Copyright (2012) American Chemical Society.

Dedication

I dedicate this work to my parents Amir Fatima and Salimuddin Khan for their endless love, encouragement, and support all through my life. You taught me perseverance, strength and commitment…

ABSTRACT OF THE DISSERTATION

Strategies and Technologies for Improving Air Quality Around Ports

by

Mohammad Yusuf Khan

Doctor of Philosophy, Graduate Program in Chemical and Environmental Engineering
University of California, Riverside, March 2013
Dr. David R. Cocker III, Chairperson

Increased activity at ports is an indication of economic development and growth; however, it also puts public health, regional air quality and global climate at risk because the exhaust from the marine diesel engines is not subjected to the stringent regulations as on-road engines. This dissertation characterizes the effectiveness of strategies and technologies to mitigate criteria pollutants and the long-lived greenhouse gas, carbon dioxide (CO_2) from marine diesel engines. The dissertation also provides insight into the current state-of-art of gaseous and particulate matter portable emission measurement system (PEMS). Results from a project show how to determine the measurement allowance for PEMS in order to provide accurate measurements for the development of emission inventories and subsequently, air pollution mitigating regulations.

In-use gaseous emissions from the two main engines were measured at sea for the first time in order to evaluate the performance of a Code of Federal Regulations (CFR) compliant PEMS against instruments meeting the simplified measurement method (SMM) complaint with International Maritime Organization (IMO).

For the first time, emissions were measured from a modern container vessel with newest engine technologies. The vessel was operated on marine gas oil, a cleaner fuel, in regulated waters and on heavy fuel oil in unregulated waters. Impact of cleaner fuel and newest technologies on the engine was assessed. A simple equation was developed to estimate time required to completely switch fuels which can be used by vessel owners to comply with regional/international fuel regulations.

Vessel speed reduction (VSR), which is a worldwide acceptable strategy for ocean-going vessels (OGVs), was evaluated. The study showed that putting a speed limit on a container OGVs as they sail near ports and coastlines could cut emissions of air pollutants by up to 70%. This study also found that by reducing the vessel speed by a mere 3-6 knots from cruise speed will result in significant reductions of criteria pollutants and carbon dioxide.

Towards the goal of reducing emissions and dependency on fossil fuels, this dissertation explores benefits of consuming hydrotreated algae biofuel in small marine diesel engines for the first time. Significant particulate matter ($PM_{2.5}$) and nitrogen oxides (NO_x) benefits were reported with slight improve in fuel economy when fuel was switched from ultra low sulfur diesel (ULSD) to 50:50 blend of ULSD and algae fuels.

The dissertation investigates the benefits associated with the hybridization of the tugboat. A conventional tugboat was retrofitted with one auxiliary engine, shaft generators, addition of lithium polymer batteries and an energy management system. Up to 30% reduction in NO_x, $PM_{2.5}$ and CO_2 was found. The energy management system in the hybrid tugboat allows the use of the auxiliary engine for propulsion as opposed to the only main engines during transit mode, thus leading to the significant reductions.

Another section of this dissertation provides an evaluation of latest PM-PEMS under different environmental and in-use conditions and features performance, accuracy and precision of PM-PEMS compared to the gravimetric reference method. The research from this study shows current PM-PEMS typically underreport the PM emissions compared to the reference method, with the exception of PEMS with photo-acoustic technology which incorporated a gravimetric filter. All PM-PEMS under evaluation performed poorly when encountered with sulfate laden PM during diesel particulate filter (DPF) regeneration.

Table of Contents

List of Figures

List of Tables

List of Acronyms

$	US Dollar
%	Percentage
°C	Centigrade
°F	degree Fahrenheit
µg	Microgram
µm	Micrometer
A50	50% ULSD 50% Algae Biofuel
AE	Auxiliary Engine
AJ	Alta June
ARB	Air Resources Board
AS	Actual Speed
ASD	Azimuthing Stern Drives
ATS	After-treatment System
BSFC	Brake Specific Fuel Consumption
bsPM	Brake-specific Particulate Matter
BTU	British Thermal Unit
C	Carbon
CARB	California Air Resources Board
CAT	Caterpillar
CCN	Cloud Condensation Nuclei

CD	Carolyn Dorothy
CFR	Code of Federal Regulations
CI	Cetane Index
CLD	Chemiluminescent Detector
CO	Carbon Monoxide
CO	Critical Orifice
CO_2	Carbon Dioxide
CoA	Certificate of Analysis
CPC	Condensation Particle Counter
CS	Cyclone Separator
CSV	Comma Separated Value
CVS	Constant Volume Sampling
d	Day
DC	Direct Current
DOC	Diesel Oxidation Catalyst
DPF	Diesel Particulate Filter
DR	Dilution Ratio
EC	Elemental Carbon
ECA	Emission Control Area
ECM	Engine Control Module
EEIA	The Energy and Environmental Analysis, Inc.
EF	Emission Factor

EMA	Engine Manufacturers Association
EMI	Electromagnetic Interference
EPA	Environmental Protection Agency
f	Conversion Factor
FC	Fuel Consumption
FID	Flame Ionization Detector
fSMPS	Fast Scanning Mobility Particle Sizer
FTP	File Transfer Protocol
g	Gram
g/hp-h	Gram Per Horsepower-hour
g/kW-hr	Gram Per Kilowatt-hour
GFM	Gravimetric Filter Module
GPS	Global Positioning System
h	Hour
H	Hydrogen
H_2O	Water
HCLD	Heated Chemiluminescent Detector
HD-OBD	Heavy Duty On Board Diagnostics
HFID	Heated Flame Ionization Detector
HFO	Heavy Fuel Oil
HL	Heated Line
hp	Horsepower

HPLC	High Performance Liquid Chromatography
hr	Hour
HRD	Hydrotreated Renewable Diesel
HVO	Hydrotreated Vegetable Oil
IC	Ion Chromatography
IMO	International Maritime Organization
INST	Instrument
IR	Infra-red
ISO	International Organization for Standardization
JD	John Deere
kg	Kilogram
knots	Nautical Miles
kPa	Kilopascal
kW	Kilowatt
L	Liter
lb	Pound
LCA	Life Cycle Analysis
LII	Laser Induced Incandescence
LR	Lloyd's Register
LS	Light Scattering
m	Meter
m/m	mass/mass

MA	Measurement Allowance
MARAD	Maritime Administration of the US Department of Transportation
MASC	Measurement Allowance Steering Committee
ME	Main Engine
MEL	Mobile Emission Laboratory
mg/hp-h	Milligram per Horsepower-Hour
MGO	Marine Gas Oil
MI	Michigan
min	Minute
mm	Millimeter
MS	Maximum Speed
MSS	Micro Soot Sensor
MW	Megawatt
N	Nitrogen
NDIR	Non-Dispersive Infrared
NDUV	Non-Dispersive Ultraviolet
NIOSH	National Institute for Occupational Safety and Health
nm	Nanometer
nmi	Nautical Miles
NO	Nitrous Oxide
NOx	Nitrogen Oxides
NSD	Number Size Distribution

NTC	NOx Technical Code
OC	Organic Carbon
OEM	Original Equipment Manufacturer
OGV	Ocean Going Vessel
PA	Photo-acoustic
PEF	Pollutant Emission Factor
PEMS	Portable Emission Measurement System
PERE	Pollutant Emitted in Rest of ECA
PEV	Pollutant Emitted in VSR Zone
PM	Particulate Matter
$PM_{2.5}$	Particulate Matter with diameter <2.5 micrometer
PM-	
PEMS	Particulate Matter-Portable Emission Measurement System
ppm	parts per million
PPMD	Portable Particulate Mass Device
PSD	Particle Size Distribution
PTFE	Teflo Filter
QCM	Quartz Crystal Microbalance
R_2	Coefficient of Determination
RED	Rest of ECA Distance
RH	Relative Humidity
rpm	Revolution Per Minute

s	Second
S	Sulfur
SAE	Society of Automotive Engineer
scf	Standard Cubic Feet
scfm	Standard Cubic Feet Per Minute
SCR	Selective Catalyst Reduction
sec	Second
SEE	Standard Estimation Error
SFOC	Specific Fuel Oil Consumption
SMM	Simplified Measurement Method
SMPS	Scanning Mobility Particle Sizer
SO_2	Sulfur Dioxide
SO_3	Sulfur Trioxide
SOC	State of Charge
SOx	Sulfur Oxides
SSD	Slow Speed Diesel
SwRI	Southwest Research Institute
T	Temperature
t_{95}	Time Required for 95% Switchover of the Fuel
TEU	Twenty-foot Equivalent Units
THC	Total Hydrocarbons
TPE	Total Pollutant Emitted

tpy	Tonne per year
UCR	University of California Riverside
ULSD	Ultra Low Sulfur Diesel
US	United States
US DOT	United States Department of Transportation
US EPA	United States Environmental Protection Agency
UV	Ultra-violet
V	Vessel Speed
VCS	Vessel Cruise Speed
VD	VSR Distance
VN	Venturi
VOC	Volatile Organic Compounds
VRS	Vessel Reduced Speed
VSR	Vessel Speed Reduction
WR	Water Removal System
wt	Weight

Chapter One: Introduction

Ports are the gateway to international trade by means of marine shipping. Globalization and continuous growth in international trade has led to the expansion of ports around the globe, imposing a substantial health hazard to the communities around ports, degrading regional air quality, and affecting global climate. The port-related emission sources include ocean-going vessels (OGVs), harbor craft, cargo handling equipment, locomotives and heavy-duty vehicles. OGVs are the major contributor to port-related emissions amongst all sources.

Marine shipping is the most efficient mode of transporting goods and about 90% of the global merchandise is transported by sea utilizing ~103,000 OGVs worldwide. However, OGVs are significant emitters of criteria pollutants[1] a consequence of the combination of using heavy fuel oil (HFO) and few emission regulations, as well as greenhouse gases including carbon dioxide (CO_2). Criteria pollutants are those pollutants included in ambient air quality standards and regulated at local and federal levels. Criteria pollutants emitted by OGVs include nitrogen dioxide (NO_2), sulphur dioxides (SO_2), carbon monoxide (CO), and particulate matter ($PM_{2.5}$).

Human exposure to fine particles from combustion sources is linked with increased risks of acute and chronic illness, such as lung cancer and cardiopulmonary disease[2]. In 2012, the United Nation heath agency re-classified diesel engine exhaust as 'carcinogenic to humans'. Recent studies have linked PM emissions from OGVs to increased number of premature deaths. PM emitted from OGVs stacks are estimated to be responsible for ~60,000

mortalities annually on a global scale[3]. NO_2 and SO_2 are linked with adverse effects on the respiratory system. Additionally, NO_x participates in the formation of ground level ozone and smog while SO_x undergoes further atmospheric oxidation to form acid rain and secondary particulate matter.

Over the past 20 years, on-road vehicles have faced stricter emission regulations, which have led to significant improvements in engine and exhaust control technologies and simultaneous reduction in emissions. In comparison to on-road vehicles, regulations for controlling OGVs emissions are fairly new. Emissions from ships are regulated by the International Maritime Organization (IMO) under Annex VI of the International Convention for the Prevention of Pollution from Ships (MARPOL) which set limits on NO_x, SO_x and PM and prohibit deliberate emissions of ozone depleting substances.

1.1. Control Strategies for OGVs

In order for regulatory agencies to protect human health and the environment from port-related emission sources, there are multiple strategies and technologies which have been implemented to reduce emissions from shipping activities. Switching to cleaner fuels in global and designated emission control areas (ECAs) and vessel speed reduction (VSR) in the vicinity of the ports are widely accepted strategies used regulators and port authorities. Alternative fuels are being considered for small marine vessels as a strategy to reduce emissions and dependency on fossil fuels. Diesel electrical hybrid systems have also emerged as one of the prevalent technology solutions for reduction of CO_2 and criteria pollutants from harbor crafts.

The IMO has set progressive reductions in fuel sulfur content. From 2010 to 2015, fuel used by all vessels operating in ECAs cannot exceed 10,000 ppm sulfur. After 2015, fuel used in ECAs may not exceed 1,000 ppm sulfur. In contrast, the sulfur content of fuel used in on-road vehicles is <15 ppm. The reduction in PM mass emissions is expected to reduce annual premature ship-related mortality by 50% in ECAs[4]. Similarly, progressive reductions in NOx emission limits have also been set. Marine diesel engines installed on or after 1 January 1990 but prior to 1 January 2000 are required to comply with Tier I emission limits (17.0 g/kW-hr). Tier II emission limit (14.4 g/kW-hr) applies on diesel engines installed on or after 1 January 2011 and Tier III emission limit (3.4 g/kW-hr) applies to diesel engines installed on or after 1 January 2016 operating in ECAs. The IMO has also specified an efficiency design index that will reduce ship fuel consumption for energy savings and greenhouse gas emission reductions for an industry that emits 3.3% of global CO_2 emissions.

Around the globe, port authorities have launched mandatory or voluntary VSR programs; for example, the Los Angeles and Long Beach San Pedro Bay Ports have a voluntary VSR program in which vessels are slowed to 12 knots in VSR zone (20 and 40 nautical miles)[5]. This voluntary program is based on the principle that the vessel speed is directly proportional to the cube of fuel consumption. Hence, small reductions in speed will produce large reductions in fuel consumption and, subsequently, CO_2 and criteria pollutants.

1.2. Control Strategies for Harbor Craft

In 2007, the United States government passed the Energy Independence and Security Act, which mandates production of at least 21 billion gallons of bio derived fuels from sources

other than corn by 2022[6]. In recent years, biofuels derived from algae feedstock has emerged as a technically viable and attractive alternative because of the following reasons: (1) high yield of fuel production per acre of land, (2) cultivation on non-arable land, (3) cultivation in fresh, saline, brackish, or wastewater, (4) algae feedstocks based on non-consumable foods, (5) algae having high lipid content for high energy density transportation fuels, and (6) algae producing additional valuable co-products, such as food ingredients. Hence, fuel derived from algae can be used in the harbor craft to curb criteria pollutants and greenhouse gas and decrease dependency on fossil fuels. Another prevalent strategy that can be used to reduce emissions is the hybridization of the harbor craft. Previous study[7] reported fuel savings and significant reduction in emissions with the hybridization of the tugboat.

1.3. Portable Emission Measurement Systems

Regulatory agencies rely upon reported emission factors for developing regulations. Therefore, accurate measurement of emissions from diesel engines is an important task. Methods that are being used to measure emissions from marine vessels and on-road diesel engines are described in NO_x Technical Code (NTC) and 40 Code of Federal Regulations (CFR) Part 1065, respectively. The purpose of the NTC is to establish mandatory procedures for testing, survey and certification of marine diesel engines to ensure that all applicable marine diesel engines comply with allowable NO_x emissions. Normally engine certification occurs on a test bed; however, the NTC allows for on-board testing for engines that cannot be certified on a test bed. The NTC allows certification to take place on-board via the Simplified Measurement Method (SMM) for these cases. In reality, both the test-bed and the in-use with SMM procedures are costly and complex, requiring the installation of

large amounts of equipment on the ship to perform emission certification. Since, portable emission measurement systems (PEMS) are approved in the 40 Code of Federal Regulations (CFR) Part 1065 for measuring in-use diesel engine emissions, the question was asked whether PEMS could provide accurate emissions measurement from marine engines. This study compares SMM and PEMS for in-use gaseous emissions from OGVs.

In the United States (US), measurements of in-use emissions from on-road diesel engines are required for regulatory purposes within a defined portion of the engine map known as Not-To-Exceed (NTE) control area. These measurements are made with Particulate Matter-Portable Emissions Measurement Systems (PM-PEMS) that are specifically developed to measure and quantify PM emissions on a mass basis under the protocols specified in the regulations. There have been numerous studies quantifying PM mass using available technologies and comparing them with the gravimetric method. These technologies have been evolving over the last decade. For in-use compliance testing, QCM and PA methods have both been developed and evaluated. Booker et al.[8] evaluated QCM technology on a prototype unit and found a good correlation with a non-portable (constant volume sampling) certification system. In an on-road study with a pre-commercial PEMS with QCM technology, however, Johnson et al.[9] showed a positive or negative measurement bias, depending upon the PM mass composition. In earlier studies of the PA measurement method, Schindler et al.[10] showed an excellent correlation, R^2 >0.95, with black carbon on a gravimetric filter. Conversely, in a recent chassis dynamometer tests, Durbin et al.[11] found 13-22% lower PM mass for a pre-commercial PA PEMS when compared to gravimetric filter mass. Another pre-commercial PM-PEMS using a combination of diffusion charging

and a gravimetric filter showed positively biased results with a poor coefficient of determination, R^2=0.55, during preliminary in-use testing program[9]. Other technologies that have been evaluated and compared to PM mass (LII, LS, combined diffusion charging and gravimetric filter, combined mobility and inertial sizing, photoelectric charging, etc.) have shown mixed results in such comparisons, with some showing good correlations[12-16], while other instruments have shown poor correlations[9, 11]. Overall, the behavior for this full range of PM measurement technologies is not fully understood and needs to be explored to better understand the sensitivity of these instruments at lower levels of PM, their reproducibility, and their linearity with the gravimetric filter method.

This research work aims at improving air quality around port communities and consequently reducing adverse health impact from diesel engines. One aspect of this research dissertation focuses on evaluating different emission measuring technologies such as portable emission measurement systems (PEMS) and sensors which are essential in quantifying in-use emissions (significantly different from laboratory measurements) and to assure proper performance of engine and after-treatment technologies. A second aspect of this dissertation is to use qualifying PEMS to evaluate strategies such as switching to cleaner fuels, alternative fuels, reducing ocean-going vessel speed in scope of reducing emissions and dependency on fossil fuels.

1.4. Outline of Dissertation

Chapter 2 presents the most comprehensive and definitive evaluation of current, regulatory compliant, PM-PEMS technologies that are commercially available for use under in-use

operating conditions. This study characterizes four PM measurement systems based on different measurement principles. At least three different units were tested for each PM-PEMS to account for variability. These PM-PEMS were compared with a UC Riverside's mobile reference laboratory (MEL) to account for measurement error in the PM-PEMS systems.

Chapter 3 provides the first comparison between the PEMS and SMM emissions measurement approaches. The SMM compliant with IMO's NTC and the PEMS compliant with EPA's 40 CFR Part 1065 were compared for two in-use large ships. Emission measurements were conducted near prescribed large ship certification load points. Particulate mass was also quantified during this study in addition to the measurement of gaseous components in the exhaust. This chapter also provides modal and overall emission factors (EFs) from a large marine diesel engine tested that are representative of a significant number of in-use uncontrolled marine diesel engines.

Chapter 4 investigates the impact of alternative fuel (renewable algae fuel) on gaseous and particulate emissions from a marine diesel engine. This study reports in-use emission rates from a marine vessel operating on a hydrotreated algae biofuel for the first time. Emission measurements were made on a four-stroke marine diesel engine from a Stalwart class vessel to compare the emission profile from burning ultralow sulfur diesel (ULSD) to a 50:50 blend of ULSD and algae biofuel (A50). Emission measurements were made using the in-use SMM system, which is compliant with International Organization for Standardization (ISO) 8178 guidelines and the MARPOL Annex VI NOx Technical Code for $PM_{2.5}$, NO_x, CO_2, CO and SO_x emissions.

Chapter 5 reports the emissions benefits from two mitigation strategies, cleaner engines and cleaner fuels, from a 2010 container vessel. This chapter provides the first comparison of Tier I certification values with in-use data obtained from a modern container vessel at sea. Additional information is provided on the transition in emissions, particle size, and particle number during fuel switch. A non-linear equation representing the fuel mixing process is verified as an approach to estimate the time required to switch the fuels.

Chapter 6 presents emission benefits associated with greenhouse gas and criteria pollutants by operating OGVs at reduced speed. Emissions were measured from Panamax and Post-Panamax class container vessels as their vessel speed was reduced from cruise to 15 knots or below. This chapter also provides comparison between measured and calculated EFs at low loads. Scenarios are presented to estimate total pollutant emitted (TPE) in ECA and emission benefits on extending the VSR zone from 24 to 200 nautical miles in ECA.

Chapter 7 presents reduction in emissions of criteria pollutants and greenhouse gases are by retrofitting the tugboat with one auxiliary engine, shaft generators, addition of lithium polymer batteries and an energy management system.

Chapter 8 summarizes the major findings of this dissertation.

1.5. Literature Cited

1. www.epa.gov/airquality/urbanair/
2. Lewtas, J. Air pollution combustion emissions: Characterization of causative agents and mechanisms associated with cancer, reproductive and cardiovascular effects. Mutat. Res. 2007, 636, 95-133.

3. Corbett, J. J. Mortality from Ship Emissions: A Global Assessment. Environ. Sci. Technology. 2007, 41 (24), 8512-8518.
4. Winebrake, J. J.; et al. Mitigating the Health Impacts of Pollution from Oceangoing Shipping: An Assessment of Low-Sulfur Fuel Mandates. Environ. Sci. Technol. 2009, 43 (13), 4776-4782.
5. CARB. Public Workshop Vessel Speed Reduction for Oceangoing Vessels. Sacramento. September 2008; http://www.arb.ca.gov/ports/marinevess/vsr/docs/090908speakingnotes.pdf
6. United States 110th Congress. The Energy Independence and Security Act of 2007, PL 110-140; U.S. Government Printing Office: Washington, D.C., 2007.
7. CARB. Evaluating Emission Benefits of a Hybrid Tug Boat. Final Report. October 2010.
8. Booker, D.R. Giannelli, R.A., Hu, J., 2007, *Road Test of an On-Board Particulate Matter Mass Measurement System*, SAE 2007-01-1116.
9. Johnson, K.C., Durbin, T.D., Jung, H., Cocker, D.R., Bishnu, D., Giannelli, R., 2011, *Environ. Sci. Technol.*, 45 (14), pp 6073-6079.
10. Schindler, W., Haisch, C., Beck, A.H., Niessner, R., Jacob, E., Rothe, D., 2004, A Photoacoustic Sensor System for Time Resolved Quantification of Diesel Soot Emissions, SAE 2004-10-0968.
11. Durbin, T.D., Johnson, K.C., Cocker, D.R and Miller, J.W., 2007, Evaluation and Comparison of Portable Emission Measurement Systems and Federal Reference Methods for Emissions from a Back-Up Generator and a Diesel Truck Operated on

a Chassis Dynamometer, Environ. Sci. Technol. 2007, 41, 6199-6204. http://eprints.cert.ucr.edu/448/

12. Lehmann, U., Niemela, V., and Morh, M., 2004, New Methods for Time Resolved Diesel Engine Exhaust Particle Mass Measurements, Environmental Science and Technology. 38:5704-5711.
13. Matter, U., Siegmann, H.C., Burtscher, H., 1999, Dynamic Field Measurements of Submicron Particles from Diesel Engines. Environ. Sci. Technology, 33, 1946-1952.
14. Maricq M.M., Xu N., Chase R.E., 2006, Measuring Particulate Mass Emissions with Electrical Low Pressure Impactor, Aerosol Science and Technology (2006) Vol 40: 68-79.
15. Podsiadlik, D.H., Chase, R.E., Lewis, D., Spears, M., 2003, Phase-Based Teom Measurements Compared With Traditional Filters for Diesel PM, SAE 2003-01-0783.
16. Witze, P.O., Maricq, M.M., Chase, R.E., Podsiadlik, D.H., Xu, N., 2004, Time-Resolved Measurements of Exhaust PM for FTP-75: Comparison of LII, ELPI, and TEOM Techniques. SAE 2004-01-0964.

Chapter Two: Characterization of PM-PEMS for In-Use Measurements from Heavy-Heavy Duty Vehicles

2.1. Abstract

This study provides an evaluation of the latest Particulate Matter-Portable Emissions Measurement Systems (PM-PEMS) under different environmental and in-use conditions. It characterizes four PM measurement systems based on different measurement principles. At least three different units were tested for each PM-PEMS to account for variability. These PM-PEMS were compared with a UC Riverside's mobile reference laboratory (MEL). PM measurements were made from a class 8 truck with a 2008 Cummins diesel engine with a diesel particulate filter (DPF). A bypass around the DPF was installed in the exhaust to achieve a brake specific PM (bsPM) emissions level of 25 mg/hp-h. PM was dominated by elemental carbon (EC) during non-regeneration conditions and by hydrated sulfate ($H_2SO_4.6H_2O$) during regeneration. The photo-acoustic PM-PEMS performed best, with a linear regression slope of 0.90 and R^2 of 0.88 during non-regenerative conditions. With the addition of a filter, the photo-acoustic PM-PEMS slightly over reported than the total PM mass (slope = 1.10, R^2 = 0.87). Under these same non-regeneration conditions, a PM-PEMS equipped with a quartz crystal microbalance (QCM) technology performed the poorest, and had a slope of 0.22 and R^2 of 0.13. Re-tests performed on upgraded QCM PM-PEMS showed a better slope (0.66), and a higher R^2 of 0.25. In the case of DPF regeneration, all PM-PEMS performed poorly, with the best having a slope of 0.20 and R^2 of 0.78. Particle

size distributions (PSD) showed nucleation during regeneration, with a shift of particle size to smaller diameters (~64 nm to ~13 nm) with elevated number concentrations when compared to non-regeneration conditions.

2.2. Introduction

Particulate matter (PM) is known for its potential to cause health problems. Regulatory agencies around the world are targeting in-use gaseous and PM emissions to ensure low emissions levels are maintained throughout the course of the engine's lifetime in real world driving conditions. In the United States (US), measurements of in-use emissions are required for regulatory purposes within a defined portion of the engine map known as Not-To-Exceed (NTE) control area. These measurements are made with Particulate Matter-Portable Emissions Measurement Systems (PM-PEMS) that are specifically developed to measure and quantify PM emissions on a mass basis under the protocols specified in the regulations.

PM is a complex mixture of extremely small particles and liquid droplets. It mainly consists of elemental and organic carbon (EC/OC), absorbed hydrocarbons and inorganic compounds (sulfate, water, etc.). There are numerous technologies by which PM mass can be quantified. These technologies utilize different measuring principles, such as a quartz crystal microbalance (QCM), photo acoustic (PA) detection, combined mobility and inertial sizing, laser-induced incandescence (LII), light scattering (LS), combined diffusion charging and gravimetric filter, and photoelectrical charging.[1, 2]

There have been numerous studies quantifying PM mass using available technologies and comparing them with the gravimetric method. These technologies have been evolving over

the last decade. For in-use compliance testing, QCM and PA methods have both been developed and evaluated. Booker et al.[3] evaluated QCM technology on a prototype unit and found a good correlation with a non-portable (constant volume sampling) certification system. In an on-road study with a pre-commercial PEMS with QCM technology, however, Johnson et al.[4] showed a positive or negative measurement bias, depending upon the PM mass composition. In earlier studies of the PA measurement method, Schindler et al.[5] showed an excellent correlation, $R^2 > 0.95$, with black carbon on a gravimetric filter. Conversely, in a recent chassis dynamometer tests, Durbin et al.[6] found 13-22% lower PM mass for a pre-commercial PA PEMS when compared to gravimetric filter mass. Another pre-commercial PM-PEMS using a combination of diffusion charging and a gravimetric filter showed positively biased results with a poor coefficient of determination, $R^2 = 0.55$, during preliminary in-use testing program.[4] Other technologies that have been evaluated and compared to PM mass (LII, LS, combined diffusion charging and gravimetric filter, combined mobility and inertial sizing, photoelectric charging, etc.) have shown mixed results in such comparisons, with some showing good correlations,[7-11] while other instruments have shown poor correlations.[4, 6] Overall, the behavior for this full range of PM measurement technologies is not fully understood and needs to be explored to better understand the sensitivity of these instruments at lower levels of PM, their reproducibility, and their linearity with the gravimetric filter method.

The measurement of PM mass under in-use driving conditions is complex and has higher uncertainty in comparison to laboratory measurements. Therefore, it is important to characterize and quantify difficulties in making these measurements with PEMS. The US

Environmental Protection Agency (EPA), the California Air Resources Board (CARB) and the Engine Manufacturers Association (EMA) formed a measurement allowance steering committee (MASC) to develop a program to account for uncertainties in PM-PEMS measurements. These uncertainties were subsequently accounted for in regulations relating to in-use emissions measurements via a measurement allowance (MA). The MASC approach for the PM measurement allowance was similar to that used for the gas phase program (Johnson et al., 2009). This included laboratory testing and Monte Carlo modeling at Southwest Research Institute (SwRI), followed by in-use testing using the University of California at Riverside's (UCR) Mobile Emission Laboratory.[12]

This study describes the in-use characterization of the PM PEMS as part of the PM MA program. A series of tests were performed, specifically designed to quantify the performance of commercially available PM-PEMS and to determine their validity as PM measurement systems for regulatory use. In comparison with previous studies of PM-PEMS[4], this study provides the latest evaluation of PM-PEMS as the technology stands at the start of the in-use compliance testing program. Unique to this study was that several PM-PEMS with multiple serial numbers were evaluated over a repeatable series of different on-road driving conditions with variations in environmental conditions and elevations. Approximately 100 tests were performed for each unit to statistically quantify differences between like models. Additionally one PM-PEMS was upgraded during this research and retested, where it showed significant improvements. The MEL provided a unique testing platform in that it contains a full 1065-compliant constant volume sampling (CVS) system with gravimetric PM measurements, while being fully operational under on-road driving conditions.[13, 14]

Measurements were made from a 2009 class 8 heavy-duty diesel vehicle, equipped with an original equipment manufacturer (OEM) Diesel Particulate Filter (DPF) with a bypass to simulate a cracked DPF. This study focused on PM emission levels targeted at 0.025 g/hp-h, which is at the regulatory limit during non-regeneration conditions and close to the heavy duty on board diagnostics (HD-OBD) PM threshold, which is currently set at 0.07, but will eventually be reduced to 0.03 g/hp-h for model year 2016 and later.[15] In addition to this study, PM PEMS were also evaluated during regeneration-only conditions. This study represents the most comprehensive and definitive evaluation of current, regulatory compliant, PM-PEMS technologies that are commercially available for use under in-use operating conditions.

2.3. Experimental Methods

2.3.1. Test Vehicle

Measurements were made from a 2009 class 8 truck equipped with a 2008 Cummins 15 liter heavy-duty diesel engine. The engine was equipped with a DPF, and was certified to meet the 0.01 g/hp-h PM standard. The vehicle was selected to represent a heavy-duty diesel vehicle with DPF-out bsPM emissions of approximately 0.001 g/hp-h. The MEL provided the load for the testing, with a combined weight of the tractor and trailer of 65,000 lbs. The vehicle odometer reading was 64,000 miles at the beginning of the study. A bypass system was set-up for the after-treatment system (ATS), designed to simulate a cracked DPF but with a properly functioning diesel oxidation catalyst (DOC). The bypass included a DOC and was successful in meeting the targeted bsPM emissions level of 25 mg/hp-h (0.025

g/hp-h) for non-regeneration conditions in both the validation and re-test phases. The bypass system was not used during regeneration, where accumulated soot was removed from the DPF.

2.3.2. PM-PEMS Description

Overall, four PM measurement systems were used for this study (Table 2-1). The nomenclature used for these PM measuring systems distinguishes them on the basis of their ability to report mass emissions, as opposed to measuring concentrations, and the measurement principle used. Systems that are capable of providing bsPM measurements and that meet the criteria defined for PEMS for in-use compliance testing under CFR40 Part 1065 regulations are called PEMS. Systems that are only designed to provide PM mass concentration in the exhaust are called instruments, or INST. The two types of PM-PEMS systems that were tested in this study are denoted as PEMS2(QCM) and PEMS3(PA). At least three different units of PEMS2(QCM) and PEMS3(PA) were tested. These units are denoted as 1, 2, 3 and 4 in Table 2-1. By testing different units, the consistency of the measurement principle and instrument design can be evaluated. The other two PM systems that were utilized in this study are referred as INST4(LS) and INST5(EM+A). These instruments are already integrated into the MEL. Another PEMS, PEMS1(DC+F), was evaluated for possible inclusion in this study, but it was not included on the basis of preliminary testing results from SwRI.

Table 2-1: Test Matrix for PM-PEMS In-Use Evaluations

PM-PEMS ID	Manufacture	Product Name	Principle of Detection	In-Use Testing
PEMS1(DC+F)	Horiba	TRPM	Diffusion charging + gravimetric filter	no
PEMS2(QCM)1,2,3	Sensors Inc	PPMD	Quartz crystal microbalance	yes
PEMS3(PA)1,2,3,4	AVL	MSS 483	photo acoustic	yes
PEMS3(PA+F)1,2,3,4	AVL	MSS 483+GFM	photo acoustic + gravimetric filter	yes[1]
INST4(LS)	TSI	DustTrak 8530	90° light scattering	yes
INST5(EM+A)	Dekati	DMM	electrical mobility + aerodynamic impaction	yes

[1]Although the AVL's MSS483 GFM was tested where only one serial number conditioning unit and filter module were evaluated, but three different serial number MSS483's were tested

The PEMS2(QCM) system is Sensor's Portable Particulate Mass Device (PPMD). The PPMD measurement principle is based on the QCM technology that employs piezoelectric crystals. Particles in the exhaust are deposited on the crystal surfaces after being charged. The total mass deposited is calculated from the change in frequency of the oscillating crystal due to deposited PM mass. This technology has the potential to quantify all types of PM, although there has been some concern related to the sensitivity of the instrument, and the possible need for crystal greasing to help the particles stick to the surface of the crystal.[4, 6]

The PEMS3(PA) system is AVL's Micro Soot Sensor (MSS) model 483. This PM-PEMS is based on a photo-acoustic light absorption sensing principle. It measures a periodic pressure wave caused by the absorption of a modulated IR laser beam by particles, and the resulting periodic heating and cooling of the exhaust gas. The resulting periodic pressure wave is recorded by a microphone, and it's amplitude is enhanced using a resonant acoustic cell. This system is specially designed for soot, and therefore, performs well for soot dominated PM[5, 17, 18] and poor for the organic and inorganic fraction of PM.[4] In an effort to characterize total PM mass, the PEMS3(PA) manufacturer upgraded their soot measurement with a prototype Gravimetric Filter Module (GFM) to enhance their measurement approach with a gravimetric filter that essentially calibrates the PA signal to a gravimetric mass. This prototype module was not used in the preliminary laboratory testing at SwRI. In this study, the MSS unit with the addition of GFM is denoted as PEMS3(PA+F).

INST4(LS) is TSI's DustTrak 8520. This PM system utilizes an optical light scattering measurement technique that is strongly influenced by particle size.[6, 19] The light emitted from the laser diode is scattered by particles, and the amount of light scatter determines the

particle mass concentration. The total amount of light emitted from the laser diode that is scattered by particles determines the particle mass concentration based on a calibration factor. ISNT4(LS) was calibrated to diesel exhaust using measurements by the MEL back in 2005.[6]

INST5(EM+A) is a DMM 230 that combines different aerosol measurement principles: electrical charging and detection, and aerodynamic inertial impaction.[20] The particle stream is charged by a corona discharger, and the electrical mobility of the particles is used to detect particles below 30 nm. Inertial size separation is done in a six stage low pressure cascade impactor to estimate the mass concentration of particle sizes ranging from 30 nm to 532 nm.

2.3.3. PEMS Installation and Operation

PEMS2(QCM) and PEMS3(PA) were mounted on a frame installed on the tractor for all the in-use testing, while INST4(LS) and INST5(EM+A) were mounted within the MEL. INST4(LS) and INST5(EM+A) sampled from the MEL's CVS. The operation for all PM systems was performed according to the manufacturer's specifications. It should be noted that PEMS2(QCM) was re-tested after the manufacturer upgraded the system. The PEMS2(QCM) was upgraded for the re-tests with higher sensitivity and improved crystal burn-in procedures to allow for higher loadings, which reduced the need to reuse crystals.

2.3.4. MEL Operation

The MEL's primary tunnel flow rate was set to 2700 standard cubic feet per minute (scfm) and the secondary tunnel was set to provide a secondary dilution of 2.27:1. These dilution

conditions created a CVS sample temperature that averaged 80˚C, with a single standard deviation of 20˚C throughout the test program.

2.3.5. MEL PM Measurements

PM mass concentrations were determined gravimetrically on pre-weighed 46.2 mm diameter 2- μm pore Teflo® filters (Whatman). Loaded Teflo® filters were weighed using a Mettler Toledo UMX2 microbalance following the guidelines within the Code of Federal Regulations.[21] Teflo® filters were subsequently extracted with High Performance Liquid Chromatography (HPLC) grade water and isopropyl alcohol, and analyzed for sulfate ions using a Dionex DX-120 ion chromatograph. Sulfate PM on the Teflo® filter was assumed to be in hydrated form ($H_2SO_4.6H_2O$), as predicted using the aerosol thermodynamic model ISORROPIA.[22-24] Parallel 2500 QAT-UP Tissuquartz Pall (Ann Arbor, MI) 47 mm filters (preconditioned at 600ºC for a minimum of 5 hours) were used to collect PM for subsequent elemental and organic carbon (EC/OC) analysis following the NIOSH[25] method using a Sunset Laboratory (Forest Grove, OR) thermal/optical carbon aerosol analyzer. Particle size distributions were measured using a fast Scanning Mobility Particle Sizer (fSMPS). During this test program, the fSMPS was operated in the size range of 8 to 188 nm with a 5 second scan time, compared to the 60 to 90 seconds for a more traditional SMPS.[26] A TSI condensation particle counter (CPC) 3760 was used to count the particle number.

2.3.6. Calculation Method

Three different calculation methods are allowed in 40 CFR Part 1065 to determine in-use brake specific PM emissions. In this study, the method 2 calculation from the PM MA was

applied to calculate emission factors. The method 2 calculation adjusts the exhaust flow measurement by a ratio of the CO_2-based fuel flow to the ECM reported fuel flow. This method is presented in its simple form in Equation 1, and with the full formula details in Khalek et al.[27]

$$Method2 = \frac{\sum g}{\sum[\frac{Carbon_{fuel}}{ECM_{fuel}} \times Work]} \quad (1)$$

2.3.7. Reference Accuracy

Prior to the in-use testing, the MEL was cross compared with SwRI at an emission level of 0.025 g/hp-h for PM was subjected to a 1065 audit. The MEL was, on average, lower than SwRI by about 6% on a simulated NTE transient cycle.[12] Some of this difference could be attributed to line losses, since the sample transfer line from the engine cell to the MEL was longer than the transfer line used in the engine cell itself. The 6% difference is well within the measurement variability of other round robin studies[30], and suggests the MEL is a reasonable reference tool for comparing PM PEMS in-use and for quantifying in-use uncertainties.[4]

2.3.8. Test Routes

The in-use routes were designed to be similar to those used in a previous PM-PEMS study[4] to provide a range of environmental conditions, and included segments near sea level, in coastal regions, and in desert regions, and with longer uphill incline segments and segments at elevations up to 1500 m. Over the different courses, the temperatures varied from 10-43ºC, several large power line transmissions were crossed providing potential

electromagnetic interference (EMI), and several railroad track crossings and pot holes provided vibration disturbances.

2.4. In-use PM Results

This section includes results from the comparison of PM systems with MEL reference method, and results for PM composition and particle size distributions (PSD). During testing, the MEL demonstrated a carbon balance within 2% and a high R^2 of 0.98, thus suggesting the data provided in this research is of high quality.

2.4.1. PM Analysis Basis

The PM analysis was done on a brake specific basis for the in-use testing. Only PM emissions measured within the NTE work zone, as mentioned earlier, were used for this comparison. The NTE work zone excludes operation when the engine is at low loads, a condition where the brake specific emissions are exaggerated by low values of the work term. The results presented in this study are based on a subset of the actual data sampled due to data yield from issues found during testing and post processing.

2.4.2. PEMS bsPM results

Comparisons between the PEMS and the gravimetric PM measurements of the MEL were made using correlations to evaluate the bias of the different systems. A summary of the results of this correlation analysis is provided for individual units (Table 2-2) and for the combined results for all units (Table 2-3).

2.4.3. PEMS2(QCM) bsPM

The correlations between PEMS2(QCM) and the MEL are shown in Figure 2-1. The correlations for all units of PEMS2(QCM) were poor. The overall correlation for non-regeneration tests showed an $R^2 = 0.13$, a slope of 0.22, and a positive intercept of 4.3 mg/hp-h. In moving from unit 1 to unit 3, both the slope (0.26 to 0.14) and R^2 (0.24 to 0.04) decreased. The PM concentration increased for the testing going from unit 1 to unit 3 in an effort to reduce sample times, which may be one of the factors contributing to the decreasing correlation going from unit 1 to unit 3.[12] Unit 3 also had a large zero intercept at 7.7 mg/hp-h, which may be a result of changing its crystal usage logic.[12] The PEMS2(QCM) non-regeneration mean bias at the 20 mg/hp-h bsPM emissions was -10 mg/hp-h, and at 30 mg/hp-h (i.e., the 2016 OBD threshold) the mean bias was -18 mg/hp-h. The standard error estimate (SEE) between PEMS2(QCM) and the MEL was relatively high (5.2 mg/hp-h). The two-tailed, paired t-test between the PEMS and MEL bsPM correlations suggests the mean differences were statistically significant at greater than a 99% confidence level, even though the SEE was relatively high. The PEMS2(QCM) regeneration results also showed a low overall correlation with an $R^2 = 0.36$ and a slope of 0.08 (Table 2-3).

Table 2-2: Non-regeneration PEMS bsPM correlation by unit 1, 2, 3 and 4 (mg/hp-h)

PEMS	Slope				Intercept				R^2			
	1	2	3	4	1	2	3	4	1	2	3	4
PEMS2(QCM)	0.26	0.25	0.14		2.3	3.0	7.7		0.24	0.13	0.04	
PEMS3(PA)		0.95	0.83	0.86		-1.0	-0.4	-0.4		0.86	0.93	0.95
PEMS3(PA+F)		1.16	1.01	1.07		-1.4	-0.3	-0.9		0.86	0.89	0.95
INST4(LS)	1.00	0.70	0.74	0.76	-3.4	-0.7	-1.1	-0.7	0.80	0.75	0.81	0.79
INST5(EM+A)	1.32	0.39	0.37	0.81	-9.0	0.4	2.8	-5.2	0.56	0.57	0.50	0.73

Table 2-3: PEMS PM bsPM correlation results combined (mg/hp-h)

PEMS	Slope	Intercept	R^2	SEE	t-test
Non-Regeneration Conditions					
PEMS2(QCM)	0.22	4.3	0.13	5.2	3E-65
PEMS3(PA)	0.90	-0.8	0.88	2.9	4E-54
PEMS3(PA+F)	1.10	-1.2	0.87	3.6	4E-54
INST4(LS)	0.76	-1.0	0.74	4.3	1E-96
INST5(EM+A)	0.59	-1.3	0.32	8.3	1E-78
PEMS2(QCM)_UPGRADE	0.66	5.1	0.25	6.8	3E-03
Regeneration Conditions					
PEMS2(QCM)	0.08	2.82	0.36	2.05	2E-03
PEMS3(PA)	-0.01	0.49	-0.68	0.09	1E-03
PEMS3(PA+F)	-0.04	7.38	-0.12	3.52	8E-02
INST4(LS)	-0.06	1.43	-0.24	2.03	1E-05
INST5(EM+A)	0.20	-0.36	0.78	1.44	9E-06

The PEMS2(QCM) system was upgraded to reduce the negative bias and large data spread. The PEMS2(QCM)_UPGRADE also showed a negative bias relative to the MEL, with a correlation slope of 0.84 when forced through zero, and 0.66 when not forced through zero. The intercept was 5.1 mg/hp-h with an R^2 of 0.25. The slope increased for the re-test, suggesting better accuracy with the upgraded unit. The R^2 and SEE were about the same for both studies, suggesting the precision did not change significantly between the two studies.

Previous studies with the same MEL showed that the PEMS2(QCM) was overestimating PM compared to the reference method with a slope of 1.5.[4] The composition was based on a similar PM composition, but with higher bsPM emissions. The change in response for PEMS2(QCM) from 1.5 to 0.22 suggests that revisions and upgrades can have a significant effect on the instruments behavior. Part of the reason for the change in response could be from configuring the PEMS for different concentrations levels, as described in Johnson et al.[12]

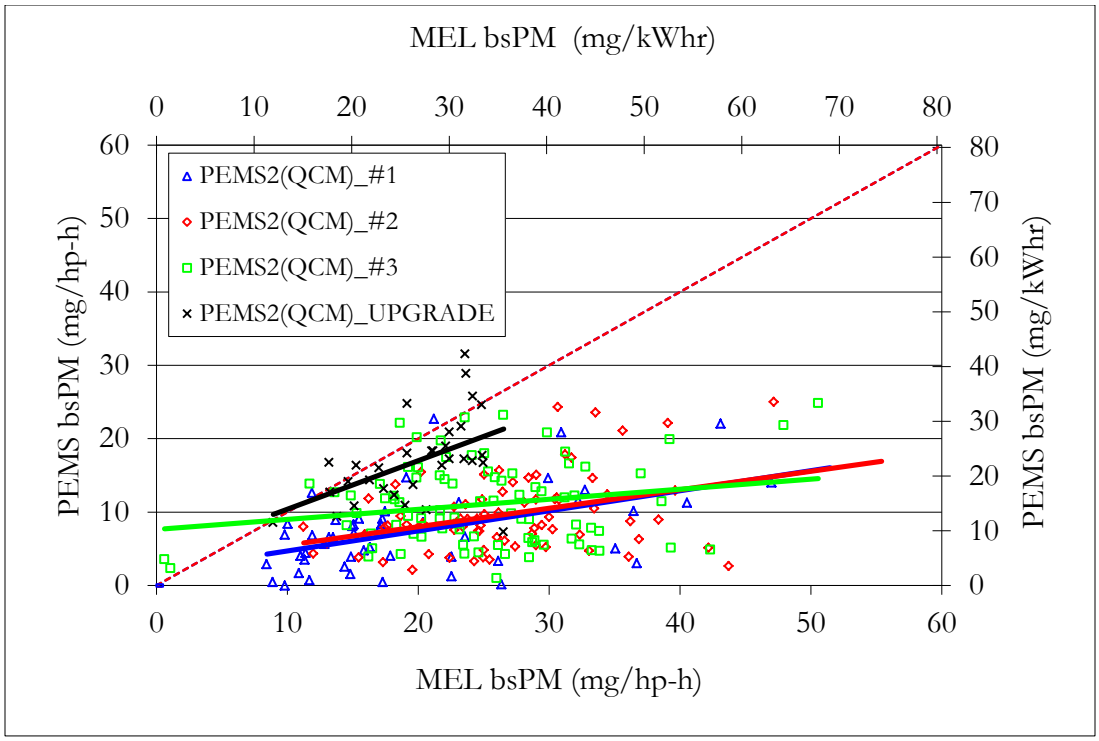

Figure 2-1: PEMS2(QCM) non-regeneration bsPM correlation unit by unit

2.4.4. PEMS3(PA) bsPM

The correlation plots for the different units of PEMS3(PA) are provided in Figure 2-2. The overall correlation for PEMS3(PA) showed an $R^2 = 0.88$, a slope of 0.90, and a negative intercept of 0.8 mg/hp-h for non-regeneration tests. The slope and R^2 were relatively consistent between unit 2 through unit 4, where the slope varied from 0.95 to 0.83 and the R^2 varied from 0.86 to 0.95. The PEMS3(PA) non-regeneration mean bias at the 20 mg/hp-h bsPM emissions was -2.8 mg/hp-h, and at 30 mg/hp-h the mean bias was -3.8 mg/hp-h, or 13% of the OBD threshold. The SEE between the PEMS3(PA) and the MEL was relatively low at 2.9 mg/hp-h. The two-tailed, paired t-test between the PEMS3(PA) and

MEL bsPM correlation results suggest the mean differences were statistically significant at a greater than 99% confidence level.

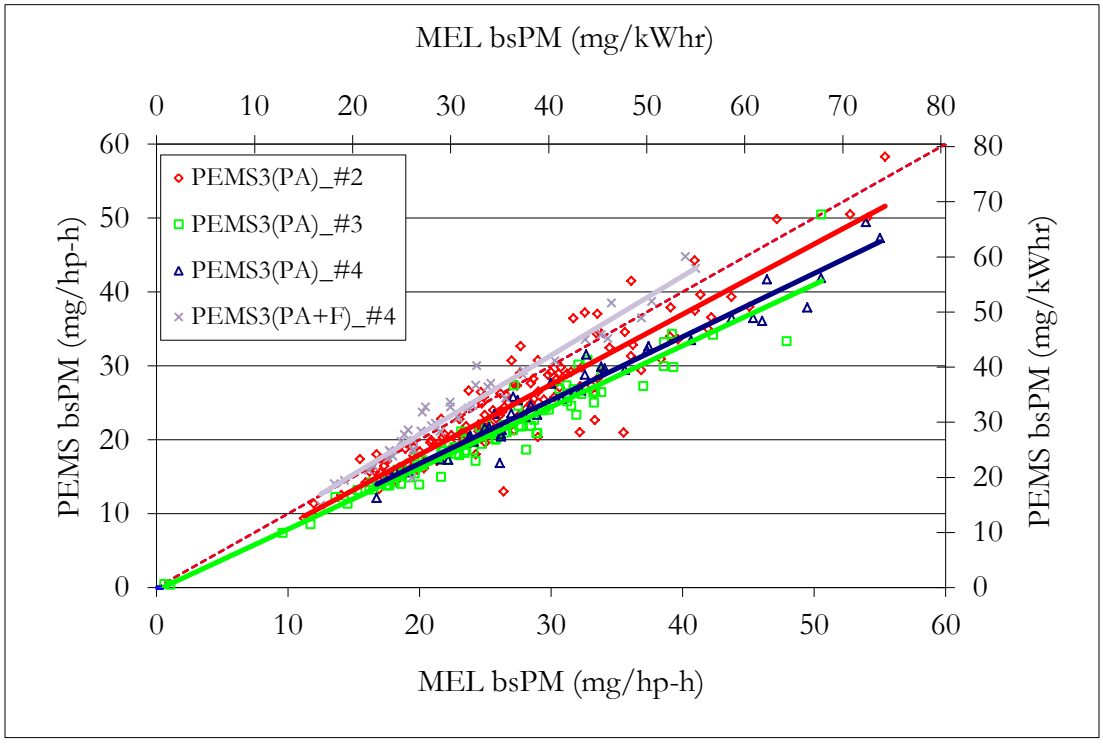

Figure 2-2: PEMS3(PA) non-regeneration bsPM correlation unit by unit. PEMS3(PA+F) is added to compare unit 4 against PEMS3(PA)

The PEMS3(PA) system showed a very similar correlation compared to a previous study, where the slope averaged 0.91 and the R^2 was 0.95.[4] Between the previous study and this study, four units have been tested with the same MEL where the slope and R^2 were relatively similar, thus suggesting this PEMS measurement technology is mature and reliable.

The PEMS3(PA) regeneration results showed a low overall correlation, with an $R^2 = -0.68$ and a slope of -0.01. The negative slope and R^2 suggests there was no correlation between

the reference measurement and the PEMS3(PA) measurement. The PEMS3(PA) regeneration results were also poor during the previous work by Johnson et al.[4]

PEMS3(PA) was upgraded with a prototype gravimetric filter system at the beginning of this research, and is denoted PESM3(PA+F), as discussed earlier. The PEMS3(PA+F) results showed a slope and R^2 of 1.1 and 0.87, respectively, for the non-regeneration conditions. This was the only PEMS during this current evaluation to show a slope greater than one. The PEMS3(PA+F) reduced the mean bias to 6% of the OBD threshold on an absolute basis. The PEMS3(PA+F) regeneration evaluation still showed a negative slope and a poor R^2 suggesting the gravimetric filter compensation system does not work for all PM compositions.

Further analysis of the PEMS3(PA+F) gravimetric filter showed that the PEMS system did not capture the same mass as the reference filter, with the PEMS filter showing only trace amounts of sulfuric acid PM (< 10 μg) while the reference system had in excess of 1000 μg for a comparable sample duration. This suggests a possible particle dilution/formation issue with the PEMS micro-dilution system, which has much lower flow rates and a higher surface area to volume ratio compared to the reference system. The PEMS2(QCM) system also uses a similar dilution process, and had issues with a low response or non-detection for nano-sized sulfuric acid particles.[4] Additional studies are needed to understand the reason for the PEMS2(QCM) and PEMS3(PA+F) low response for regeneration conditions.

One of the PEMS3(PA+F) events had a dominant fraction of organic PM. The agreement with the reference system for this case could be improved for PEMS3(PA+F) by using a model-based approach. This approach was based on a model[28] that uses a combination of

hydrocarbon levels, catalyst loading, fuel sulfur levels and ATS temperature to help estimate the amount of material that condenses on a particle surface during dilution. Using this model, the agreement between PEMS3 and the reference method was improved from 55-60% negative bias to a 10% negative bias. Further development of models to account for the dynamics of dilution processes could help improve filter-based PM-PEMS that are used for generalized in-use PM inventories and models.

2.4.5. INST4(LS) & INST5(EM+A)

INST4(LS) showed a reasonable correlation of $R^2 = 0.74$, a slope 0.76 (Table 2-3), and a negative intercept of -1 g/hp-h for the non-regeneration PM tests. However, there was no correlation for regeneration conditions with an negative R^2 of 0.24. The good correlation for the non-regeneration events suggests this instrument has some correlation with the MEL reference method for the PM composition and size distribution for the non-regeneration, bypassed PM. However, the instrument does not correlate with the gravimetric reference system for regeneration type PM, as has been reported in other studies.[4] It should be note that the good correlation of INST4(LS) with the MEL for non-regeneration can probably be attributed to the previous calibration to the MEL PM mass back in 2005.

INST5(EM+A) showed a lower correlation of $R^2 = 0.32$ and a slope 0.59 (Table 2-3) compared to INST4(LS) for the non-regeneration tests. This is somewhat surprising since the INST5(EM+A) detection method is more sophisticated than that for INT4(LS) and should detect a wider range of particles with different compositions and particle size distributions. In the case of regeneration tests, INST5(EM+A) performed best relative to all PEMS with a slope of 0.20 and $R^2 = 0.78$. INST4(LS) and INST5(EM+A) showed a lower

slope and R^2 in this study compared to the previous study.[4] This suggests INST4(LS) and INST5(EM+A) measurement system may be affected by the change the PM emission level.

2.4.6. Overall PM-PEMS Performance

Results for the combined data sets for all PEMS and INSTs are presented in Figure 2-3. All PEMS and INSTs, except for the upgraded PEMS3(PA+F), showed a negative bsPM bias relative to the MEL reference method for both the non-regeneration and regeneration cases. PEMS3(PA) showed the best overall correlation and PEMS2(QCM) the lowest overall correlation, with the correlations for INST4(LS) and INST5(EM+A) in-between those units. PEMS2(QCM) also showed the highest positive zero intercept, while the other PEMS showed slightly negative zero intercepts. PEMS2(QCM)_UPGRADE improved its correlation with the MEL, although precision did not change significantly, as shown in Table 2-3.

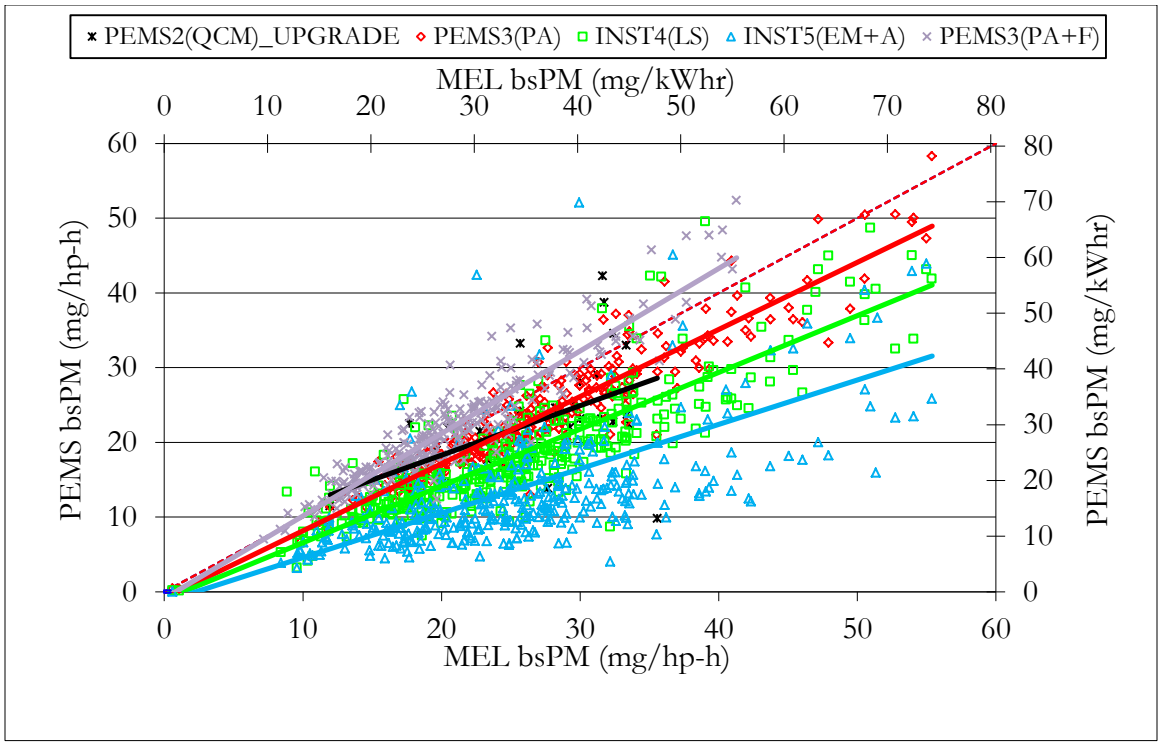

Figure 2-3: PEMS and INST non-regeneration bsPM correlation combined

The performance of the PEMS was also evaluated in terms of their operational characteristics, ease of use, and failures. The PEMS problems ranged from issues related to testing under in-use conditions, operational issues, and post processing issues. The in-use issues ranged from electrical and mechanical connections, crystal usage for short NTE's, valve switching, measurement signals, and crystal behaviors. Operational problems occurred during startup, commissioning, and with the systems prior to testing in-use. Typical issues included incorrect system configurations, procedures that didn't work, and issues with the startup software and other recommended practices that didn't function as discussed in manual. The post processing issues included data filtering, bsPM differences between

processor versions, data identification, and calculation methods not being available. The impact of these errors on the results was a factor of approximately 1.3 to 1.5, depending on the PEMS and the unit number. All of these issues are discussed in detail elsewhere.[12] Both the PEMS2(QCM) and PEMS3(PA) had issues that impacted their respective data yields. The PEMS2(QCM) had more issues overall, with data yield of 61% out of 347 valid events. The PEMS3(PA) had fewer issues, with an average data yield of 70%. This data yield was impacted by unit 1, which had a low yield of 15% due to the prototype gravimetric filter module and not the PEMS3(PA) system. PEMS3(PA) units 2, 3 and 4 had a relatively high yield, averaging more than 90%.

2.4.7. PM Composition

The PM composition was a strong function of whether the PM was generated under non-regeneration or regeneration conditions. The non-regeneration PM was dominated by EC (~90%), with small amounts of OC (~9%) and trace amounts of sulfur.[12] For these measurements, EC levels were well above the detection limits, while the OC and sulfur measurements were near the detection limits. Additional analysis was performed by SwRI using a direct filter injection system for a gas chromatograph (US Patent # 5109710). During this analysis, SwRI analyzed five selected MEL Teflon filters and 5 from SwRI (from the MA model development work). The results showed that the MEL filters were between 10 to 20% OC, SwRI steady state filters were 32% to 57% OC, and the SwRI transient filters were between 14% and 16% OC.[27] These results suggest that the OC fraction for the in-use transient testing may be on the same order as suggested by UCR's results. It also suggests

that the steady state testing may have a different composition than the transient and in-use testing results.

The regeneration filter samples collected were typically composed of predominately nucleated hydrated sulfate particles ($H_2SO_4.6H_2O$), as shown by others.[29] A separate analysis of EC, OC and sulfur measurements was performed for selected regeneration filters. These results showed only trace amounts of EC and OC, and a dominate amount of sulfur (~98%). This suggests that nearly all the PM mass was hydrated sulfate particles for the regeneration cases.

2.4.8. Particle Size Distribution (PSD)

Particle number (CPC 3760) and size distributions (fSMPS) were measured throughout the testing. The PSDs for typical non-regeneration and regeneration cases are provided in the Figure 2-4. The size distributions showed an average number diameter of 64 nm for the non-regeneration cases and 13 nm for the regeneration cases. Higher particle number concentrations (~5 times) were observed during the regeneration cases in comparison to non-regeneration cases. The combination of the regeneration particle composition being dominated by sulfate and number averaged diameter of 13 nm suggests the particles contributing to the PM mass were formed predominantly from the conversion of SO_2 to SO_3 over the catalytic surfaces of the DPF, as discussed previously.[4, 29] These nanoparticles represent a homogeneous nucleation that formed during simultaneous dilution and condensation inside the CVS tunnel. Thus, it is possible that the PEMS and MEL may see different particles diameters due to their different locations, but typically particle formation with similar dilution ratios and temperatures should form similar mass levels. The correlation

between the reference and the PEMS and INST was poorest for the regeneration tests compared to the non-regeneration tests. It is unclear, however, if the reason for the poor correlation for all PEMS and INST is due to the composition, particle size, or both, or other instrument issues. Small particle size probably contributed to a low signal response for several PM PEMS instruments. Specifically, small particles do not scatter light well, thus affecting INST4(LS), and small particles affect the ability for INST5(EM+A) to use its assumption of a log normal distribution being centered at 100 nm for its impactor electrometers.

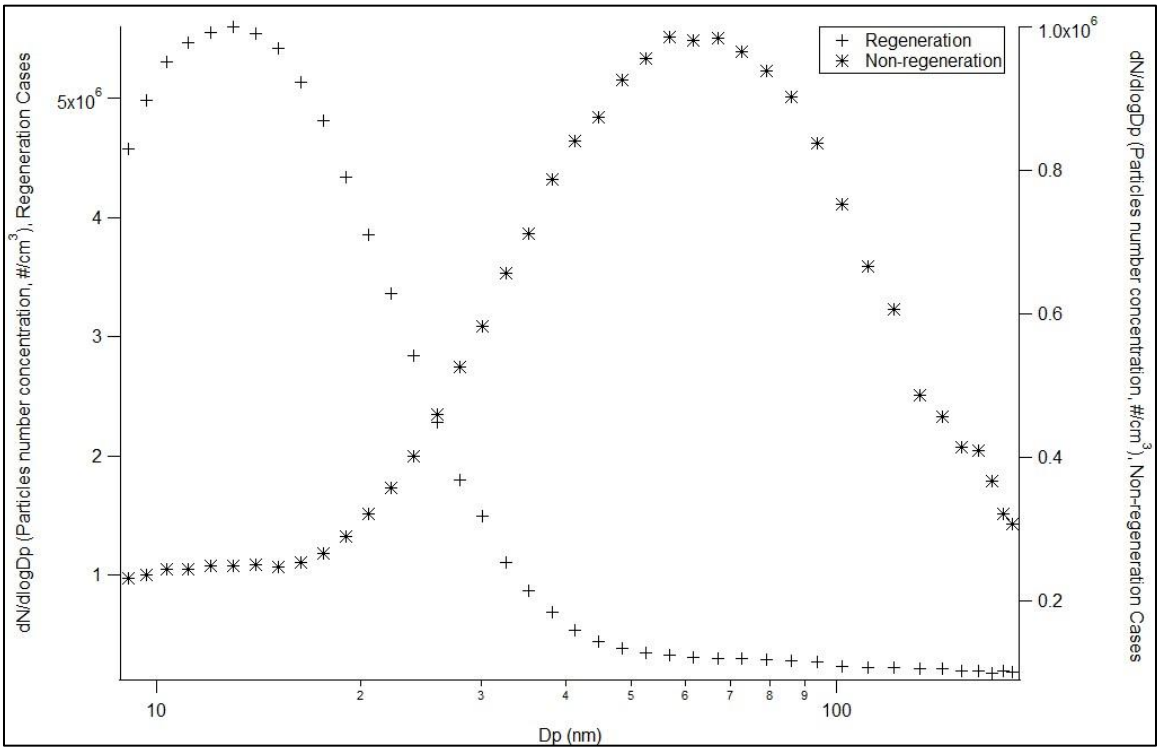

Figure 2-4: PM number size distribution (dN/dlogDp) for a typical non-regeneration and regeneration conditions. Note that the x-axis is on logarithmic scale

2.5. Conclusions

This research provides the latest evaluation of PM PEMS performance, accuracy, and precision compared to the gravimetric reference method. The research from this study shows current PM PEMS typically underreport the PM emissions compared to the reference method, with the exception of the PEMS3(PA+F) which incorporated a gravimetric filter. Both PEMS2(QCM) and PEMS3(PA) showed very similar unit-to-unit performance with PEMS3(PA) being precise. The changes in performance between older and newer versions of the same PEMS is also of interest. The variability between different versions was low for some PM-PEMS, but for others there was about a factor of 5 differences between different versions. The large variability between newer and older versions of the same PM-PEMS for some PEMS suggests these PEMS are very sensitive to parameters changes and the version number of a PEMS should be included as part of future publications.

Regenerations continue to be difficult for PM PEMS to quantify. During this and a previous in-use study PM PEMS were only able to quantify about 20% of the mass of the gravimetric reference method. INST5(EM+A) technology showed the best regeneration correlation during both studies. The filter based PEMS3(PA+F) system was unable to correlate well with the MEL when the PM was composed of hydrated sulfate nano-particles, but it has the potential to correlate with organic dominated PM. Micro-dilution may be the root cause for the low correlation for the sulfuric acid nanoparticles for the PM-PEMS. More analysis and evaluation is needed to fully characterize the non-soot dominated PM.

INST4(LS) and INST5(EM+A) correlation slope decreased between this study and the previous study. The lower slope could be due to a measurement issue at lower concentrations for the current study. This suggests these PEMS would significantly underreport at the levels of a properly functioning DPF at the sub 1 mg/hp-h. It is also known from internal work that at the sub 1 mg/hp-h emission level, the reference method is at the detection limits of its measurement capability. At this level, INST4(LS) is below its detection limits, but INST(EM+A) still has a fairly strong measurement signal. Since INST5(EM+A) has a strong signal and the reference method is at its detection limit, INST5(EM+A) may be the only suitable measurement tool to help characterize sub 1 mg/hp-h emissions such as during DPF regeneration.

In general, this research has shown that PM PEMS have continued to evolve, and have improved in their correlation with the gravimetric filter for some PEMS, but not all. Overall, some PM PEMS are suitable to quantify DPF failures at the OBD-HD thresholds to within 10%. Other PM PEMS could significantly under or over report these PM emissions depending on what versions of the PM-PEMS is used. This study also uncovered some issues with firmware, hardware, and post processing upgrades that can have a significant impact on the reported emissions. The implications from this study suggest that not all PM-PEMS are at the same level of development maturity with respect to correlations with gravimetric filter mass and that new PM PEMS need to be carefully evaluated before they are widely adopted for emission inventory or regulatory purposes. The inclusion of the gravimetric filter has shown to improve the PM PEMS performance, but these benefits are not equal for all PM compositions and additional studies are needed.

2.6. Acknowledgements

The California Air Resources Board (CARB), US EPA, and Engine Manufacturer's Association (EMA) funded this work. The authors acknowledge the support of the Measurement Allowance Steering Committee (MASC) for assistance in developing and carrying out this program. The authors acknowledge Sensors Inc., and AVL for providing the PM-PEMS as an in-kind contributions. We also acknowledge Cummins for their engineering assistance on controlling the regenerations and managing DPF soot levels. Lastly, we acknowledge Mr. Donald Pacocha and Mr. Joe Valdez, University of California at Riverside, for their contribution in setting up and executing this field project, the data collection and quality control.

2.7. Literature Cited

1. Baron, P.A., Willeke, K., 2001, *Aerosol Measurement: Principles, Techniques, and Applications*. John Wiley: New York.
2. Mohr, M., Lehmann, U., Rutter, J., 2005, Comparison of Mass-Based and Non-Mass-Based Particle Measurement Systems for Ultra-Low Emissions from Automotive Sources. Environ. Sci. Technology, 39, 2229-2238.
3. Booker, D.R. Giannelli, R.A., Hu, J., 2007, *Road Test of an On-Board Particulate Matter Mass Measurement System*, SAE 2007-01-1116.
4. Johnson, K.C., Durbin, T.D., Jung, H., Cocker, D.R., Bishnu, D., Giannelli, R., 2011, *Environ. Sci. Technol.*, 45 (14), pp 6073-6079.

5. Schindler, W., Haisch, C., Beck, A.H., Niessner, R., Jacob, E., Rothe, D., 2004, A Photoacoustic Sensor System for Time Resolved Quantification of Diesel Soot Emissions, SAE 2004-10-0968.
6. Durbin, T.D., Johnson, K.C., Cocker, D.R and Miller, J.W., 2007, Evaluation and Comparison of Portable Emission Measurement Systems and Federal Reference Methods for Emissions from a Back-Up Generator and a Diesel Truck Operated on a Chassis Dynamometer, Environ. Sci. Technol. 2007, 41, 6199-6204. http://eprints.cert.ucr.edu/448/
7. Lehmann, U., Niemela, V., and Morh, M., 2004, New Methods for Time Resolved Diesel Engine Exhaust Particle Mass Measurements, Environmental Science and Technology. 38:5704-5711.
8. Matter, U., Siegmann, H.C., Burtscher, H., 1999, Dynamic Field Measurements of Submicron Particles from Diesel Engines. Environ. Sci. Technology, 33, 1946-1952.
9. Maricq M.M., Xu N., Chase R.E., 2006, Measuring Particulate Mass Emissions with Electrical Low Pressure Impactor, Aerosol Science and Technology (2006) Vol 40: 68-79.
10. Podsiadlik, D.H., Chase, R.E., Lewis, D., Spears, M., 2003, Phase-Based Teom Measurements Compared With Traditional Filters for Diesel PM, SAE 2003-01-0783.
11. Witze, P.O., Maricq, M.M., Chase, R.E., Podsiadlik, D.H., Xu, N., 2004, Time-Resolved Measurements of Exhaust PM for FTP-75: Comparison of LII, ELPI, and TEOM Techniques. SAE 2004-01-0964.

12. Johnson K.C., Durbin T.D., Jung H., Cocker III D.R., Khan, M.Y., 2010, Validation Testing for the PM-PEMS Measurement Allowance Program, Final Report by the University of California Riverside for the California Air Resources Board under contract No. 07-620, November 2010. http://eprints.cert.ucr.edu/505/
13. Cocker, D.R., Shah, S.D., Johnson, K.C., Miller, J.W., and Norbeck, J.M., 2004a, Development and Application of a Mobile Laboratory for Measuring Emissions from Diesel Engines. 1. Regulated Gaseous Emissions. Environ. Sci. Technol. 38, 2182.
14. Cocker, D.R., Shah, S.D., Johnson, K.C., Zhu, X., Miller, J.W., and Norbeck, J.M., 2004b, Development and Application of a Mobile Laboratory for Measuring Emissions from Diesel Engines. 2. Sampling and Toxics and Particulate Matter. Environ. Sci. Technol. 38, 6809.
15. CARB, 2010, California Air Resources Board, Final Regulation 1971.1 (e) Monitoring Requirements for Diesel/Compression-Ignition Engines (8) Particulate Matter (PM) Filter Monitoring (8.2)(8.2.1) Filtering Performance.
16. Johnson K.C., Durbin T.D., Cocker III D.R., Miller W.J., Bishnu D.K., Maldonado H. Moynahan N, Ensfield C., Laroo C.A., 2009, On-Road Comparison of a Portable Emission Measurement System with a Mobile Reference Laboratory for a Heavy Duty Diesel Vehicle, Atmospheric and Environment. http://eprints.cert.ucr.edu/338/
17. Bell, A., G. Phil., (1881), Mag. J. Sci., XI, 510–528.

18. Harren, Frans J.M., Gina, Cotti, Jos Oomens, and Sacco te Lintel Hekkert, 2000, Photoacoustic Spectroscopy in Trace Gas Monitoring, Encyclopedia of Analytical Chemistry R.A. Meyers (Ed.) pp. 2203–2226, John Wiley & Sons Ltd, Chichester.
19. Hinds, W. C., 1998, Aerosol Technology, John Wiley: New York.
20. Ristimaki, J., Virtanen, A., Marjamaki, M., Rostedt, A., Keskinen, J., 2002, On-line measurement of size distribution and effective density of submicron particles. J. Aerosol Sci., 33, 1541-1557.
21. CFR. Code of Federal References, 2010, *Protection of the environment. Title 40. Section 86 and 89.*
22. Fountoukis, C. and Nenes, A., 2007, ISORROPIA II: A Computationally Efficient Aerosol Thermodynamic Equilibrium Model for K+ - Ca2+ - Mg2+ - NH4+ - SO42- - NO3- - - Cl- - H2O Aerosols, Atmos. Chem. Phys., 7, 4639-4659.
23. ISORROPIA, 2009, http://nenes.eas.gatech.edu/ISORROPIA.
24. Nenes, A., Pilinis, C., Pandis, S.N., 1998, ISORROPIA: A New Thermodynamic Model for Multiphase Multicomponent Inorganic Aerosols, Aquat. Geochem., 4, 123-152.
25. NIOSH, 1996, *NIOSH Manual of Analytical Methods; National Institute of Occupational Safety and Health: Cincinnati, OH.*
26. Shah, S., D., and Cocker, D., 2005, A Fast Scanning Mobility Particle Spectrometer for Monitoring Transient Particle Size Distributions, J. Aerosol Sci. Vol. 39:519-526, 2005.
27. Khalek, I.A., Bougher, T.L., Mason, R.L., Buckingham, J.P., 2010, PM-PEMS Measurement Allowance Determination, Final Report by Southwest Research

Institute for the Heavy Duty In-Use Testing Steering Committee, SwRI Project 03.14956.12, June.

28. Clerc J.C., and Johnson J.H., 1982, A Computer Heat Transfer and Hydrocarbon Adsorption Model for Predicting Diesel Particulate Emissions in Dilution Tunnels, SAE 821218 October 18, 1982.
29. Swanson, J.; Kittelson, D.; Watts, W.; Gladis, D.; Twigg, M., 2009, Influence of Storage and Release on Particle Emissions from New and Used CRTs; Atmos. Environ., 43, 3998-4004.
30. Traver, M. L., 2002, Inter-laboratory Crosscheck of Heavy Duty Vehicles Chassis Dynamometers, CRC Project No. E-55-1, May 2002.

Chapter Three: Measuring In-Use Ship Emissions with International and US Federal Methods

3.1. Abstract

Regulatory agencies have shifted their emphasis from measuring emissions during certification cycles to measuring emissions during actual use. Emission measurements in this research were made from two different large ships at sea to compare the Simplified Measurement Method (SMM) compliant with the International Maritime Organization (IMO) NO_x Technical Code with the Portable Emission Measurement Systems (PEMS) compliant with the United States Environmental Protection Agency (USEPA) 40 Code of Federal Regulations (CFR) Part 1065 for on-road emission testing. Emissions of nitrogen oxides (NO_x), carbon dioxide (CO_2) and carbon monoxide (CO) were measured at load points specified by International Organization for Standardization (ISO) to compare the two measurement methods. The average percentage errors calculated for PEMS measurements were 6.5%, 0.6% and 357% for NO_x, CO_2 and CO, respectively. The NO_x percentage error of 6.5% corresponds to a 0.22 to 1.11 g/kW-hr error in moving from Tier III (3.4 g/kW-hr) to Tier I (17.0 g/kW-hr) emission limits. Emission factors (EFs) of NO_x and CO_2 measured via SMM were comparable to other studies and regulatory agencies estimates. However, $EF_{PM2.5}$ for this study was up to 26% higher than that currently used by regulatory agencies. The $PM_{2.5}$ was comprised predominantly of hydrated sulfate (70-95%), followed by organic carbon (11-14%), ash (6-11%) and elemental carbon (0.4-0.8%).

3.2. Introduction

Over the past 20 years, on-road vehicles have faced stricter emission regulations[1], which have led to significant improvement in engine and exhaust control technologies and simultaneous reduction in emissions. In comparison to on-road vehicles, regulations for controlling ship emissions are fairly new.[2] Emissions from ships are regulated by the International Maritime Organization (IMO) under Annex VI of the International Convention for the Prevention of Pollution from Ships (MARPOL) which set limits on NO_x, sulfur oxides (SO_x) and particulate matter (PM) and prohibit deliberate emissions of ozone depleting substances.

Exhaust from large marine diesel engines contributes significantly to the anthropogenic burden, thereby affecting the chemical composition of the atmosphere, global climate and air quality in coastal areas.[3-7] Key emissions from ships include NO_x, SO_x, CO_2, CO, unburned hydrocarbons, and PM. These emissions are released into the marine boundary layer at relatively high local concentrations. PM emitted from ship stacks is estimated to be responsible for ~60,000 mortalities annually on a global scale.[8] Moreover, emissions of NO_x and volatile organic compounds (VOCs) react in the presence of sunlight to form ground level ozone and secondary particulate, which can harm human health and vegetation.

The main propulsion engines on large ships are defined as "Category 3" slow speed diesel engines by IMO and typically range in size from 2,500 to 70,000 kW. Further these engines typically burn a heavy fuel oil (HFO) with high viscosity and sulfur content. In contrast to fuel dependent emissions, such as SO_2 and CO_2, emissions of NO_x are dependent on the

combustion process. In slow speed diesel engines, combustion occurs at higher temperatures for a longer period of time, which improves combustion efficiency but increases thermal fixation of nitrogen in the combustion air to form NO_x.[9] Thus, the NO_x emission limits set by Regulation 13 of IMO's MARPOL Annex VI are directly related to the rated speed of the engine.[2]

The purpose of the NO_x Technical Code (NTC) is to establish mandatory procedures for testing, survey and certification of marine diesel engines to ensure that all applicable marine diesel engines comply with allowable NO_x emissions. Normally engine certification occurs on a test bed; however, the NTC allows this on-board testing for engines that cannot be certified on a test bed. The NTC allows certification to take place on-board via the Simplified Measurement Method (SMM) in such cases. The details of the SMM are available elsewhere.[10] In reality, both the test-bed and the in-use with SMM procedures are costly and complex, requiring the installation of large amounts of equipment on the ship to perform emission certification. Further, under the current certification scheme, a ship's engines are allowed to be certified while operating on distillate fuel (nitrogen free) both on the test bed and in-use even though large ships typically operates on HFO. Using a distillate fuel effectively biases the certified NO_x emission to a lower value, as the fuel bound nitrogen can account for 6-10%of a ship's NO_x emissions.[11]

Since PEMS are currently approved in the 40 Code of Federal Regulations (CFR) Part 1065 for measuring in-use diesel engine emissions,[12] the question was asked whether PEMS could also provide accurate emissions measurement from large marine ships. Use of PEMS for on-board certification of NO_x emissions could then be performed quickly, accurately and at

lower cost when operating on their standard operating fuel (HFO). PEMS could also be used for yearly surveys to ensure that the large ships engine emissions remain in compliance with the NO_x emission standards. Additionally, to meet upcoming proposed IMO Tier III NO_x reductions, it is envisioned that pre and post intake or exhaust gas treatment devices will be used to meet the NO_x emission requirements. Consequently, it will be very difficult for engines with such systems to be certified in a conventional test-bed environment and these systems will likely require on-board, in-use certification. Under the current SMM provision, this certification will be very cumbersome and costly to the ship owner.

One of the major goals of this research was to evaluate whether PEMS are a viable tool for in-use marine ship engine certification. Recently, these gaseous PEMS have been evaluated against US Environment Protection Agency (EPA) CFR methodology for in-use emission measurement from on-road vehicles.[13] As a result, a "measurement allowance" was developed for PEMS complying with 40 CFR Part 1065.[14] A measurement allowance for PEMS is defined as the measurement error in the quantification of gaseous pollutant when compared with the laboratory method. Similarly, in this study, SMM and PEMS are compared to account for differences between methods. The difference, if it exists, could be used to establish a measurement allowance for gaseous PEMS for large ships which might then allow the submission of a proposal to IMO for inclusion of PEMS into the NTC to allow its use for on-board certification.

This research provides the first comparison between the PEMS and SMM emissions measurement approaches. The SMM compliant with IMO's NTC and the PEMS compliant with EPA's 40 CFR Part 1065 were compared for two in-use large ships. Emission

measurements were conducted near prescribed large ship certification load points. Particulate mass was also quantified during this study in addition to the measurement of gaseous components in the exhaust. This study also provides modal and overall emission factors (EFs) from a large marine diesel engine tested that is representative of a significant number of in-use uncontrolled marine diesel engines.

3.3. Experimental Details

In-use emission measurements were made from two container ships with C-3 category main propulsion engines. One large ship was a Panamax class built in 1997 with the capacity to carry 4,000 to 6,000 containers and had a Tier 0 main propulsion engine. The other large ship was a post-Panamax class launched in 2010 that can carry approximately 10,000 containers and had a main propulsion engine meeting Tier I NO_x standards. Overall emissions from the two main engines were measured in order to evaluate the performance of a CFR compliant PEMS against instruments meeting the SMM.

3.3.1. Engine and Fuel Specifications

The main propulsion engine on ship 1 was a two stroke, slow speed Sulzer 9RTA84C diesel engine with a maximum rated power of 36,740kW at 102 rpm. A significant number of large ships use engines of this size. Ship 2 was propelled by a slow speed Hyundai B&W 11K98ME7 diesel engine with a 68,530kW at 97 rpm and is representative of the propulsion engines used on larger container ships that are being built today. Engine parameters including load (kW), speed (rpm), intake manifold temperature, boost pressure and fuel consumption were monitored manually from the engine computer during the testing. Both

engines consumed HFO in international waters that met ISO 8217 specifications. Since HFO properties depend strongly on the source, a one liter fuel sample was drawn from the main engine final filter drain, immediately upstream of the injector rail. The fuel samples were subsequently analyzed for a number of fuel properties (Table 3-1).

Table 3-1: Selected fuel properties from all trips

HFO Properties	**Units**	**Trip 1**	**Trip 2**	**Trip 3**
Density at 15.5°C	kg/m^3	950.1	962.2	988.2
Viscosity at 50°C	mm^2/s	262.3	367	368.6
Sulfur	%m/m	3.14	2.15	2.51
Ash	%m/m	0.07	0.03	0.07
Vanadium	mg/kg	276	57	262
Nickel	mg/kg	56	21	55
Net Specific Energy	mg/kg	40.09	40.26	40.30

3.3.2. Test Cycles

Comparison between emission measurements with SMM and PEMS compliant instruments were made (Table 3-2) as close as practically possible to the engine loads as specified in ISO 8178-4 E3[15] test cycle (100%, 75%, 50% and 25% of maximum rated power).

Table 3-2: Operating load points for emission measurements

Container Ship Tests			**Engine Model**	**Operating Loads**
Trip 1	Jul-2009	Ship 1	Sulzer 9RTA84C	29%, 52%, 73%, 81%
Trip 2	Aug-2009	(Panamax Class)		28%, 44%, 69%, 83%
Trip 3	Sep-2010	Ship 2 (Post Panamax Class)	Hyundai MAN B&W 11K98ME7	24%, 47%, 75%, 90%

Three sets of consecutive emission measurements were made at each test mode. The duration of each measurement was five to seven minutes. The order of test modes was from

high load to low load. Gaseous readings were recorded at a one-hertz frequency. Average concentrations and standard deviations were calculated to ensure steady state measurements.

3.3.3. Emission Measurements

3.3.3.1. Measurement of Gaseous Emissions by SMM

The sampling system flow diagram is shown in Figure 3-1. Two Horiba PG-250 multi-gas analyzers (Table 3-3) were used to measure raw and diluted gas concentrations of NO_x (0-2,500 ppm), CO (0-5,000 ppm), CO_2 (0-20%), SO_2 (0-3,000 ppm) and O_2 (0-20%). This instrument is compliant with IMO's NTC for the measurement of NO_x, CO and CO_2. Note that the NTC only allows the use of a chemiluminescent detector (CLD) or a heated chemiluminescent detector (HCLD) for analyzing NO_x. Peltier coolers were installed between the sampling probe and Horiba analyzers to remove water and minimize the interference of H_2O on CO and CO_2 measurements. A J.U.M., Model 109A, heated flame ionization (HFID) analyzer was used to measure total hydrocarbons (THC). A separate heated filter and sample line (191±10°C) were used for the THC measurements as required by the protocol. Analyzer checks with calibration gases both before and after tests were made to account for instrument drift. Calibration adjustments were made manually to the raw data. SO_2 emissions provided in this study are calculated from the sulfur level in the fuel per ISO 8178.[15]

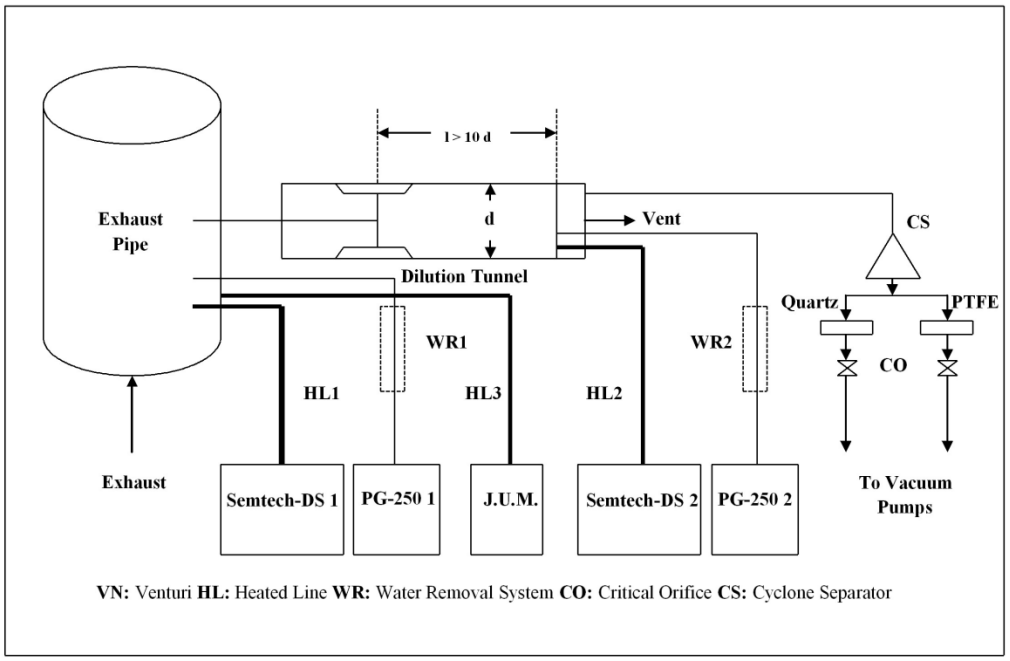

Figure 3-1: Sampling system flow diagram

Table 3-3: SMM and PEMS detection method and measurement ranges for gaseous pollutants

Gaseous Pollutant	SMM		PEMS	
	Detector	Range	Detector	Range
NO_x	Heated Chemiluminescence[a]	0-2500 ppmv	Non-Dispersive Ultraviolet (NDUV)[b]	0-3000 ppmv
CO_2	Non-Dispersive Infrared (NDIR)[a]	0-20%	Non-Dispersive Infrared (NDIR)[b]	0-20%
CO	Non-Dispersive Infrared (NDIR)[a]	0-5000 ppmv	Non-Dispersive Infrared (NDIR)[b]	0-80000 ppmv
THC	Heated Flame Ionization Detector[†]	0-10000 ppmC	Heated Flame Ionization Detector[b]	0-40000 ppmC

[a]Horiba PG-250; [b]Sensors Semtech-DS; [†] (J.U.M. Model 109A)

3.3.3.2. Measurement of Gaseous Emissions by PEMS

Two Sensors' Semtech-DS PEMS (Table 3-3) were utilized in this study, so that raw and dilute emissions could be measured simultaneously (Figure 3-1). The PEMS are capable of

measuring NO_x (0-3,000 ppm), CO_2 (0-20%), CO (0-80,000 ppm), THC (0-40,000 ppmC) and O_2 (0-20%) in a single unit and are compliant with US EPA's 40 CFR Part 1065. The Semtech-DS uses the same measurement principles as the SMM for CO/CO_2 (NDIR) and THC (FID). However, NO_x is measured using a non-dispersive ultra violet (NDUV) detection method. It uses only one heated line (maintained at 191°C) to transfer the exhaust sample from the stack to THC analyzer. After THC analysis, a sample conditioning system within the Semtech-DS removes any remaining heavy hydrocarbons, thereby minimizing contamination of the optical detectors (NDIR & NDUV). Calibrations were made before and after each test using Semtech-DS software. Raw data was adjusted for calibration by the Semtech-DS software.

3.3.3.3. Measurement of Particulate Mass

Sampling and analysis of particulate mass conformed to ISO 8178-2 requirements.[16] A partial flow dilution system with single venturi was installed (Figure 3-1). A 2.5 μm cyclonic separator was installed downstream of dilution tunnel to remove particles larger than 2.5 μm (aerodynamic diameter). $PM_{2.5}$ was collected on 47 mm diameter 2 μm pore Teflo® filters (Pall Gelman, Ann Arbor, MI) and $PM_{2.5}$ mass was determined by weighing filters using a Mettler Toledo UMX2 microbalance following the requirements of CFR part 1065. Before and after the collection, the Teflo® filters were conditioned for 24 hr in an environmentally controlled room (RH = 40%, T = 25°C) and weighed daily until two consecutive weight measurements were within 3 μg. The Teflo® filters were subsequently extracted with HPLC grade water and isopropyl alcohol and analyzed for sulfate ions using a Dionex DX-120 ion chromatograph. A factor of 2.15 was applied to the mass of sulfate ions as sulfate on the

Teflo® filter was assumed to be in hydrated form ($H_2SO_4.6H_2O$) as predicted using the aerosol thermodynamic model ISORROPIA.[17-19] Parallel 2500 QAT-UP Tissuquartz Pall (Ann Arbor, MI) 47 mm filters (preconditioned at 600°C for a minimum of 5 hours) were used to collect $PM_{2.5}$ for subsequent elemental and organic carbon (EC/OC) analysis following aerosol analyzer (±20% measurement uncertainty).

3.3.4. Calculation Method

Emission factors were calculated using the emission concentration as measured by SMM, calculated exhaust flow rate and the engine load obtained from engine computer. The carbon balance method was used to calculate exhaust flow rate. Emission factors are provided in grams per kilowatt-hour (g/kW-hr) for Trip1 and 2 and a conversion factor, *f* (Table 3-4), is provided to calculate EFs in g/kg fuel burned (eq 1). Emission factors for Trip 3 are provided elsewhere.[21]

$$(Pollutant_i)_{g/kW-hr} \times f = (Pollutant_i)_{\frac{g}{kg} of\ fuel} \quad (1)$$

3.4. Results and Discussions

3.4.1. Comparison of Two Methods

3.4.1.1. Laboratory comparison

The PEMS and SMM were compared under well controlled laboratory conditions. Steady state tests were performed using a light duty vehicle with an uncontrolled diesel engine fueled by ultra-low sulfur diesel (ULSD) and operating on a chassis dynamometer. Excellent correlations (R^2 = 1.00, slope of 1.01) were found for both NO_x and CO_2 measurements.

However, CO concentrations had a lower correlation (R^2 = 0.91) with the PEMS positively biased (slope = 1.45). Further, a percentage error, which is defined as the ratio of the difference between the PEMS and SMM measured values divided by value measured by SMM method, was calculated for each measured gaseous pollutant. The average PEMS percentage errors for NO_x, CO_2 and CO measurements were 0.03%, 0.12% and 77%, respectively. Thus controlled laboratory tests suggest that PEMS measurements are equivalent to the IMO's instruments for NO_x and CO_2 and will not require a measurement allowance for in-use NO_x emission measurement while CO PEMS readings are highly biased.

3.4.1.2. In-use NO_x comparison

PEMS and SMM were next compared on large ship during three trips at sea. Parity charts for NO_x comparing SMM and PEMS measurements are shown in Figure 3-2. Excellent correlation of R^2 = 1.00, slope of 0.97 and positive intercept of 134 was observed. The average percentage error for PEMS measurement (NDUV) was 6.5%. A 6.5% error in PEMS NO_x measurement for emission limits ranging between 3.4 (Tier III) and 17 g/kW-hr (Tier I) would correspondingly result in an absolute measurement error of 0.22 to 1.11 g/kW-hr. A two-tailed, paired *t*-test between the PEMS's and SMM's NO_x concentrations suggest that the mean difference between PEMS and SMM measurements was statistically significant at greater than 99% confidence level.

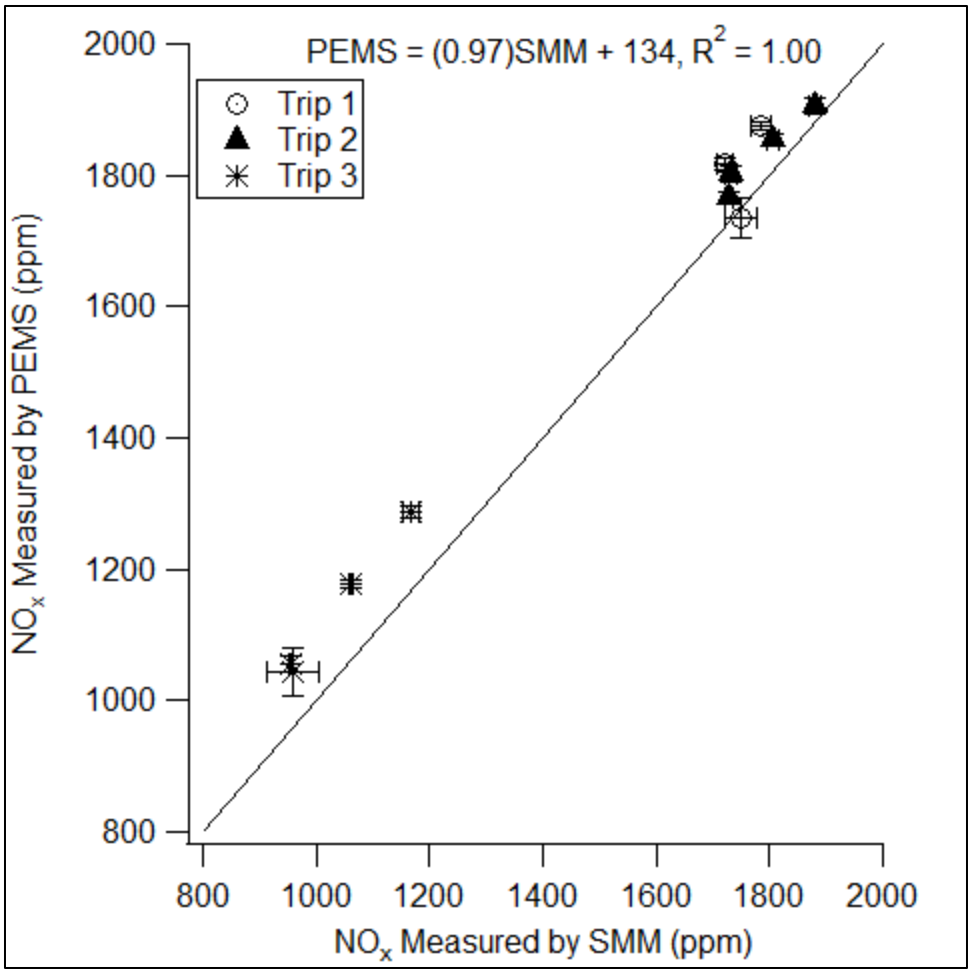

Figure 3-2: SMM and PEMS NO_x parity chart. Solid line represents 1-1 line

NDUV measurement is generally insensitive to other diesel exhaust gases such as CO_2 and H_2O but it has some sensitivity towards SO_2. As shown in the laboratory work, NO_x measured with NDUV in the PEMS agreed well with the SMM methods when the engine burned ULSD (sulfur content ≤ 0.0015% by weight) fuel. However, ships burn fuels containing up to 3.5 % by weight of sulfur and SO_2 will interfere with the NO_x measurements since it absorbs in the range of 200-400 nm of the UV spectrum and exhibits

strong UV absorption spectrum between 200-240 nm and 290-310 nm.[22-26] Furthermore, NO and NO_2 in Semtech-DS absorb at 225±1.5 nm and 350±5 nm, respectively. Data in this research show a positive interference with NO, as expected; however, the magnitude was small considering that fuels had sulfur content up to 3.14% by weight. In general, an independent SO_2 calibration gas should be used to determine potential positive interference on NO_x measurements when NDUV methods are used. Based on the potential for interference and barring any additional investigation, it might be possible that some or all of the 6.5% error could be due to the effects of SO_2 interference.

3.4.1.3. In-use CO_2 and CO comparison

Parity charts for CO_2 and CO (Figure 3-3 and 3-4) showed results similar to laboratory tests. The overall correlation for CO_2 showed an $R^2 = 1.0$, a slope of 0.96 and a positive intercept of 0.22. The average percentage error for PEMS CO_2 was 0.6%. A two-tailed, paired t-test between the SMM and PEMS CO_2 concentration correlations suggest that the mean difference was statistically significant at greater than 95% confidence level. PEMS CO measurements were biased high as expected from lab study. Moreover, the CO correlation deteriorated when methods where compared on ships. An overall correlation for CO showed an $R^2 = 0.51$, a slope of 6.29 with negative intercept of 158. The average CO percentage error increased from 77% in laboratory tests to 357% for in-use tests. CO measurement error is attributed to the fact that slow speed diesel engines are highly efficient and therefore emit low CO (up to 200 ppm in the present study) whereas the PEMS measurement range is up to 80,000 ppm. This low CO concentration in the exhaust is within the PEMS instrumental noise. Therefore, variation in CO bias for PEMS is only a random

value due to noise and the PEMS is therefore unsuitable for the measurement of CO in the ship's exhaust.

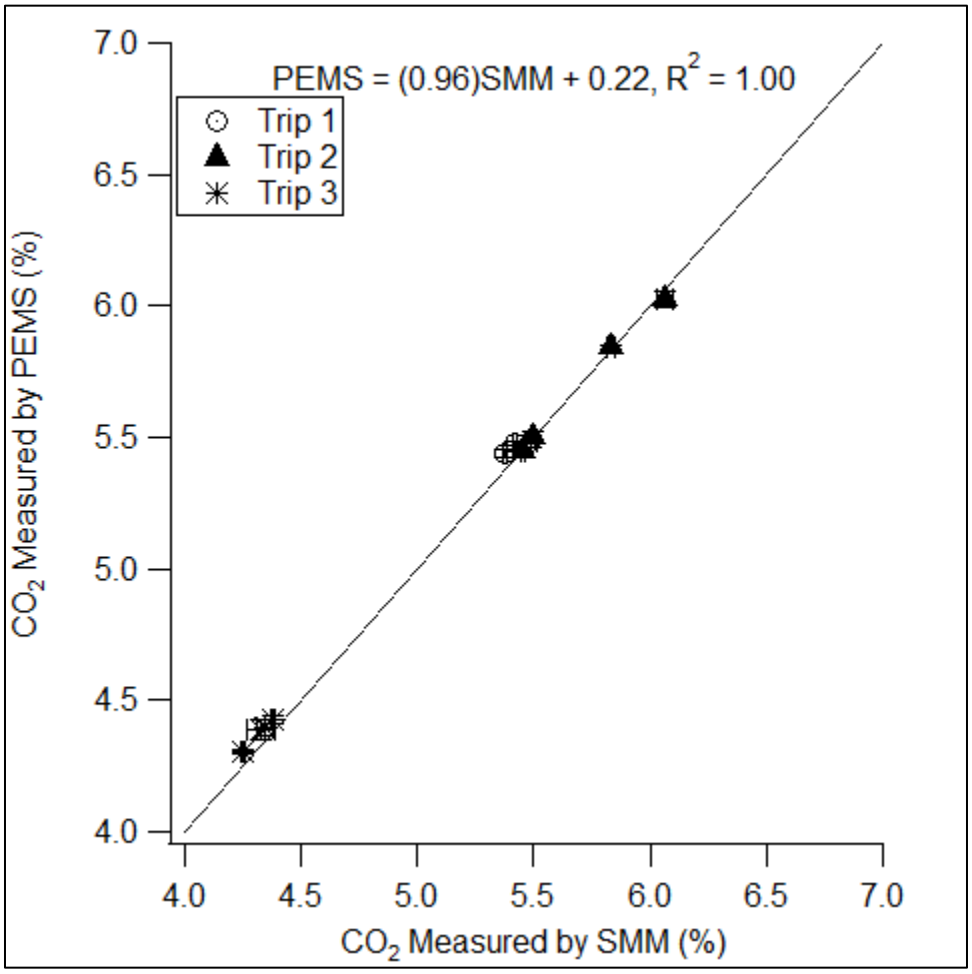

Figure 3-3: SMM and PEMS CO_2 parity chart. Solid line represents 1-1 line

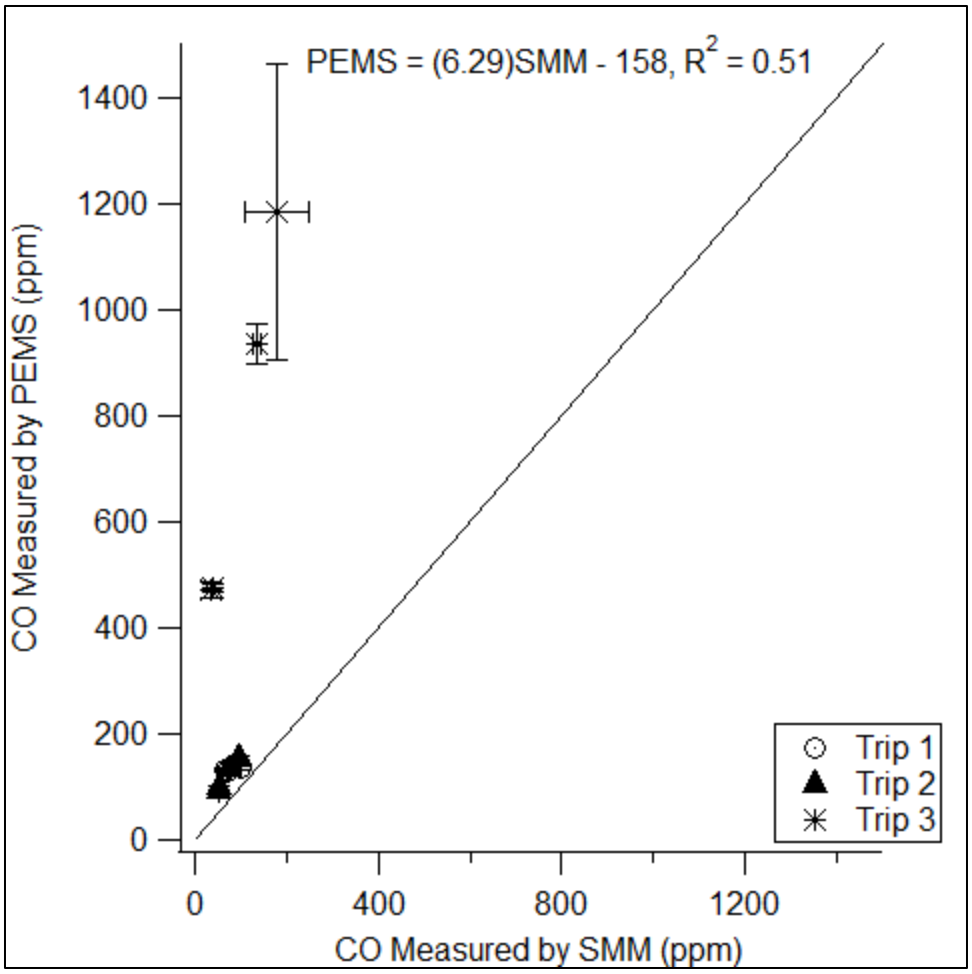

Figure 3-4: SMM and PEMS CO parity chart. Solid line represents 1-1 line

3.4.2. Gaseous and Particulate Emissions: Sulzer 9RTA84C

Modal gaseous (CO_2, NO_x, CO, THC and SO_2) and particulate mass EFs for Trips 1 and 2 are summarized in Table 3-3. Emission factors for CO_2, NO_x and CO were within ~10% for both trips across ISO load points. Modal EF_{CO2} from both trips showed that the engine operates most efficiently near 50% load. During Trip 1, the SMM compliant THC device for measuring THC failed on multiple tests; therefore, EF_{THC} were calculated based on the measurements made by PEMS. No significant difference was observed for PEMS THC

measurements on Trips 1 and 2. SO_2 and $PM_{2.5}$ EFs are highly dependent on the sulfur content of the fuel. Trips 1 and 2 consumed fuel with sulfur content of 3.14% and 2.15%, respectively. Therefore, on average EF_{SO2} and $EF_{PM2.5}$ were ~30% and ~26% lower for Trip 2 compared to Trip 1. Overall, good agreement was found between emissions from the two trips.

The summation of speciated PM (EC, OC, $H_2SO_4 \cdot 6H_2O$ and ash) agreed well (<7%) with the total gravimetric $PM_{2.5}$ for all modes except 100% (11%). Figure 3-5 represents the fraction of speciated $PM_{2.5}$ against total $PM_{2.5}$ across ISO load points for Trip 1. The hydrated sulfate fraction dominated the total PM and it increased from 0.70 to 0.95 as load increased from 25% to 100%. Conversely, the fraction of OC (11-14%), EC (0.4-0.8%) and ash (6-11%) decreased with increased in engine load. Fuel sulfur conversion to sulfate increased from 2.3% to 5.5% as the engine load increased from 29% to 81%, consistent with previous studies.[27, 28]

Table 3-4: Gaseous and particulate modal emission factors from Trip 1 and 2 in g/kW-hr. *f* is a conversion factor to convert g/kW-hr to g/kg of fuel

Targeted Load	Actual Load	CO_2	NO_x	CO	THC	SO_2	$PM_{2.5}$	*f*
		g/kWhr						
Trip 1								
25%	29%	577	19.5	0.57	0.30	11.4	1.19	1.82
50%	52%	555	18.5	0.41	0.30	10.9	1.44	1.86
75%	73%	561	19.5	0.36	0.26	11.0	2.14	1.82
100%	81%	576	19.1	0.35	0.25	11.3	2.19	1.75
Trip 2								
25%	28%	584	18.9	0.60	0.30	7.9	0.91	1.71
50%	44%	533	16.6	0.44	0.28	7.2	1.07	1.88
75%	69%	612	20.6	0.39	0.26	8.3	1.60	1.63
100%	83%	579	19.0	0.35	0.22	7.8	1.56	1.73

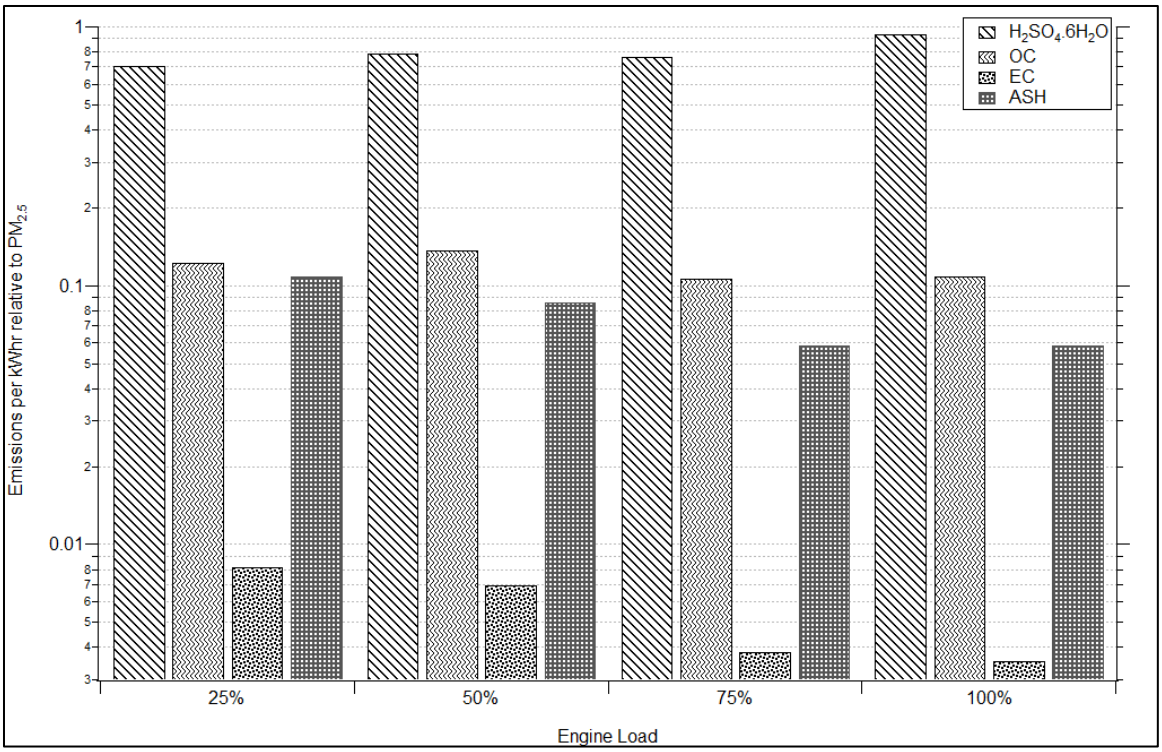

Figure 3-5: Emissions of $H_2SO_4.6H_2O$, OC, EC and ash per kW-hr relative to $PM_{2.5}$

3.4.3. Overall Weighted Emission Factors

The overall weighted emission factor for different gaseous and particulate pollutants was calculated using the weighting factors defined in the ISO 8178-4 E3 test cycle for heavy-duty marine engines.[15] The overall weighted EF is calculated as:

$$E_{WM} = \frac{\sum_{i=1}^{i=n}(m_i \,.\, WF_i)}{\sum_{i=1}^{i=n}(p_i \,.\, WF_i)} \qquad (2)$$

Where:

E_{WM} = Overall weighted emission factor (g/kW-hr)

m_i = Emission factor for i mode (g/hr)

WF_i = Weighted factor for i mode

p_i = Engine load for i mode

The overall weighted EFs for NO_x, $PM_{2.5}$, SO_2, CO_2 and CO are summarized in Table 3-5. Overall, weighted EFs for EC, OC, ash and $H_2SO_4 \cdot 6H_2O$ for Trip 1 were 0.01, 0.22, 0.12, 1.64 g/kW-hr, respectively. Assuming EF_{EC}, EF_{OC} and EF_{ash} to be constant across all studies, and correcting the EF of the sulfate fraction of the $PM_{2.5}$ for the differences in fuel sulfur content using eq. 3, the USEPA[30] and CARB $PM_{2.5}$ data (Table 3-5) were found to be 26% and 10% lower, respectively, than the summation of EC, OC, ash and hydrated sulfate fraction of the $PM_{2.5}$ when compared to the Trip 1 results. Overall EF_{NOx} for uncontrolled marine diesel engines in this study are ~7-8% and ~3-5% higher than USEPA/CARB and Lloyds study[29], respectively. Variation among EF_{SO2} is attributed to variable sulfur content in each study. Measured EF_{CO2} is also within 10% of regulatory agencies estimates for both Trips 1 and 2. However, measured EF_{CO} are ~one-fourth of the estimated values of regulatory agencies.

$$(H2SO4.6H2O)_{Trip_i} = \frac{(S\%)_{Trip_i}}{(S\%)_{Trip_1}} (H2SO4.6H2O)_{Trip_1} \quad (3)$$

Table 3-5: Comparison of measured and previous reported overall weighted emission factors

	NO_x	$PM_{2.5}$	SO_2	CO_2	CO	Sulfur Content
			g/kW-hr			%
Trip 1	19.3	2.00	11.1	565	0.37	3.14
Trip 2	19.6	1.49	8	593	0.40	2.15
Agrawal et al., 2010	19.77	2.40	11.53	617	0.29	3.01
USEPA, 2009	18.1	1.31	10.3	620	1.4	2.7
CARB, 2008	18.1	1.5	10.5	620	1.38	2.5
Lloyds, 1995	18.7	1.23	–	–	–	–

3.5. Conclusions

Two different methods; IMO's SMM and USEPA's on-road certified PEMS were compared during three different trips on in-use container ships. Excellent correlation was observed for CO_2 measurements. PEMS measurements for NO_x were 6.5% higher on average than SMM which was could be attributed to some sensitivity of the NDUV wavelength light absorption to SO_2. This measurement error would become insignificant when lower sulfur fuel is burned in C3 marine engines. The PEMS, as currently configured, was unable to measure the typically low concentrations of CO in slow speed marine diesel engine exhaust. However, since IMO only regulates NO_x and sulfur content in fuel, PEMS can provide a simpler and more convenient method to perform on-board emission certification.

The emission factors from two different trips from the same ship were reproducible. Modal and weighted emission factors are provided for criteria pollutants (NO_x, CO, SO_2 and $PM_{2.5}$) and CO_2. Hydrated sulfate dominates the composition of PM and the fuel sulfur conversion to sulfate was consistent with the few studies available on emissions from ships.

3.6. Acknowledgement

The authors express their gratitude to the US Environmental Protection Agency (US EPA) for their financial support and the shipping company for volunteering their ship to carry out this project successfully. An appreciation is extended to all the crew members and administrative staff of the ship for their support and cooperative efforts during the emission testing. The authors are grateful to Dr. Varalakshmi Jayaram, Mr. Charles Buffalino and Mr.

Kurt Bumiller for their help with the test preparations, and Ms. Kathalena Cocker and Mr. James Gutierrez for their help and support in the Analytical Lab.

3.7. Literature Cited

1. United States Environmental Protection Agency, **2012**. http://www.epa.gov/oms/hd-hwy.htm#regs.
2. International Maritime Organization, **2005**. The protocol of 1997 (MARPOL Annex VI).http://www.imo.org/OurWork/Environment/PollutionPrevention/AirPollution/Pages/The-Protocol-of-1997-(MARPOL-Annex-VI).aspx.
3. Capaldo, K.; et al. Effects of ships emissions on sulphur cycling and radiative climate forcing over the ocean. Nature **1999**, 400 (6746), 743-746.
4. Duce, R.A.; et al. Impacts of atmospheric anthropogenic nitrogen on the open ocean. Science **2008**, 320 (5878), 893-897.
5. Lauer, A; et al. Assessment of Near-Future Policy instruments for oceangoing shipping: Impact on atmospheric aerosol burdens and the earth's radiation budget. Environ. Sci. Technol. **2009**, 43 (15), 5592-5598.
6. Agrawal, H.; et al. Primary particulate matter from ocean-going engines in the southern California air basin. Environ. Sci. Technol. **2009**, 43 (14), 5398-5402.
7. Song, S.K.; et al. Influence of ship emissions on ozone concentrations around coastal areas during summer season. Atmos. Environ. **2010**, 44 (5), 713-723.
8. Winebrake, J.J.; et al. Mitigating the health impacts of pollution from oceangoing shipping: an assessment of low-sulfur fuel mandates. Environ. Sci. Technol. **2009**, 43 (13), 4776-4782.

9. ENTEC UK Limited. Quantification of Emissions from Ships associated with Ship Movements between Ports in European Community, **2002**.
10. IMO. Prevention of air pollution from ships and NOx Technical Code, International Maritime Organization, **1997**.
11. CARB. Emissions Estimation Methodology for Ocean-Going Vessels. http://www.arb.ca.gov/regact/2008/fuelogv08/appdfuel.pdf
12. CFR. Protection of the Environment. Title 40. Part 86 and 89. U.S. Code of Federal Regulations.
13. Durbin, T.D.; et al. Evaluation and comparison of portable emission measurement systems and federal reference methods for emissions from a back-up generator and a diesel truck operated on a chassis dynamometer, Environ. Sci. Technol. **2007**, 41, 6199-6204United States Environmental Protection Agency, 2012. http://www.epa.gov/oms/hd-hwy.htm#regs.
14. Johnson, K.C.; et al. On-road comparison of a portable emission measurement system with a mobile reference laboratory for a heavy-duty diesel vehicle. Atmospheric Environment. **2009**, 43 (18) 2877-2883.
15. ISO. ISO 8178-4, Reciprocating internal combustion engines-exhaust emission measurement. Part-4: Test cycles for different engine applications, **1996**.
16. ISO. ISO 8178-2, Reciprocating internal combustion engines: exhaust emission measurement. Part-2: Measurement of gaseous and particulate exhaust emissions at site; International Organization of Standardization, **1996**.

17. Fountoukis, C. and Nenes, A., 2007, ISORROPIA II: A Computationally Efficient Aerosol Thermodynamic Equilibrium Model for K+ - Ca2+ - Mg2+ - NH4+ - SO42- - NO3- - - Cl- - H2O Aerosols, Atmos. Chem. Phys., 7, 4639-4659.
18. ISORROPIA, 2009, http://nenes.eas.gatech.edu/ISORROPIA.
19. Nenes, A., Pilinis, C., Pandis, S.N., 1998, ISORROPIA: A New Thermodynamic Model for Multiphase Multicomponent Inorganic Aerosols, Aquat. Geochem., 4, 123-152.
20. NIOSH. NIOSH Manual of Analytical Methods; National Institute of Occupational Safety and Health: Cincinnati, OH, **1996**.
21. Khan, M.Y.; et al. Benefits of two mitigation strategies for container vessels: cleaner engines and cleaner fuels, Environ. Sci. Technology, **2012**, 46 (9), pp 5049-5056.
22. Plach, H.J. and Troe, J.; Absorption study of the dissociation of SO2 and SO in shock waves. International Journal of Chemical Kinetics, Vol. 16, 1531-1542 (**1984**).
23. Syty, A. Determination of sulfur dioxide by ultra violet spectrometry. Analytical Chemistry, Vol 45, No. 9. (**1973**)
24. Somesfalean, G.; et al. All-diode-laser ultraviolet absorption spectroscopy for sulfur dioxide detection. Applied Physics B 80, 1021-1025 (**2005**)
25. Vattulainen, J.; et al. Experimental determination of SO_2, C_2H_2, and O_2 UV absorption cross sections at elevated temperature and pressures. (**1997**)
26. Xu, F.; et al. Concentration evaluation method using broadband absorption spectroscopy for sulfur dioxide monitoring. Applied Physics Letters, 88, 231109 (**2006**).

27. Agrawal, H.; et al. In-use gaseous and particulate matter emissions from a modern ocean going container vessel, Atmospheric Environment 42 (**2008**) 5504-5510.

28. Agrawal, H.; et al. Emissions from main propulsion engine on container ship at sea. Journal of Geophysical Research, Vol. 115, D23205, 7 PP., **2010**.

29. Lloyd's Register. *Lloyd's Register Engineering Services*, **1995**.

30. U.S. Environmental Protection Agency (USEPA). Current Methodologies in Preparing Mobile Source Port-Related Emission Inventories. Final Report. April 2009. http://www.epa.gov/cleandiesel/documents/ports-emission-inv-april09.pdf

Chapter Four: Impact of Algae Biofuel on In-Use Gaseous and Particulate Emissions from a Marine Vessel

4.1. Abstract

In-use emission rates for a marine vessel operating on hydrotreated algae biofuel are reported for the first time. Emission measurements were made on a 4-stroke marine diesel engine from a *Stalwart* class vessel to compare the emissions profile from burning ultra-low sulfur diesel (ULSD) to a 50/50 blend of ULSD and Algae biofuel (A50). In-use emission measurements followed the International Organization for Standardization (ISO) 8178-4 D2 certification test cycle protocol. Particulate matter ($PM_{2.5}$), nitrogen oxides (NO_x), carbon monoxide (CO) and greenhouse gas (CO_2) were sampled in accordance with the ISO 8178-2 protocol for each mode of the test cycle. Switching fuel from ULSD to A50 resulted in significant ~35% lower $PM_{2.5}$ emissions for 25% and 50% load and an overall weighted $PM_{2.5}$ reduction of ~25%. Overall reductions of 30% and 20% were observed in elemental carbon (EC) and organic carbon (OC), respectively. $PM_{2.5}$ was dominated by OC (77-94%) for both fuels. NO_x emissions were reduced by ~10% on switching from ULSD to A50. Overall the emissions of CO_2 and CO were reduced by 5% and 18% indicating a slight improvement in fuel economy for this engine while operating on A50.

4.2. Introduction

Particulate matter ($PM_{2.5}$) and other criteria pollutants released from marine vessel engines significantly affect air quality and present a substantial health hazard to communities near ports and inland waterways.[1-8] Human exposure to fine particles from combustion sources is linked with increased risks of acute and chronic illness, such as lung cancer and cardiopulmonary disease.[9] A criteria pollutant such as nitrogen oxides (NO_x) is also linked with adverse effects on the respiratory system in addition to the formation of ground-level ozone and smog. Moreover, the continuous rise in global surface temperature due to the combustion of fossil fuels has spurred worldwide interest in reducing carbon dioxide (CO_2) emissions by investigating the impacts and operational consequences of alternative fuels.

In recent years, biofuels derived from algae feedstock has emerged as a technically viable and attractive alternative because of the following reasons :[37,38,43] 1) high yield of fuel production per-acre of land, 2) cultivation on non-arable land, 3) cultivation in fresh, saline, brackish or wastewater, 4) algae feedstocks are based on non-consumable foods, 5) algae have high lipid content for high energy density transportation fuels, and 6) algae produces additional valuable co-products such as food ingredients. In a recent study by Pienkos and Darzins,[11] productivity for soybeans and algae was compared. They estimated that low productivity algae (10 g m^{-2} d^{-1}, 15% oil content) can produce 633 gal $acre^{-1}$ of algae fuel compared to 48 gal $acre^{-1}$ of soybean fuel. However, cost analysis provided in the same study estimated the price of algae bio-crude to be $25 per gallon for low productivity algae and $2.50 per gallon for high productivity algae (50 g m^{-2} d^{-1}, 50% oil content).

In 2007, the United States government passed the energy independence and security act, which mandates production of at least 21 billion gallons of bio-derived fuels from sources other than corn by 2022.[10] Furthermore, the United States Navy established a goal in 2009 of increasing the Navy and Marine Corps use of alternative energy to 50% by 2020.[12] The Navy in turn developed a fuel qualification plan[13] to ensure non-petroleum fuels have similar or better performance than petroleum fuels. Examples of performance tests includes compatibility with current Navy fuels, tolerance to seawater compensation, flash point characteristics, long-term storage capabilities, resistance to bio-contamination, and evaluation of whether the biofuel will negatively impact the current Navy fuels logistics, as well as many others. The goal of this process is to ensure that any fuel will serve as a drop-in replacement requiring no modifications to existing infrastructure or propulsion systems.

One of the fuels being qualified for ship propulsion is hydrotreated renewable diesel (HRD) fuel. This fuel was produced to Navy specifications by Solazyme, Inc. Solazyme uses standard industrial fermentation equipment and proprietary heterotrophic microalgae that grow in the dark. The highly productive microalgae consume the sugars from waste organic material and can produce > 80% oil in just a few days at commercial levels.[44] The algal oil is subsequently processed by the Honeywell UOP/Eni Ecofining™ process to produce HRF-76, the renewable version of F-76.[45] The UOP/Eni Ecofinning™ process uses two stage hydrogenation. The first stage completely hydrogenates any oxygen containing molecules and the second stage employs catalytic hydro-isomerization to produce a branched paraffin rich diesel fuel that has good cold flow properties.[46] The fuel was specifically designed and processed to be blended 50/50 by volume with NATO F-76 fuel, which is the military diesel

fuel typically used by the Navy for ship propulsion. The 50/50 blend of HRD with F-76 has already successfully completed most of the specifications in the fuel qualification plan, and it is currently under-going full scale engine testing and platform demonstrations.[39]

In an on-going effort to evaluate alternative fuels for marine fleets, the US Navy, the Maritime Administration of the US Department of Transportation (MARAD), Great Lakes Maritime Academy in Traverse City, Michigan and University of California at Riverside worked together to test a 50/50 blend of ULSD/Algae Biofuel (A50) in an engine on the *T/S State of Michigan* vessel. The objective of the project was to evaluate marine application of algae renewable fuel. The goals were to conduct limited performance and operational tests of the blended fuel on board a marine vessel and to quantify the emissions profile when switching from ultra-low sulfur diesel (ULSD) to A50. Emission measurements were made from a marine diesel engine using the in-use Simplified Measurement Methods (SMM) system which is compliant with ISO 8178 guidelines and the MARPOL Annex VI NO_x Technical Code[14] for $PM_{2.5}$, NO_x, CO_2, carbon monoxide (CO) and sulfur oxides (SO_x) emissions.

4.3. Experimental Methods

4.3.1. Vessel and Engine Description

The vessel selected for the test was a Stalwart class (T-AGOS) modified tactical general ocean surveillance ship built in 1986. The vessel is representative of many the United States Department of Transportation (U.S. DOT) and the Navy vessels that operate throughout the U.S. inland and ocean waters. The vessel has four main diesel generators (Caterpillar

D398; 12 cylinder, 48.3 L total displacement, 600 kW maximum power rating @ 1200 rpm) that are electrically interconnected via a bus to drive two 1600 kW propulsion motors and to provide electrical power for hoteling purposes.

4.3.2. Test Fuels

Fuel characteristics influence engine exhaust emissions. Due to difference in densities of ULSD and hydrotreated Algae fuel, adequate blending of the fuels was a major concern. Therefore, MARAD and the fuel supplier developed a blending methodology to mix and blend the fuels to ensure proper mixing and constant density throughout the fuel before it was loaded into the fuel tank of the vessel. Information on fuel blending methodology is presented elsewhere.[39]

Multiple samples of the ULSD fuel were taken from the ULSD fuel and the A50 blend of the same ULSD fuel with the algae fuel delivered to the storage tanks on the *T/S State of Michigan*. The ULSD and A50 samples were analyzed by the US Naval Research Laboratory. The average properties of both fuels are summarized in Table 4-1. All properties of the A50 are consistent within blending and analytical measurements of the A50 being a 50/50 blend of ULSD and Algal biofuel. Both fuels had Lubrizol 539D added to ensure they had adequate lubricity.

Table 4-1: Selected fuel properties for ULSD and A50 fuels

Certificate of Analysis			
Properties	**Units**	**ULSD**	**Blend (A50)**
Density @ 15°C	kg/m^3	829	804
Viscosity @ 40°C	mm^2/s	2.3	2.5
Carbon Content	mass %	86.4	85.9
Hydrogen Content	mass %	13.6	14.4
Sulfur Content	ppm	10.3	3.9
Ash	mass %	0.05	0.00
Calorific Value	MJ/kg	42.938	43.400

4.3.3. Test Cycles

In-use emission measurements were collected from the diesel generator engine during vessel operation on the Great Lakes of North America. Emission measurements were performed in ascending order of the mode numbers stated in the ISO 8178-4 D2 test cycle.[49] Best efforts were made to operate the engine at load points specified in the D2 test cycle. Due to practical operating constraints, 100% load was not achieved and therefore, 92% load (maximum achievable load) was considered as ISO mode 1 of the D2 test cycle. The actual load points for both fuels are provided in Table 4-2.

Table 4-2: Actual load points (Percent Load and kW) for the marine diesel generator engine

ISO 8178-4 D2		**Mode 1**	**Mode 2**	**Mode 3**	**Mode 4**	**Mode 5**
Fuel	Load	100	75	50	25	10
ULSD	(%)	92	82	60	26	17
	(kW)	554	490	359	159	101
Blend (A50)	(%)	92	80	61	28	15
	(kW)	551	482	368	167	91

4.3.4. Sampling and Analysis

The methods for sampling and analysis of gases and particulate matter (PM) conformed to ISO 8178-2 requirements. A partial flow dilution system with a single venturi was used and attached directly to the stack negating the need for a heated transfer line.[36] Concentrations of CO, CO_2 and NO_x were measured in both the raw exhaust gas and dilution tunnel using a Horiba PG-250 portable multi-gas analyzer. The dilution ratio determined from CO_2 and NO_x concentrations, agreed within 5%, which is typical of these measurements.

$PM_{2.5}$ samples were collected off the dilution tunnel, following a 2.5 μm cyclone onto pre-weighed 47-mm diameter 2-μm pore Teflo filters (Pall Gelman, Ann Arbor, MI). Loaded Teflo filters were weighed using the same Mettler Toledo UMX2 microbalance used for the clean filters following the guidelines within the Code of Federal Regulations.[16] Filters were conditioned for 24 hr in an environmentally controlled room (RH = 40%, T = 22ºC) and weighed daily until two consecutive weight measurements were within 3 μg before and after $PM_{2.5}$ collection. Elemental and organic carbon (EC/OC) analysis was performed on $PM_{2.5}$ samples collected on 2500 QAT-UP Tissuquartz Pall (Ann Arbor, MI) 47 mm filters that were preconditioned at 600ºC for a minimum of 5 hours. A 1.5 cm^2 punch from the quartz filter was analyzed with a Sunset Laboratory (Forest Grove, OR) thermal/optical carbon aerosol analyzer according to the NIOSH 5040 reference method.[17]

4.3.5. Overall Weighted Emission Factors

The overall weighted emission factors for different gaseous and particulate pollutants were calculated based on the weighting factors established in the ISO 8178-4 D2 test cycle. The equation for calculating the overall EF is:

$$EF_x = \frac{\sum_{i=1}^{i=n}(m_i \times WF_i)}{\sum_{i=1}^{i=n}(p_i \times WF_i)} \quad (1)$$

where EF_x is the overall weighted emission factor of pollutant x (g $kW^{-1}hr^{-1}$), m_i is emission factor for the i^{th} mode (g hr^{-1}), WF_i is the i^{th} mode weighting factor, and p_i is the engine load for the i^{th} mode.

4.4. Results

Measurements were made for modes 1 through 5 and then repeated twice following the same protocol for each fuel so that triplicate results were obtained for each mode. EFs are reported as grams per kilowatt-hour (g $kW^{-1}hr^{-1}$) based on the concentration of measured species, recorded engine load and calculated exhaust flow rate. The exhaust flow rate for the engine was calculated using the carbon balance method specified in ISO 8178-2. This method assumes complete conversion of fuel carbon to carbon dioxide on combustion.

4.4.1. Gaseous Emissions

The modal and overall weighted EFs of NO_x, CO and CO_2 for both fuels are summarized in Table 4-3. The overall weighted EF_{NOx} was 7.9 g $kW^{-1}hr^{-1}$ and 7.1 g $kW^{-1}hr^{-1}$ for ULSD and A50 respectively. The EF_{NOx} values are approximately 28% (ULSD) and 35% (A50) lower

than the IMO MARPOL Annex VI Tier 1 NO_x limits (10.9 g $kW^{-1}hr^{-1}$). Maximum NO_x reductions (~13%) were observed at the 50% and 25% engine loads. An overall EF_{NOx} reduction of 10% was observed upon switching from ULSD to A50. The EF_{CO} were low for both fuels with an overall reduction of 18% observed for A50 compared to ULSD fuel. Modal EF_{CO2} (760-1396 g $kW^{-1}hr^{-1}$) across all load points was typical of medium speed diesel engines. At the lower loads, diesel engines are fuel inefficient; therefore, high EF_{CO2} were observed at the 25% and 10% engine loads. The greatest reductions in EF_{CO2} were observed at the 50% load (9% reduction) and 25% load (10% reduction) similar to EF_{NOx} and EF_{CO}. An overall 5% reduction in weighted EF_{CO2} was observed for A50 versus the ULSD. Per ISO 8178-1,[34] sulfur dioxide (SO_2) concentrations were calculated based on sulfur content in the fuel with ULSD (0.007 g $kW^{-1}hr^{-1}$) and A50 (0.003 g $kW^{-1}hr^{-1}$) having nearly zero SO_2 emissions.

Table 4-3: Modal and overall weighted EFs of gaseous emissions for ULSD and A50 fuels. Percent reduction in emissions upon switching from ULSD to A50

Test Mode			ULSD			BLEND (A50)			% Reduction		
ISO	ULSD	A50	NO_x	CO	CO_2	NO_x	CO	CO_2	NO_x	CO	CO_2
			g/kW-hr			g/kW-hr					
100	92	92	7.1	1.15	838	6.3	1.01	831	11%	12%	1%
75	82	80	7.2	1.15	790	6.7	0.98	784	8%	15%	1%
50	60	61	8.0	1.34	834	6.9	0.99	760	13%	26%	9%
25	26	28	9.4	2.07	1046	8.2	1.74	944	13%	16%	10%
10	17	15	10.5	3.89	1387	10.5	3.83	1396	1%	2%	-1%
Overall Weighted EFs			**7.9**	**1.44**	**866**	**7.1**	**1.19**	**822**	**10%**	**18%**	**5%**

4.4.2. Particulate Emissions

The modal and overall EFs of $PM_{2.5}$, EC and OC are provided in Figure 4-1. Significant reductions (up to 35%) in $PM_{2.5}$ were observed at 50% and below engine load on consuming

A50 versus ULSD. At higher engine loads (75% and 100%), $PM_{2.5}$ was only reduced by 6% and 7%, respectively. The overall weighted $EF_{PM2.5}$ reduction is 25%. $PM_{2.5}$ emissions were dominated by OC for both fuels. As load decreased, the fraction of EC in total $PM_{2.5}$ decreased from 23% to 6% while the fraction of OC increased (77% to 94%) for ULSD. Similarly, when the engine burned A50, the EC fraction decreased from 18% to 7% and the OC fraction increased from 82% to 93% of total $PM_{2.5}$ as the load was decreased. Overall, only minor changes were observed in EC and OC relative concentrations when switching from ULSD (weighted average of 16% EC and 84% OC) to A50 (weighted average of 14% EC and 86% OC). Substantial reductions (30%-34%) in EF_{EC} were observed across all loads except at 10% engine load where EF_{EC} was only reduced by 6%. Conversely, 25%-28% reduction in EF_{OC} was found at lower loads (50% and below) while only slight changes in EF_{OC} was obtained at 100% (-2%) and 75% (4%) engine load. Overall a reduction of 30% and 20% in weighted EF_{EC} and EF_{OC}, respectively, was obtained on consuming A50 fuel.

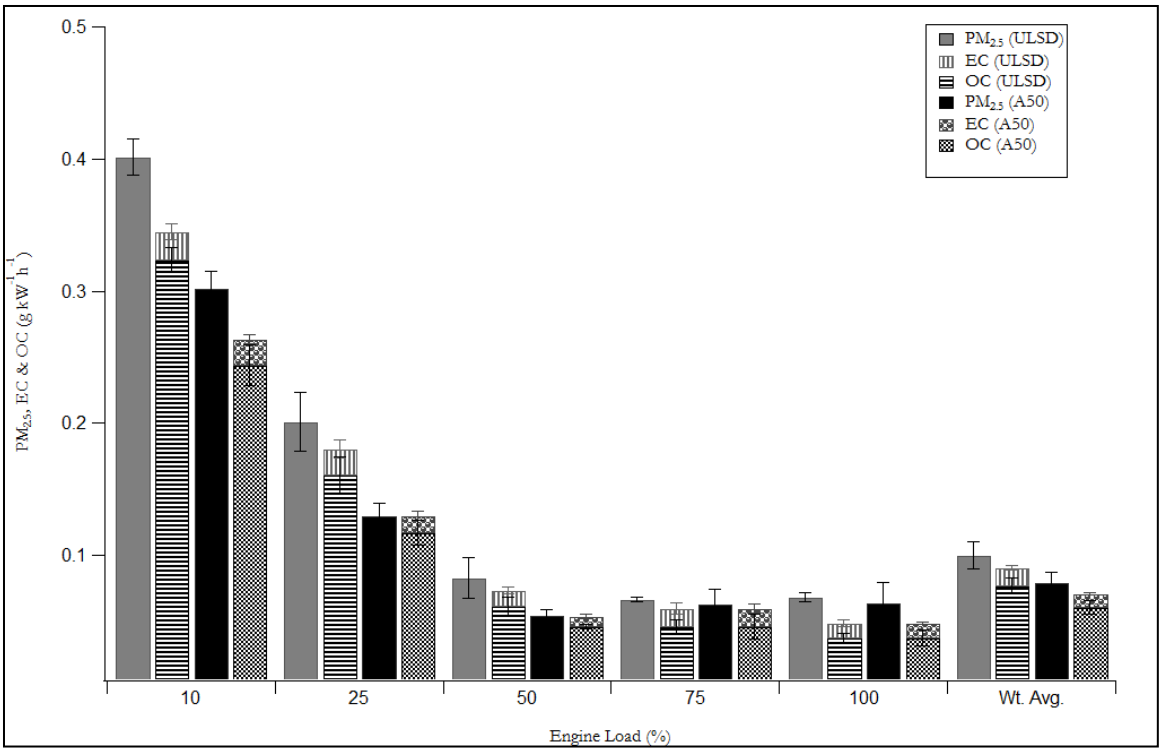

Figure 4-1: Modal and overall weighted EFs of $PM_{2.5}$, EC and OC for both fuels

An important quality check for this study was a check of whether total $PM_{2.5}$ mass was conserved. Specifically, the total mass collected on the teflo filter was compared with the sum of the EC and OC masses. When the OC was multiplied by a factor[30] of 1.2 to account for hydrogen and oxygen in the OC, a regression slope of 1.02 (R^2 = 0.99) and 1.05 (R^2 = 0.99) was found for total mass on quartz with respect to total $PM_{2.5}$ on teflo filter for ULSD and A50 fuel, respectively (Figure 4-2).

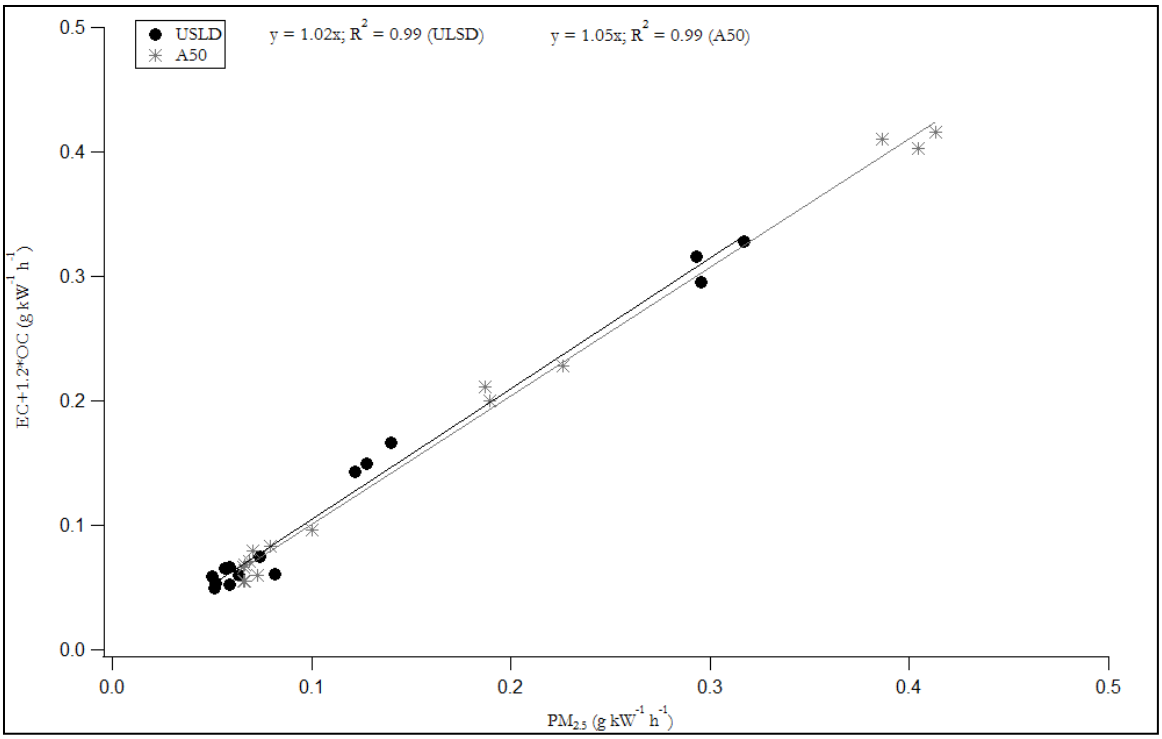

Figure 4-2: Comparison of total mass on quartz and Teflo filter for ULSD and A50 fuels

4.5. Discussion

With the exception of CO_2 at 10% engine load and OC at 100% engine load, all pollutants showed some reduction (1-35%) for the A50 relative to the USLD fuel. However, based on a two-tailed, paired t-test, reductions in $EF_{PM2.5}$ and EF_{OC} at modes of 75% and 100% were not statistically significant. Similarly, at 10% engine load, reductions for gaseous pollutants and EC were not statistically significant. For all other engine loads and for overall weighted engine load, the two-tailed, paired t-test suggests that the mean differences are statistically significant at a greater than 95% confidence level. The ISO 8178-4 D2 test cycle, which was developed based upon normal in-use engine operation, indicates that 85% of the time the

engine operation is in the range of 25% to 75% of the maximum engine load. Therefore, it is reasonable to expect that the overall weighted EFs and percent reduction of gaseous and particulate emissions for ULSD and A50 fuels are applicable to diesel generator engines, which operate primarily in this engine load region.

In diesel engines, more than 99% of the fuel carbon is converted into CO_2. Therefore, a reduction in CO_2 emissions on burning A50 should be similar to the reduction in fuel consumption (FC) on burning A50. Approximately 8% and 9% fuel savings were observed at 50% and 25% engine loads (Figure 4-3). Clearly, the major fuel benefits occur at intermediate load points (Figure 4-3) where the engine spends a significant amount of time during normal operation conditions. A 4.5% reduction in overall weighted fuel consumption was found. A slightly better fuel economy on consuming A50 can be partially explained by the higher calorific value of A50 (Table 4-1). The higher Cetane Index, which correlates with a higher Cetane Number, of the A50 is likely another factor contributing to a higher fuel economy for the A50.

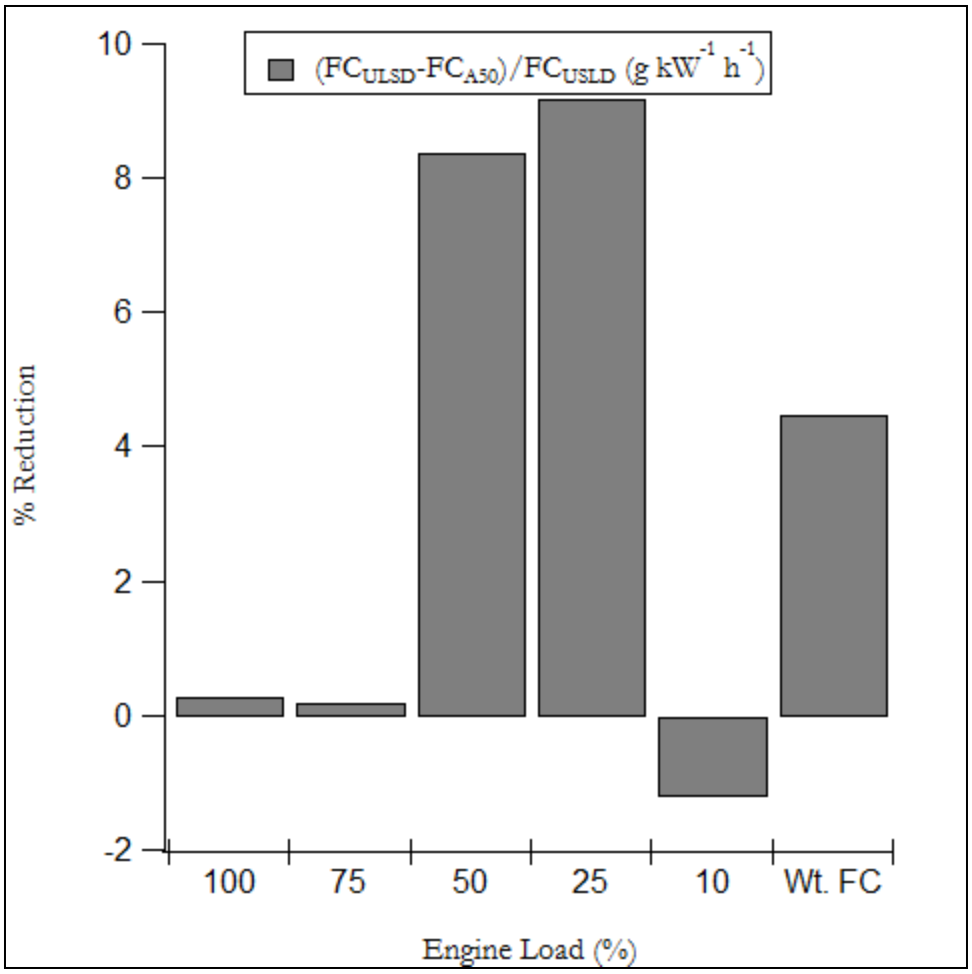

Figure 4-3: Reduction in fuel consumption (FC) by A50

Trade-off in emission benefits between NO_x and PM from diesel engines has always presented a challenge to engineers trying to reduce both simultaneously. Most studies[18-28] on biodiesel fuels focus on engine/chassis dynamometer tests of on-road engines operating predominantly on transient cycles. These studies show an increase in NO_x (-5.9% to 6.6% for B20 and 2%-17% for A50) emissions and large reductions in CO (3-30% for B20 and 18-40% for A50) and PM (4-37% for B20 and 4-63% for A50) mass emissions. Research on

biodiesel effects on marine diesel engines is limited. Recent et al.[29] found reduction in NO_x up to ~24% and ~3% increase in CO_2 emissions from small marine craft diesel engines (21.3 and 38 kW) on consuming B100 (recycled cooking fat and vegetable oil). In a more comparable study[1] with maximum engine power of 500 hp on a ferry consuming a B50 blend of soy-based biodiesel and ULSD, Jayaram et al., noted 7% and 25% reductions in CO and $PM_{2.5,}$ respectively, with no significant change in NO_x emissions. Another recent study[30] on a one cylinder 400 kW marine diesel engine also found NO_x as well as PM emissions to be similar for low-sulfur fossil fuels and biogenic fuels.

The only study to evaluate the impact of algae derived fuel was carried out by Fisher et al.[31] on an engine dynamometer. They compared gaseous and particulate emissions from a 39 kW off-road diesel engine consuming different fuels and blends including B20 and B100 algae biodiesel for two different engine loads (50% and 75%). Both algae blends reduced EF_{NOx} by up to 10%; however, higher PM emissions were observed for B100 algae-biodiesel relative to ULSD at 75% engine load. Moreover, the OC fraction of the PM for B100 was higher than ULSD at the operating conditions studied by Fisher et al. In contrast to fuel saving with algae renewable diesel observed in the current study, Fisher et al. found a fuel penalty of 10-12% for B100 with respect to ULSD due to the ~13% lower heating value of the algae derived biodiesels used in their study compared with ULSD. All of the foregoing studies, including the algae biodiesel studied by Fisher et al., involved fatty acid methyl ester biodiesels. Hydrotreated biodiesels have properties closer to petroleum diesels and Fischer-Tropsch diesels.

There have been a few studies in which vegetable oil was converted to paraffins by a refinery-based hydrotreatment process. In a study conducted by Kuronen et al.[40], emission profiles on consuming 100% hydrotreated vegetable oil (HVO) was compared with standard European diesel fuel (EN 590:2004) on two city buses. Cetane number and density of HVO was 82.9 and 779 kg/m^3 in comparison to 55.5 and 839 kg/m^3 for EN590 diesel fuel. Depending upon the vehicle, aftertreatment technique and test cycle, significant reduction in emissions (PM: 28% to 46%; NO_x: 7% to 14%; CO: 5% to 78%) was observed. In other studies[41, 42], usage of 100% HVO resulted in approximately 10-18% reduction in NOx and ~28% reduction in PM.

In the current study, the A50 used had a higher cetane index (CI) of 65 compared with ULSD (CI of 51). Previous studies[32,33] have shown trends of decreasing NO_x emissions with increasing cetane index for both diesel and biodiesel fuels. Density is another fuel property that has been shown to impact NO_x emissions. Higher densities have been correlated with higher NO_x emissions for both diesel and biodiesel fuels. Therefore, the lower density of A50 (804 kg m^{-3}) with respect to ULSD (829 kg m^{-3}) coupled with the higher CI likely contributed to the ~10% reduction in EF_{NOx} for the engine studied.

The analysis of the fuels did not include measurement of the aromatic content, but the hydrogen Content of the fuels was measured. Since there is no reason to expect any significant concentration of oxygen or nitrogen in the fuels it is assumed that both fuels are only hydrocarbons. Based on the hydrogen content of the fuels (13.6% for the ULSD and 14.4% for the A50) the carbon content is 86.4% ULSD and 85.9% for the A50. Thus C/H = 0.53 for ULSD and = 0.51 for A50. A Coordinating Research Council study[47] which

evaluates chemical and physical properties of fuels, suggests that these fuels would be composed primarily of normal, iso-paraffins and cyclo-paraffins.

An overall reduction of ~18% and ~25% in CO and $PM_{2.5}$, respectively, can be explained by the difference in CI and aromatic content of both fuels tested. Higher CI promotes shorter ignition delays, providing more time for the fuel consumption process to be completed and hence reducing the formation of CO and PM. Aromatic content in the fuel contributes to incomplete fuel oxidation in the locally fuel rich zones which leads to the formation of CO and PM. Although aromatic content was not directly measured, the cetane index, density and carbon/hydrogen ratio are indicative of a relatively low aromatic content. Moreover, the neat algae fuel was additive free besides the addition of Lubrizol 539D for lubricity which was also added to ULSD fuel. The 100% algae biofuel had a measured cetane number of >74.7 and a density of 775.8 kg/m^3 at 15°C, which is consistent with a fuel with a very low or 0% aromatic concentration.[48] Therefore, A50 had lower aromatic content than the ULSD fuel. These factors lead one to expect lower CO and $PM_{2.5}$ emissions from A50 relative to ULSD for the engine under test.

This study has demonstrated that algae biofuel derived through the hydrotreated process has the potential to substantially reduce criteria pollutants without modifying the engine or infrastructure in the vessel. However, a life cycle assessment (LCA) of algae fuel production (cultivation, harvesting, lipid extraction, conversion to renewable diesel, byproduct management) is necessary for sustainable full-scale production and assessing environmental impacts. In a recent field-to-wheels LCA analysis performed by Life Cycle Associates, LLC, using the Argonne National Laboratories GREET model, concluded that the Solazyme's

Soladiesel algae biofuels (hydrotreated fuel) produced 85-93% lower greenhouse gas emissions than standard petroleum based ULSD.[35] Such results are encouraging for the nascent algae industry, but obtaining a high productivity yield while reducing the capital and operating costs remains a challenge for commercializing algal oil.

4.6. Acknowledgements

The authors express their gratitude to the U. S. DOT / Maritime Administration for their financial support, the Great Lakes Maritime Academy for volunteering their vessel to carry out this project successfully, and to all personnel who assisted in making the necessary modifications. Appreciation is extended to all the crew members and administrative staff of the ship for their support and cooperative efforts during the emission testing. We especially thank Ms. Jen Murphey of Great Lakes Maritime Academy for taking care of the receipt and return of all our emission measurement equipment. The authors are grateful to Mr. Kurt Bumiller for his help with the test preparations, Ms. Kathalena Cocker and Mr. Jesus Sahagun for their help and support in the Analytical Lab.

4.7. Literature Cited

1. Jayaram, V.; Agrawal, H.; Welch, W.A.; Miller, J.W.; Cocker, D.R. Real-time gaseous, PM and Ultrafine Particle Emissions from a Modern Marine Engine Operating on Biodiesel. Enivron. Science and Technology. 2011, 45, 2286-2292.

2. Corbett, J. J.; Winebrake, J. J.; Green, E. H.; Kasibhatla, P.; Eyring, V.; Lauer, A. Mortality from ship emissions: A global assessment. Environ. Sci. Technol. 2007, 41 (24), 8512–8518.
3. Deniz, C.; Durmusoglu, Y. Estimating shipping emissions in the region of the Sea of Marmara, Turkey. Sci. Total Environ. 2008, 390 (1), 255–261.
4. Lucialli, P.; Ugolini, P.; Pollini, E. Harbour of Ravenna: The contribution of harbour traffic to air quality. Atmos. Environ. 2007, 41 (30), 6421–6431.
5. Saxe, H.; Larsen, T. Air pollution from ships in three Danish ports. Atmos. Environ. 2004, 38 (24), 4057–4067.
6. Schrooten, L.; De Vlleger, I.; Panis, L. I.; Styns, K.; Torfs, R. Inventory and forecasting of maritime emissions in the Belgian sea territory, an activity-based emission model. Atmos. Environ. 2008, 42 (4), 667–676.
7. Vutukuru, S.; Dabdub, D. Modeling the effects of ship emissions on coastal air quality: A case study of southern California. Atmos. Environ. 2008, 42 (16), 3751–3764.
8. Corbett, J. J.; Fischbeck, P. S. Emissions from Waterborne Commerce Vessels in United States Continental and Inland Waterways. Environ. Sci. Technol. 2000, 34 (15), 3254–3260.
9. Joellen Lewtas. Air pollution combustion emissions: Characterization of causative agents and mechanisms associated with cancer, reproductive and cardiovascular effects. Mutation Research 636 (2007) 95-133.
10. The Energy Independence and Security Act of 2007, PL 110-140; U.S. Government Printing Office: Washington, DC.

11. Pienkos, P.T. and Darzins, A., The promise and challenges of microalgal-derived biofuels. Biofuels, Bioprod. Bioref. 3:431-400 (2009).
12. United States Navy. The Department of the Navy's Energy Goals. http://www.navy.mil/features/Navy_EnergySecurity.pdf
13. Office of Naval Research. Future Naval Fuels Program. http://www.onr.navy.mil/Science-Technology/Departments/Code-33/All-Programs/332-naval-materials/Future-Naval-Fuels.aspx.
14. International Maritime Organization, Annex VI of MARPOL 73/78 "Regulations for the Prevention of Air Pollution from Ships and NOx Technical Code"
15. ISO. ISO 8178-2, Reciprocating Internal Combustion Engines: Exhaust Emission Measurement. Part-2: Measurement of Gaseous Particulate Exhaust Emissions at Site; International Organization for Standardization, 1996.
16. United States Environmental Protection Agency (USEPA). Protection of the Environment. Title 40. Sections 86 and 89. U.S. Code of Federal Regulations.
17. NIOSH. NIOSH Manual of Analytical Methods; National Institute of Occupational Safety and Health: Cincinnati, OH, 1996.
18. McCormick, R.L.; Tennant, C.J.; Hayes, R.R., Regulated Emissions from Biodiesel Tested in Heavy-Duty Engines Meeting 2004 Emission Standards. Society of Automotive Engineers 2005, SAE 2005-01-2200.
19. Sze, C.; Whinihan, J.K.; Olson, B.A.; Schenk, C.R., Impact of Test Cycle and Biodiesel Concentration on Emissions. Society of Automotive Engineers 2007, SAE 2007-01-4040.

20. McCormick, R.L.; Williams, A.; Ireland, J., Effects of Biodiesel Blends on Vehicle Emissions. National Renewable Energy Laboratory 2006, NREL/MP-540-40554.
21. U.S. Environmental Protection Agency, A comprehensive Analysis of Biodiesel Impacts on Exhaust Emissions. Draft Technical Report 2002, EPA420-P-02-001.
22. Sharp, C.A.; Howell, S.A.; Jobe, J., The effect of Biodiesel Fuels on Transient Emissions from Modern Diesel Engines, Part I Regulated Emissions and Performance. Society of Automotive Engineers 2000, SAE 2000-01-1967.
23. Graboski, M.S.; Ross, J.D.; McCormick, R.L., Transient Emissions from No. 2 Diesel and Biodiesel Blends in a DDC Series 60 Engine. Society of Automotive Engineers 1996, SAE 961166.
24. Schumacher, L.G.; Borgelt, S.C., Fosseen, D., Heavy-duty engine exhaust emission tests using methyl ester soybean oil/diesel fuel blends. Bioresour. Technology. 1996, 57(1), 31-36.
25. Alam, M.; Song, J.; Acharya, R., Combustion and Emissions Performance of Low Sulfur, Ultra Sulfur and Biodiesel Blends in a DI Diesel Engine. Society of Automotive Engineers 2004, SAE 2004-01-3024.
26. Cheng, A.S.; Buchholz, B.A.; Dibble, R.W., Isotopic Tracing of Fuel Carbon in the Emissions of a Compression-Ignition Engine Fueled with Biodiesel Blends. Society of Automotive Engineers 2003, SAE 2003-01-2282.
27. Durbin, T.D.; Cocker, D.R.; Sawant, A.A., Regulated Emissions from Biodiesel Fuels from on/off-road Applications. Atmospheric Environment. 2007, 41 (27), 5647-5658.

28. Eckerle, W.A.; Lyford-Pike, E.J.; Stanton, D.W., Effects of Methyl Ester Biodiesel Blends on NOx Emissions. Society of Automotive Engineers 2008-01-0078.
29. Roskilly A. P.; Nanda, S.K.; Wang, Y.D., The Performance and the Gaseous Emissions of Two Small Marine Craft Diesel Engines Fuelled with Biodiesel. Appl. Therm. Eng. 2008, 28 (8-9), 872-880.
30. Petzold, A.; Lauer, P.; Fritsche, U., Operation of Marine Diesel Engines on Biogenic Fuels: Modification of Emissions and Resulting Climate Effects. Environmental Science and Technology, 2011.
31. Fisher, B.C.; Marchese, A.J.; Volckens, J.; Measurement of Gaseous and Particulate Emissions from Algae-Based Fatty Acid Methyl Esters. SAE 2010-01-1523.
32. McCormick, R.L.; Graboski, M.S.; Alleman, T.L., Impact of Biodiesel Source Material and Chemical Structure on Emissions of Criteria Pollutants from a Heavy-Duty Engine. Environmental Science and Technology, 2001, 35, 1742-1747.
33. Graboski, M.S.; McCormick, R.L., Combustion of Fat and Vegetable Oil Derived Fuels in Diesel Engines. Progress in Energy and Combustion Science 1998, 24, 125-164.
34. International Organization for Standardization (ISO). 8178-1, 1st edition; International Organization for Standardization, 1996.
35. http://www.greencarcongress.com/2009/04/soladiesel-lca-20090422.html
36. Agrawal, H., Malloy, Q.G.J., Welch, W.A., In-use Gaseous and Particulate Matter Emissions from a Modern Ocean Going Container Vessel. Atmospheric Environment 42 (2008) 5504-5510.
37. Chisti, Y. Biodiesel from microalgae. Biotechnol. Adv. 2007, 25, 294-306.

38. Chisti, Y. Biodiesel from microalgae beats bioethanol. Trends Biotechnol. 2008, 26 (3), 126-131.
39. United States Maritime Administration (MARAD). Alternative fuel for Marine Application. http://www.marad.dot.gov/documents/MARAD_ALT_FUEL_FINAL_REPORT_%28REVISED_3-22-12%29.pdf
40. Kuronen, M., Mikkonen, S., Aakko, P., Murtonen, T., Hydrotreated vegetable oil as fuel for heavy duty diesel engines. SAE 2007. 2007-01-4031.
41. Rothe, D., Lorenz, J., New BTL Diesel Reduces Effectively Emissions of a Modern Heavy-Duty Engine" 5th International Colloquium Fuels, Technische Akademie Esslingen (TSE), January 12-13, 2005.
42. Kleinschek, G., Emission Tests with Synthetic Diesel Fuels (GTL &BTL) with Modern Euro 4 (EGR) Engine. 5th International Colloquium Fuels, Technische Akademie Esslingen (TSE), January 12-13, 2005.
43. National Algal Fuel Technology Roadmap. U.S. Department of Energy, May 2010.
44. Solazyme. www.solazyme.com/technology.
45. The Buzz, Solarzyme Completes Delivery to Navy, and Re-Ups, Al.gae Industry Magazine.com, September 16, 2010
46. Kalnes, T. N., Marker, T., Shonnard, D. R., and Koers, K. P. Green diesel production by hydrorefining renewable feedstocks. http://www.uop.com/wp-content/uploads/2011/01/UOP-Hydrorefining-Green-Diesel-Tech-Paper.pdf.
47. Chemical and Physical Properties of the Fuels for Advanced Combustion Engines, CRC Report No. FACE-1, July 2010

48. Alternative Fuel for Marine Application, Final Report, prepared for Naval Fuels and Lubes CFT by U. S. Maritime Administration (MARAD) 29 February 2012.
49. International Organization for Standardization (ISO). ISO 8178-4, Reciprocating internal combustion engine-Exhaust emission measurement-Part 4: Test cycles for different engine applications, 1996.

Chapter Five: Benefits of two mitigation strategies for container vessels: Cleaner engines and cleaner fuels

5.1. Abstract

Emissions from ocean going vessels (OGVs) are a significant health concern for people near port communities. This paper reports the emission benefits for two mitigation strategies, cleaner engines and cleaner fuels, for a 2010 container vessel. In-use emissions were measured following International Organization for Standardization (ISO) protocols. The overall in-use nitrogen oxide (NO_x) emission factor was 16.1±0.1 $gkW^{-1}h^{-1}$, lower than the Tier 1 certification (17 $gkW^{-1}h^{-1}$) and significantly lower than the benchmark value of 18.7 $gkW^{-1}h^{-1}$ commonly used for estimating emission inventories. The in-use particulate matter ($PM_{2.5}$) emission was 1.42±0.04 $gkW^{-1}h^{-1}$ for heavy fuel oil (HFO) containing 2.51 wt % sulfur. Unimodal (~30 nm) and bi-modal (~35 nm; ~75 nm) particle number size distributions (NSDs) were observed when the vessel operated on marine gas oil (MGO) and HFO, respectively. First-time emission measurements during fuel switching (required 24 nautical miles from coastline) showed that concentrations of sulfur dioxide (SO_2) and particle NSD took ~55 minutes to reach steady-state when switching from MGO to HFO and ~84 minutes in the opposite direction. Therefore, if OGVs commence fuel change at the regulated boundary, then vessels can travel up to 90% of the distance to the port before steady state values are re-established. The transient behavior follows a classic, non-linear

mixing function driven by the amount of fuel in day tank and the fuel consumption rate. Hence, to achieve the maximum benefits from a fuel change regulation, fuel switch boundary should be further increased to provide the intended benefits for the people living near the ports.

5.2. Introduction

Globalization and continuous growth in international trade has led to larger and more powerful engines on OGVs. The diesel engines on the OGVs are relatively high emitters of $PM_{2.5}$, NO_x, sulfur oxides (SO_x) and carbon dioxide (CO_2), a consequence of the combination of using heavy fuel oil and little emission regulations. Increasing ship emissions affect global climate[1-3] and regional air quality near port communities,[4,5] suggesting that mitigation strategies and controls are needed to reduce the impact of OGV emissions and shipping related PM mortalities.[6] Two mitigation strategies were investigated in this research; use of a cleaner burning modern diesel engine and the switch to cleaner, lower sulfur fuels near coastal communities.

The current emission standards do not include limits on PM mass emissions; however, it is well established that reducing fuel sulfur content is effective in lowering SO_x and PM mass emissions from combustion sources. The approach is based on the fact that SO_2 is formed during the fast reaction of fuel-sulfur with oxygen in the combustion process, and subsequently, particles form during the slower oxidation of sulfur dioxide and its hydration to sulfuric acid (Eqn. 1).

$$S + O_2 \xrightarrow{\text{(Fast)}} SO_2 \xrightarrow{1/2O_2\ \text{(Slow)}} SO_3 \xrightarrow{H_2O} \text{Sulfuric acid} \quad (1)$$

Research shows that the sulfur content for heavy fuel oil is the primary factor contributing to PM mass emissions.[28,29]

Recent shipping regulations have tightened the emission limits for NO_x, SO_x and fuel quality in global and designated emission control areas (ECAs). The IMO set progressive reductions in NO_x emissions and fuel sulfur content. From 2010 to 2015, fuel used by all vessels operating in ECAs cannot exceed 10,000 ppm sulfur. After 2015, fuel used in ECAs may not exceed 1,000 ppm sulfur. In contrast, the sulfur content of fuel used in on-road vehicles is <15 ppm. The reduction in PM mass emissions is expected to reduce annual premature ship-related mortality by 50% in ECAs.[7] In addition to the fuel change, the California Air Resources Board (CARB) currently requires that OGV main and auxiliary engines burn fuel with sulfur content equal to or less than 1.5 wt % within 24 nautical miles (nmi) of the California coastline.[8]

Particle emissions have been previously characterized from slow-speed marine engines using test rigs as well as stack and plume studies during ship transit. Kasper et al.[9] reports a mean diameter of particles of 20-40 nm for a two-stroke marine diesel engine operating on a test rig and burning a HFO with 0.6 wt % sulfur. Petzold et al.[10] reported physical properties, chemical composition, and cloud forming potential of particulate emissions from a 4-stroke, medium-speed, marine diesel engine operating on a test rig for load conditions from 10% to 110% with HFO containing 2.21 wt % sulfur. Moldanová[11] reported microphysical and chemical properties of the exhaust for various load conditions of a 2-stroke diesel engine and observed bi-modal particle mass size distribution with peaks at 0.5 μm and 7 μm. Fridell et

al.[12] used a cascade impactor to study the size distribution of particles from the exhaust of three transiting ships. Lyyranen et al.[13,14] studied particle NSDs from 4-stroke medium speed engines operating on HFO with 2.4 wt % sulfur. Murphy et al.[15] measured criteria emissions, cloud condensation nuclei (CCN) concentrations and estimated the particle number emission factors from simultaneous on-board (3.01 wt % sulfur) and aircraft measurements.

The contribution of ship emissions to local inventories require emission factors (EFs) with most researchers using data either compiled by IVL Swedish Environmental Research Institute (IVL) for ENTEC UK[26] or Lloyd's register (LR).[31] In each study, only 3 container vessels were tested to represent thousands of container vessels that sail around the globe. A similar number of measurements were made from variety of vessels (tankers, ferries, tugboat, etc.). In total, the IVL EFs, which are widely used, are based on eight measurements from slow speed diesel (SSD) engines and LR EFs are from 11 SSD engines. For practical inventory development, these EFs are applied to SSD engines irrespective of vessel type; they only depend on the type of engine, fuel and operating mode. Hence the EFs from this study are especially important as they represent the first in-use measurements from a modern container vessel using the latest Tier I engine technology.

Under the current certification scheme, engines are allowed to be certified while operating on distillate fuel (nitrogen free) both on test-bed and in-use even though the OGVs operate on HFO in international boundaries. The fuel bound nitrogen can account up to 10% of NO_x emissions which can effectively biases the certified NO_x emission to a lower value. In this study, data were collected at sea near the prescribed OGV certification load points and during fuel switching between MGO and HFO fuel. This research provides the first

comparison of Tier I certification values with in-use data obtained from a modern container vessel (launched in 2010) at sea. Additional information is provided on the transition in emissions, particle size and particle number during fuel switch. A non-linear equation representing the fuel mixing process is verified as an approach to estimate the time required to switch fuels.

5.3. Experimental Methods

5.3.1. Vessel and Engine Description

A 2010 post-Panamax container vessel was tested as it is representative of the large container vessels and slow-speed, diesel engines that being built today. The main propulsion engine (Hyundai B&W 11K98ME7) for the vessel was an electronically controlled, slow speed two-stroke, 68,530kW diesel engine rated at 97 rpm with a displacement of 22,060 liters. The engine was equipped with the latest technology to meet IMO Tier I emission specifications for vessel construction between 2000 and 2010. The engine was designed with low-NO_x slide valves, an electronic fuel injection system and improvements in the in-cylinder combustion for lowering NO_x emissions and improving fuel economy.

5.3.2. Fuel Properties

Emissions were evaluated for two fuel types: MGO and HFO. In compliance with California regulations, MGO with 0.17 wt % sulfur was used in the main engine within 24 nmi of the California coastline. Outside 24 nmi, the engine operated on HFO with 2.51 wt % sulfur. One liter fuel samples were drawn from the main engine final filter drains, immediately upstream of the injector rail, for analysis of fuel properties (Table 5-1).

Table 5-1: Selected fuel properties

		Certificate of Analysis (CoA)		UCR Samples	
Fuel	Units	HFO	MGO	HFO	MGO
Density @15C	kg/m^3	988.8	845.5	-	-
Viscosity @40C	mm^2/s	368.6	3.3	-	-
Sulfur	% m/m	2.40	0.17	2.51	0.17
Ash	% m/m	0.07	<0.01	-	-
Vanadium	mg/kg	262	<1	-	-
Density @15.5C	kg/m^3	-	-	988.2	845.2

5.3.3. Test Cycles

HFO emissions at 90%, 75%, 47% and 24% of full load were evaluated. Efforts were made to achieve loads similar to those specified in the ISO 8178-E3 test cycle (Table 5-2) to compare measured in-use emissions with the engine certification values; however, the actual loads at sea only approximate those in the E3 test cycle due to perturbations in loads caused by the interactions of the vessel and sea. Data for the engine load (kW), engine speed (rpm), and fuel consumption (kg/hr) were downloaded from the engine computer. A check of the accuracy of the gauge readings was carried out by calculating the engine efficiency using the reported engine load and fuel consumption. At 90% and 75% engine load, efficiencies were 46.9% and 47.5% which is typical of slow speed diesel engines.[35] The calculated efficiencies are typical of slow speed diesel engines. Specific fuel oil consumption (SFOC) is calculated based on fuel consumption and engine load. Measurements were also made at slower speeds, 12% and 23% of full load, while the engine operated on MGO. Additional real-time emission measurements were conducted while the engine followed typical operating conditions (including fuel switching).

Table 5-2: Engine operating conditions

Targeted modes	ISO100	ISO75	ISO50	ISO25	MGO23	MGO12	Fuel Switch	
Fuel	HFO	HFO	HFO	HFO	MGO	MGO	MGO to HFO	HFO to MGO
Load (%)	90	75	47	24	23	12	30	24
Load (kW)	61,944	51,703	31,902	16,707	15,481	8,275	20,559	16,447
Engine Speed (rpm)	97	91	78	61	59	49	67	58
SFOC ($g\,kW^{-1}h^{-1}$)	191	188	200	205	209	232	201	205

5.3.4. Sampling and Analysis

Sampling and analysis of gases and PM conformed to ISO 8178-2 requirements.[16] Briefly, testing was conducted using a partial flow dilution system with a single venturi.[17,18] The dilution tunnel was attached directly to the stack negating the need for a heated transfer line. Dilution ratios (DRs) were obtained from both CO_2 and NO_x measurements of raw and dilute exhaust gas with DRs agreeing within 5% for the two gases. CO, CO_2, NO_x and SO_2 were monitored using the Horiba PG-250 Exhaust Gas Analyzer. SO_2 EFs were calculated from the fuel sulfur content per ISO 8178-1 protocol[19] except for during the fuel switch where a Horiba Analyzer was used to monitor the continuous change in SO_2 exhaust concentration.

$PM_{2.5}$ samples were taken from the dilution tunnel after a 2.5 μm cyclone separator, collected on filter media and the mass were determined gravimetrically on pre-weighed 47-mm diameter 2-μm pore Teflo® filters (Pall Gelman, Ann Arbor, MI). Loaded Teflo® filters were weighed using a Mettler Toledo UMX2 microbalance following the guidelines within the Code of Federal Regulations (CFR).[20] Before and after the collection, the filters were conditioned for 24 h in environmentally controlled room (RH = 40%, T = 25ºC) and weighed daily until two consecutive weight measurements were within 3μg.[17] Teflo® filters

were subsequently extracted with HPLC grade water and isopropyl alcohol and analyzed for sulfate ions using a Dionex DX-120 ion chromatograph. Sulfate on the Teflo® filter PM was assumed to be in hydrated form ($H_2SO_4 \cdot 6H_2O$) as predicted using the aerosol thermodynamic model ISORROPIA.[32-34] Therefore, a factor of 2.15 was applied to the mass of sulfate ions to determine its total contribution to the PM mass. Parallel 2500 QAT-UP Tissuquartz Pall (Ann Arbor, MI) 47 mm filters (preconditioned at 600°C for a minimum of 5 hours) were used to collect $PM_{2.5}$ for subsequent elemental and organic carbon (EC/OC) analysis following the NIOSH[21] method using a Sunset Laboratory (Forest Grove, OR) thermal/optical carbon aerosol analyzer.

The real-time PM mass concentration in the dilution tunnel was monitored with a TSI DustTrak Model 8520 taken directly from the tunnel and without a 2.5 μm cyclone separator. This measurement provided assurance that the PM concentration was steady while the mass was collected on the filters. A secondary dilution tunnel was installed to obtain particle NSD using a TSI scanning mobility particle sizer (SMPS) Model-3080 with 3081 classifier and TSI 3772 condensation particle counters (CPCs).

5.4. Results and Discussion

Triplicate measurements were made consecutively across all loads. EFs are reported as grams per kilowatt-hour ($gkW^{-1}h^{-1}$) based on the concentration of measured species, recorded engine load and calculated exhaust flow rate. The exhaust flow rate for the vessel was calculated assuming complete conversion of fuel carbon to carbon dioxide (carbon balance method).

5.4.1. Modal Emission Factors

Modal EFs are determined at steady-state conditions and are important for OGVs and locomotives as those engines normally operate for long periods of time at steady state conditions or modes. Thus, modal EFs are essential to estimating inventories in a particular area. Modal EF for carbon monoxide (CO), CO_2, NO_x and SO_2 are summarized in Tables 5-3. The modal value for NO_x at 75% engine load is just below Tier I limit (17.0 $gkW^{-1}h^{-1}$) and close to the Tier 2 limit (14.4 $gkW^{-1}h^{-1}$) at 47% load. The modal EF_{CO2} also reflect fuel efficiency at different operating modes. EF_{CO2} is lowest at 75% load (590 $gkW^{-1}h^{-1}$) where OGV spend significant amount of time during transit.

Table 5-3: Modal emission factors ($gkW^{-1}h^{-1}$) of different gases for main engine. ‡Average EFs during the fuel switch

Load (%)	Fuel	CO_2	NO_x	CO	SO_2
12	MGO	749±11	26.4±1.5	0.39±0.002	0.76
23	MGO	672±1	16.8±0.1	1.9±0.09	0.68
24	HFO	644±29	14.9±0.2	1.7±0.71	10.1
47	HFO	626±15	14.4±0.1	1.2±0.07	9.86
75	HFO	590±2	16.9±0.2	0.32±0.02	9.29
90	HFO	600±5	15.2±0.1	0.36±0.004	9.44
30	MGO to HFO	654±30‡	15.8±0.5‡	2.09±0.3‡	n/a
24	HFO to MGO	651±20‡	16.1±0.3‡	1.44±0.4‡	n/a

The modal EFs for $PM_{2.5}$ mass, EC/OC, hydrated sulfate ($H_2SO_4 \cdot 6H_2O$) and ash are summarized in Table 5-4. The $PM_{2.5}$ mass was comprised of 69-82% hydrated sulfate; 10-19% OC; <5% EC; and ash. EC and OC emissions decreased with increasing load (reflecting the engine efficiency tuning at 75% load) while sulfate emissions increased with

increasing load. Fuel sulfur conversion to sulfate increased from 2.4% to 4.2% as the engine load increased from 24% to 90%, consistent with previous studies.[18,23]

Table 5-4: Modal emission factors ($gkW^{-1}h^{-1}$) of $PM_{2.5}$ and speciated $PM_{2.5}$ for main engine

Load (%)	Fuel	$PM_{2.5}$	EC	OC	$H_2SO_4.6H_2O$	Ash
12	MGO	0.28±0.04	0.0023±0.002	0.17±0.003	0.05±0.01	0.02
23	MGO	0.34±0.07	0.0034±0.0003	0.17±0.01	0.08±0.02	0.02
24	HFO	1.19±0.05	0.0087±0.002	0.22±0.006	0.79±0.05	0.14
47	HFO	1.22±0.05	0.0057±0.0004	0.19±0.002	0.90±0.06	0.14
75	HFO	1.44±0.04	0.0043±0.001	0.17±0.001	1.13±0.11	0.13
90	HFO	1.54±0.04	0.0039±0.0002	0.16±0.003	1.28±0.02	0.13

The main propulsion engine was operated at 24% (HFO) and 23% (MGO) allowing for a comparison of the $PM_{2.5}$ mass emissions. Results in Table 4 show the EF for $PM_{2.5}$ mass was reduced by ~70% by switching to MGO with lower sulfur content. This reduction is significant and shows the impact of $PM_{2.5}$ emissions on communities near coastline can be substantially mitigated by switching to a cleaner fuel MGO.[24,25]

5.4.2. Modal Data for Particulate Diameters

The SMPS provided near continuous determination of the particle NSD for different operating modes and different fuels (Figure 5-1a). The exhaust particle NSDs for MGO are monodisperse with a mobility mode diameter at ~30 nm when operating at <25% load. A slight increase in the mobility diameter is observed as load increased. In contrast, the particle NSD data for the HFO shows the aerosol is distinctly bi-modal with first mode at ~35 nm

and second mode between 70 nm and 95 nm. The shift to a larger diameter is consistent with the higher PM mass levels measured on the filters when the engine operated on HFO. Assuming constant particle density, particle volume distributions (Figure 5-1b) indicate a decrease in particulate mass with decreasing engine load.

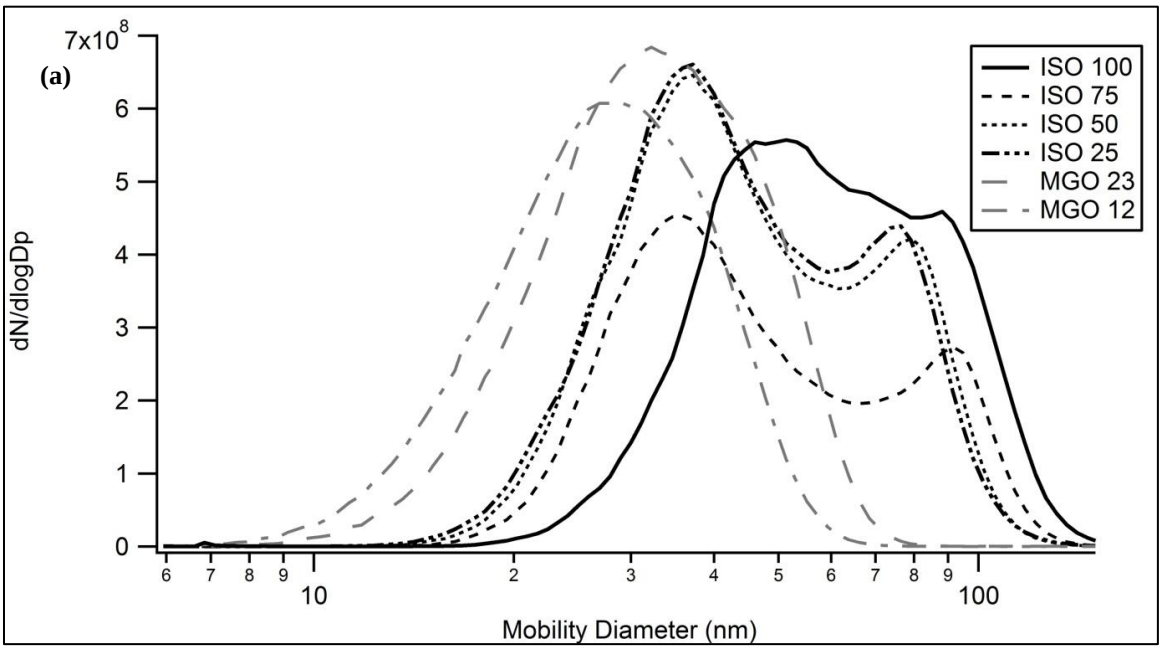

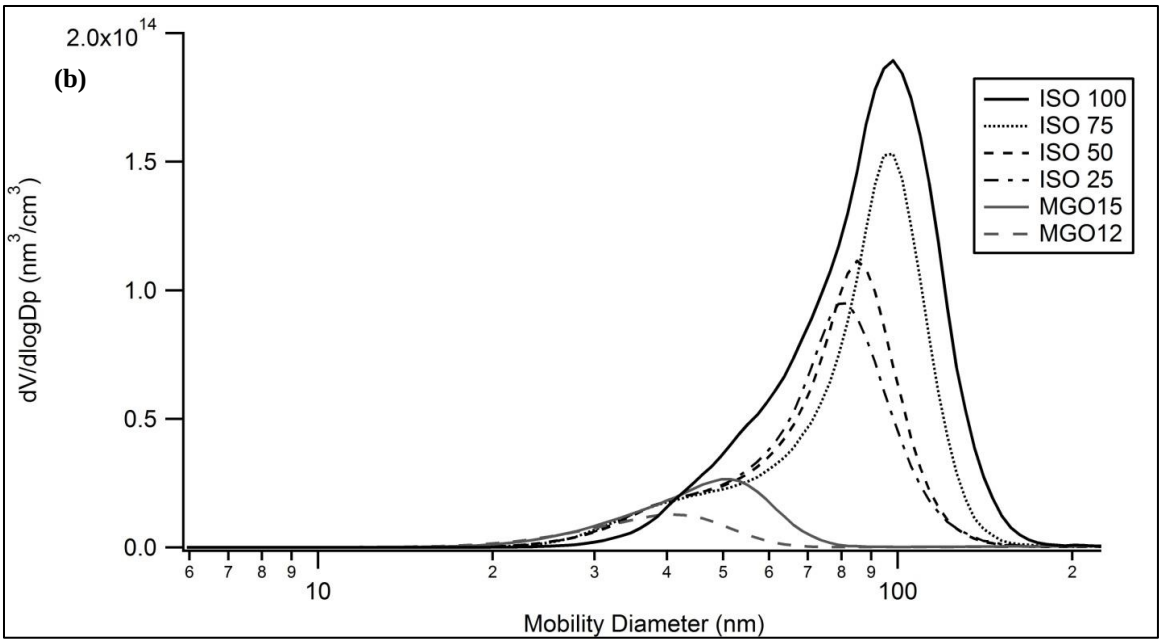

Figure 5-1: Particle number (a) and volume concentrations (b) for all operating modes

5.4.3. Overall Emission Factors

The overall measured EFs were calculated (equation 2) for an engine operating on HFO with the weighting factors established in the ISO-8178 E-3 protocols (Table 5-5). The equation for calculating the overall EF is:

$$WEF = \frac{\sum MEF \times MWF}{\sum Load \times MWF} \quad (2)$$

Where

WEF: Weighted Emission Factor ($gkW^{-1}h^{-1}$)

MEF: Modal Emission Factor (gh^{-1})

MWF: ISO weighting factor for the mode

Load: Engine load for the mode (kW)

Results show the overall EF_{CO2} was 600±2 $gkW^{-1}h^{-1}$ and similar to values reported in other studies.[17,22] As expected, the EF_{CO} of 0.5±0.04 $gkW^{-1}h^{-1}$ was much lower than that measured for CO_2 as most of the carbon (99.9%+) in the fuel was converted to CO_2. Results in Table 5-5 show the overall EF_{NOx} was about 14% lower than the Lloyd's values and 5% lower than the Tier I certification value. EF for $PM_{2.5}$ mass is strongly dependent on the sulfur content of the fuel and therefore hard to compare with previous work. Comparative values for EC[23] indicate the overall EF is lower, suggesting an improved combustion process.

Table 5-5: Comparison of measured overall emission factors with others [a]SO_2 values reported are calculated from sulfur in the fuel

	NO_x	$PM_{2.5}$	SO_2[a]	CO_2
Measured	16.1±0.1	1.42±0.04	9.44	600±2
Agrawal[17]	18.21	1.63	8.39	644
Agrawal[23]	19.77±0.28	2.40±0.05	11.53	617
Llyods service data[26]	18.7	1.23	-	-
US EPA 2009[27]	18.1	1.31	10.29	620
CARB 2008[22]	18.1	1.46	10.50	620

5.4.4. Transient Data

While OGVs generally operate at a fixed load, there are times when the engine operates in a transient mode. For example, transient modes can occur when maneuvering and entering or leaving the harbor. Another transient period is during the fuel switch from HFO to MGO or from MGO to HFO. Transient data are quite scarce, as are the opportunities for taking such measurements. During this research we continuously measured the gaseous and PM concentrations and particle NSD transitions during the fuel switching operations. As the vessel left the harbor, it operated on MGO and then beyond 24 nmi, the vessel switched

from MGO to HFO. Fuel switching takes time as the crew carefully follows a detailed checklist for fuel switching that was prepared in consultation with engine manufacturer. According to engine manufacturers, rapidly changing fuel and/or temperature will move viscosity outside the specified range and harm the fuel delivery system, including pumps and injectors. Therefore, switchover must be carried out slowly in order to avoid scuffing of fuel valves, fuel pump plungers and suction valves.[30]

Figure 5-2a shows the continuous emissions data as the vessel switched fuels. During the switch, vessel load was ~30%, except for two times at ~9:08 and ~9:43 am when small perturbations occurred. As a consequence of the constant load, the gas-phase emissions for NO_x, CO and CO_2 did not change significantly; however, the real-time EF_{SO2} and particle NSD took about ~55 minutes to reach steady state again. Figure 5-2b shows the transient behavior of the particle mode diameter and particle number concentrations during the fuel switch. The results show a new particle mode occurred within a few minutes of the fuel switch from 35 nm to 75 nm; leading to the formation of a bi-modal particle NSD within one hour. The transient particle NSD data are consistent with observations of particle NSD for steady-state mode testing using HFO.

When nearing the coastline the vessel switched from HFO to MGO at about 24% load. With the load constant, the concentrations of NO_x, CO and CO_2 were basically steady; however, the EF_{SO2} and particle NSD decreased over the ~84 minutes needed to achieve steady state (Figure 5-3a). Transient particle NSD and (Figure 5-3b) show the initial bi-modal distribution returns to a single mode, as expected for MGO. Although total particle number decreased gradually along with SO_2, high concentrations of smaller particles were observed

throughout the fuel switch which is an indication of the presence of HFO in the fuel feed even 84 minutes after the fuel switch commenced.

Except for SO_2, the averages of transient EFs (Table 5-3) for fuel switching are calculated. SO_2 concentrations exhibit non-linear change due to continuous changes in the fuel sulfur content. EF_{SO2} ($gkW^{-1}h^{-1}$) changed from 0.7 to 11 during fuel switching from MGO to HFO and 10.1 to 0.7 from HFO to MGO. In both switches, rapid change in EFs was observed (Figure 5-2a, 5-3a) during the early stage of mixing fuels which tends to slow down in the rest of the fuel switch. Because of its non-linear behavior, EF_{SO2} cannot be averaged out for the entire fuel switch and requires continuous monitoring of SO_2 concentration or an equation that can predict change in sulfur content of the mixing fuel (see Figure A-1).

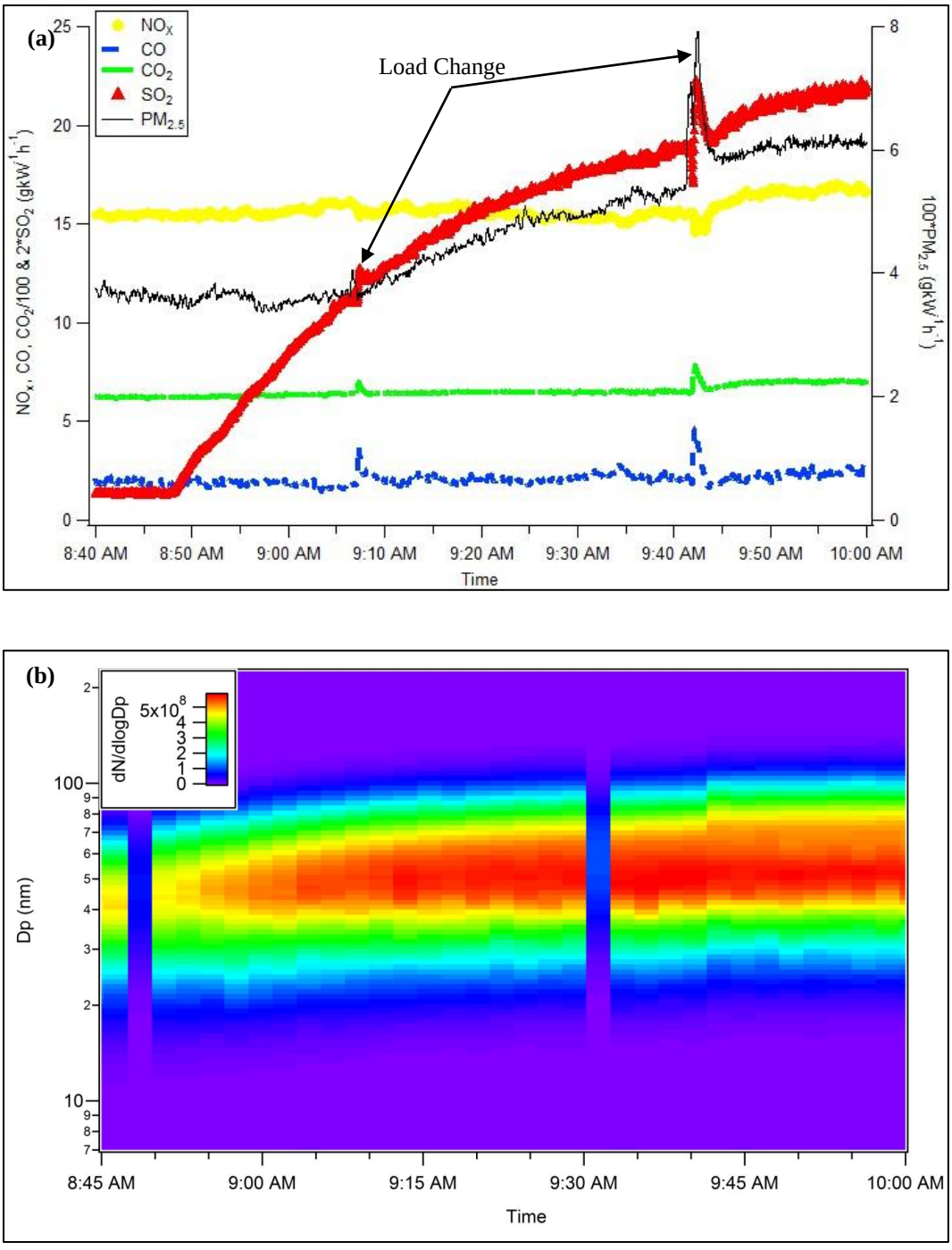

Figure 5-2: Real-time (a) gaseous EFs ($gkW^{-1}h^{-1}$) and (b) particle number concentration measurement when fuel is switched from MGO to HFO at 30% engine load respectively. Change in load was observed at 9:08 and 9:43 am. Note: CPC 3772 data was not available around 8:50 am and 9:30 am

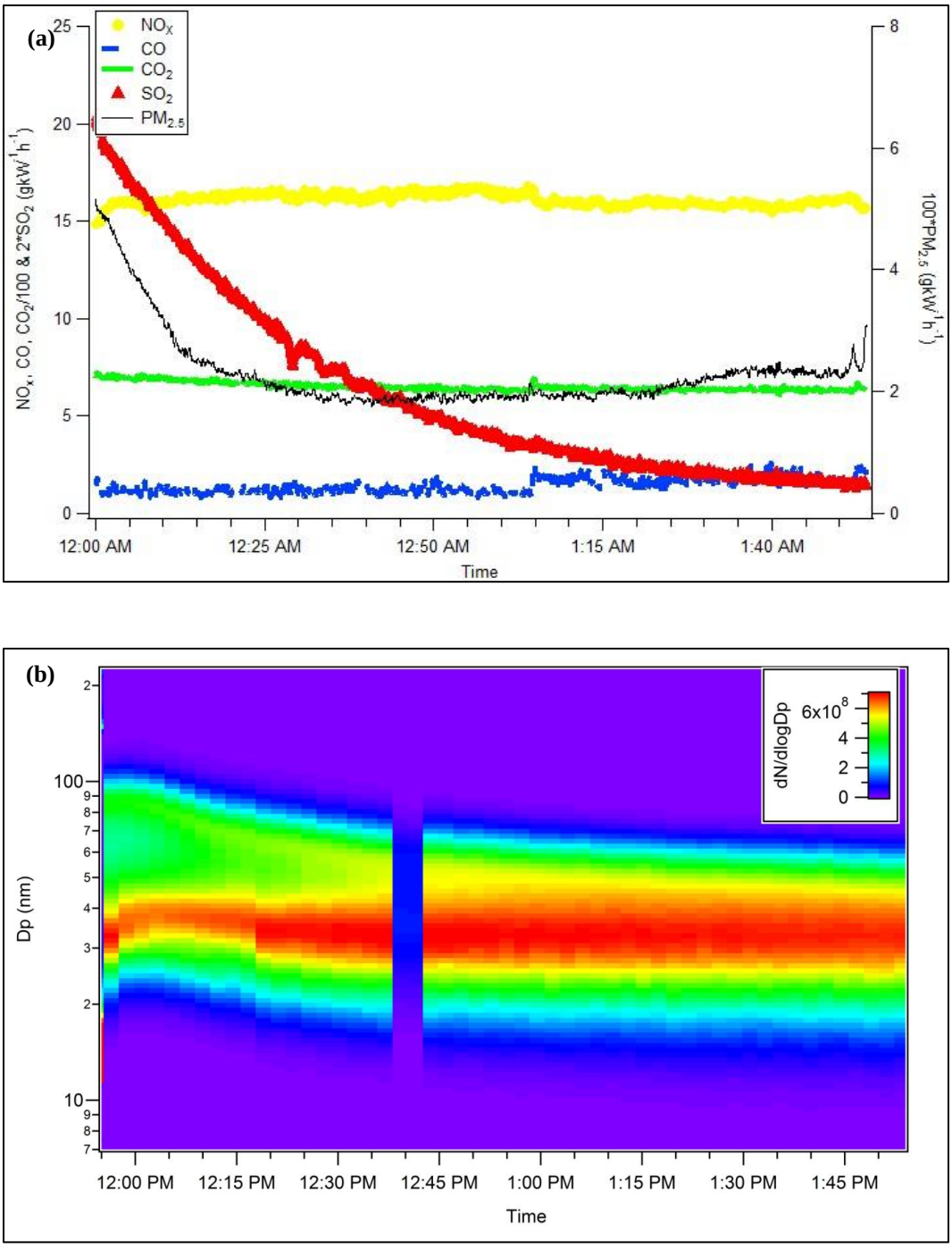

Figure 5-3: Real-time (a) gaseous EFs ($gkW^{-1}h^{-1}$) and (b) particle number concentration measurement when fuel is switched from HFO to MGO at 24% engine load respectively. Note: CPC 3772 data was not available around 12:40 am

The times measured for a fuel change during this research were substantial and surprisingly long. These results can be compared with earlier research by our group where the times were also measured (Table 5-6). Taken in total it is evident that the long times measured in this research are representative of the time required for a fuel switch to be completed when following the checklist and procedure developed by the engine manufacturer.

Table 5-6: Fuel switching time (t_{95}) for different vessels ([a]Trip I on vessel 1, [b]Trip II on vessel 1, *Current study)

Vessels	Vessel 1[a]	Vessel 1[b]	Vessel 2	Vessel 3*
$t_{MGO\ to\ HFO}$ (min)	60	70	80	55
$t_{HFO\ to\ MGO}$ (min)	-	90	-	84

5.4.5. Non-linear Mixing Equation

Because the time required for the fuel switch was about an hour, rather than minutes, a simple kinetic equation was independently developed with the goal of identifying the primary parameters that control the length of time required for 95% switchover of the fuel, t_{95}. Developing an equation required a schematic of the fuel flow system model for a marine engine (Figure 5-5) and some assumptions of: 1) ideal mixing in the day tank, 2) the rate of fuel to the engine, E >> R, the fuel rate in the return line, 3) perturbations in load due to variations in the sea state are insignificant, and 4) t_{95} is not affected by changes in fuel-viscosity. With these assumptions, t_{95} can be parameterized as a function of net fuel consumption rate, f (L min^{-1}), and volume of the fuel in the day tank, V_{DT} (L), Eqn. (3).

$$t_{95} = \frac{V_{DT}}{f} ln\ 20 \tag{3}$$

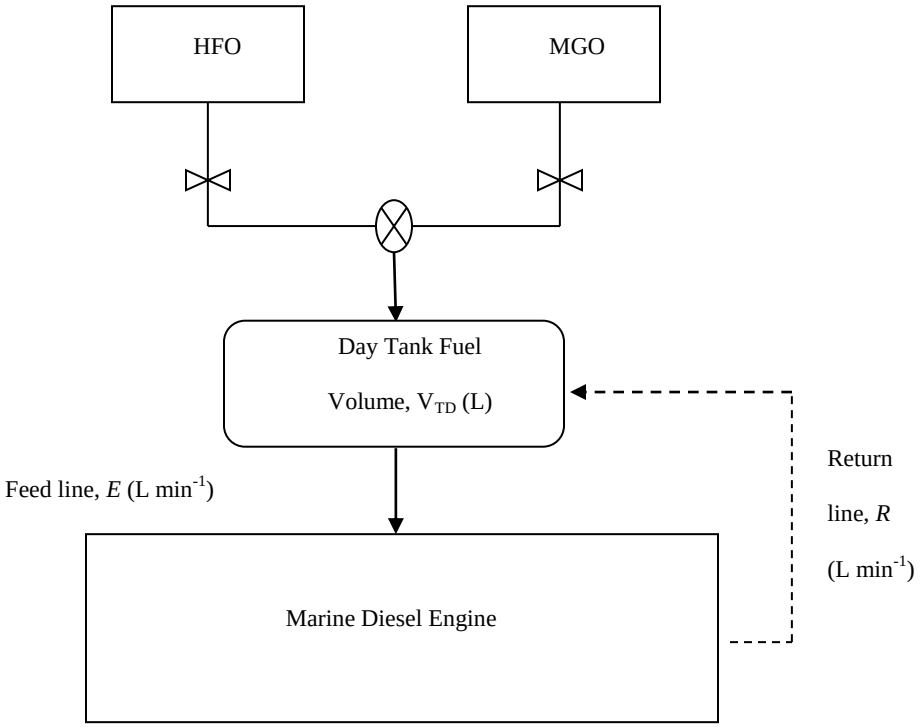

Figure 5-4: Fuel flow system for marine diesel engine

The output of this equation is compared with the observed time needed for fuel switch in this study. Comparisons are presented here as *Case I* (MGO to HFO, f = 77 L min^{-1}) and *Case II* (HFO to MGO, f = 65 L min^{-1}). V_{DT} reported for this study was 1500 L in both cases. The t_{95} calculated by the equation is equal to 59 and 69 minutes, for *Case I* and *Case II*, respectively. With 95% change in fuel for *Case I*, the expected SO_2 concentration would be 435 ppm after 65 minutes of fuel switching and agrees with calculated values from Eq. 3. Similarly, in *Case II*, expected SO_2 concentration is 50 ppm after 84 minutes of fuel switching. The comparison of measured and calculated SO_2 concentrations with time are shown in Figure A-1. Additional measurements are required to account for uncertainties associated with Eq. 3. A detailed derivation for the equation is provided in appendix A.

Note the Eq. 3 predicts the longer time to switch for *Case II* since the load and corresponding fuel rate were lower. The key parameters driving the length of time for the fuel switch are the volume fuel in day tank and the rate of fuel consumption. Eqn. 3 predicts that the time required for fuel switching for a OGV can be reduced by either decreasing the volume of fuel in the day tank or by increasing the rate of fuel consumption or both.

5.4.6. Implications

The results of the research measured the significant benefits for two mitigation strategies: cleaner engines and cleaner fuels. The actual in-use EF_{NOx} was 5% and 14% lower than the Tier I certification value and the Lloyds service data commonly used in the development of emission inventories, respectively. The overall in-use EF_{EC} and EF_{OC} were 33% and 20% lower than the comparative post panamax container vessel studied by Agrawal et al.[23], reflecting the benefits of newest engine technologies. This research also verified an equation to calculate the length of time for a fuel switch. Given that vessels do not have monitoring equipment to calculate the length of time to switch fuels, vessels may switch at the distance specified in the regulation. While this approach is practical, regulated boundaries close to the ports for burning cleaner fuels will not provide the intended protection for people's health. For example, a large container vessel operating at a speed of 15 knots and requiring 85 minutes for fuel switching will have traveled 21 nmi within the 24 nmi regulated zone with elevated SO_2 and $PM_{2.5}$ emissions. Even at lower speeds, there will be a significant increase in OGV emissions on the port communities. From a global perspective, the increase in emissions when entering the harbor will be offset by the decrease in emissions on leaving the harbor. However, the interest is on the health of people in local port communities.

Therefore, it is important to set the regulatory boundary far enough from the port so that the time required to switch to cleaner fuel becomes a trivial issue.

5.5. Acknowledgments

This study would have not been possible without the funding from the United States Environmental Protection Agency, the analytical support from Ms. Kathy Cocker, the shipping company that provided the opportunity and the helping hands of the crew on the vessel. We would also like to thanks Dr. Varalakshmi Jayaram, Mr. Charles Bufalino for test preparation and Ms. Poornima Dixit, Mr. David Torres, Mr. Charles Wardle for their support in analyses of the sample media.

5.6. Literature Cited

1. Capaldo, K., et al., Effects of ship emissions on sulphur cycling and radiative climate forcing over the ocean. Nature, 1999. 400(6746): p. 743-746.
2. Duce, R.A., et al., Impacts of atmospheric anthropogenic nitrogen on the open ocean. Science, 2008. 320(5878): p. 893-897.
3. Lauer, A., et al., Assessment of Near-Future Policy Instruments for Oceangoing Shipping: Impact on Atmospheric Aerosol Burdens and the Earth's Radiation Budget. Environmental Science & Technology, 2009. 43(15): p. 5592-5598.
4. Agrawal, H., et al., Primary Particulate Matter from Ocean-Going Engines in the Southern California Air Basin. Environmental Science & Technology, 2009. 43(14): p. 5398-5402.

5. Song, S.K., et al., Influence of ship emissions on ozone concentrations around coastal areas during summer season. Atmospheric Environment, 2010. 44(5): p. 713-723.
6. Corbett, J.J., Mortality from Ship Emissions: A Global Assessment. Environmental Science & Technology, 2007. 41(24): p. 8512-8518.
7. Winebrake, J.J., et al., Mitigating the Health Impacts of Pollution from Oceangoing Shipping: An Assessment of Low-Sulfur Fuel Mandates. Environmental Science & Technology, 2009. 43(13): p. 4776-4782.
8. Title 13 Section 2299.3. California Code of Regulations.
9. Kasper, A., et al., Particulate emissions from a low-speed marine diesel engine. Aerosol Science and Technology, 2007. 41(1): p. 24-32.
10. Petzold, A., et al., Physical Properties, Chemical Composition, and Cloud Forming Potential of Particulate Emissions from a Marine Diesel Engine at Various Load Conditions. Environmental Science & Technology, 2010. 44(10): p. 3800-3805.
11. Moldanova, J., et al., Characterisation of particulate matter and gaseous emissions from a large ship diesel engine. Atmospheric Environment, 2009. 43(16): p. 2632-2641.
12. Fridell, E., E. Steen, and K. Peterson, Primary particles in ship emissions. Atmospheric Environment, 2008. 42(6): p. 1160-1168.
13. Lyyranen, J., Jokiniemi, J. and Kauppinen, E., The effect of Mg-based additive on aerosol characteristics in medium-speed diesel engines operating with residual fuel oils. Journal of Aerosol Science, 2002. 33(7): p. 967-981.

14. Lyyranen, J., et al., Aerosol characterisation in medium-speed diesel engines operating with heavy fuel oils. Journal of Aerosol Science, 1999. 30(6): p. 771-784.
15. 15. Murphy, S.M., et al., Comprehensive Simultaneous Shipboard and Airborne Characterization of Exhaust from a Modern Container Ship at Sea. Environmental Science & Technology, 2009. 43(13): p. 4626-4640.
16. ISO, ISO 8178-2, Reciprocating Internal Combustion Engines: Exhaust Emission Measurement. Part-2: Measurement of Gaseous Particulate Exhaust Emissions at Site. International Organization of Standardization. 1996.
17. Agrawal, H., et al., In-use gaseous and particulate matter emissions from a modern ocean going container vessel. Atmospheric Environment, 2008. 42(21): p. 5504-5510.
18. Agrawal, H., et al., Emission measurements from a crude oil tanker at sea. Environmental Science & Technology, 2008. 42(19): p. 7098-7103.
19. International Organization for Standardization. 1996. First edition(8178-1).
20. Protection of the environment. Title 40. Section 86 and 89. Code of Federal Regulations.
21. NIOSH, NIOSH Manual of Analytical Methods; National Institute of Occupational Safety and Health: Cincinnati, OH. 1996.
22. CARB, California Air Resources Board, Emissions Estimation Methodology for Ocean-going Vessels. 2008.
23. Agrawal, H., et al., Emissions from main propulsion engine on container ship at sea. Journal of Geophysical Research-Atmospheres, 2010. 115.
24. IMO 2000. Study of Greenhouse Gas Emissions from Ships-Final Report. 2000.

25. Corbett, J.J., Global Nitrogen and Sulfur Emissions Inventories for Oceangoing Ships. Journal of Geophysical Research-Atmospheres, 1999. 104: p. 3457-3470.
26. Entec UK Limited. Quantification of Emissions from Ships associated with Ship Movements between Ports in the European Community. 2002.
27. USEPA, Current Methodologies in Preparing Mobile Source Port-Related Emission Inventories. 2009.
28. Baranescu, R.A., Influence of fuel sulfur on diesel particulate emissions. SAE Technical Paper Series 881174, 1988.
29. Wall, J.C., Shimpi, S.A., Yu, M.L., Fuel sulfur reduction for control of diesel particulate emissions. SAE 1988.
30. Technical considerations of fuel switching practices. API Technical Issues Workshop. June, 3, 2009.
31. Lloyd's Register. Lloyd's Register Engineering Services, 1990a, 1990b, 1993a, 1993b & 1995.
32. Nenes, A., Pilinis, C., Pandis, S.N. (1998) ISORROPIA: A New Thermodynamic Model for Multiphase Multicomponent Inorganic Aerosols, Aquat. Geochem., 4, 123-152.
33. Fountoukis, C. and Nenes, A. (2007) ISORROPIA II: A Computationally Efficient Aerosol Thermodynamic Equilibrium Model for K^+ - Ca^{2+} - Mg^{2+} - NH_4^+ - SO_4^{2-} - NO_3^- - - Cl^- - H_2O Aerosols, Atmos. Chem. Phys., 7, 4639-4659.
34. ISORROPIA. http://nenes.eas.gatech.edu/ISORROPIA.
35. MAN Diesel Low Speed. Marine Diesel Engines. Marine Diesel Engines Improvements on the

Efficiency.http://www.dtu.dk/upload/institutter/kt/nyheder/cccs_pres/man_diesel soeren_h_jensen.pdf.

Chapter Six: Greenhouse Gas and Criteria Emission Benefits Through Reduction of Vessel Speed at Sea

6.1. Abstract

Reducing emissions from ocean-going vessels (OGVs) as they sail near populated areas is a widely recognized goal and Vessel Speed Reduction (VSR) is one of several strategies that is being adopted by regulators and port authorities. The goal of this research was to measure the emission benefits associated with greenhouse gas and criteria pollutants by operating OGVs at reduced speed. Emissions were measured from one Panamax and one post-Panamax class container vessels as their vessel speed was reduced from cruise to 15 knots or below. VSR to 12 knots yielded carbon dioxide (CO_2) and nitrogen oxides (NO_x) emissions reductions (in kg/nautical mile (kg/nmi)) of approximately 61% and 56%, respectively, compared to vessel cruise speed. The mass emission rate (kg/nmi) of $PM_{2.5}$ was reduced by 69% with VSR to 12 knots alone and by ~ 97% when coupled with the use of the marine gas oil (MGO) with 0.00065% sulfur content. Emissions data from vessels while operating at sea are scarce and measurements from this research demonstrated that tidal current is a significant parameter affecting emission factors (EFs) at lower engine loads. Emissions factors at ≤20% loads calculated by methodology adopted by regulatory agencies were found to underestimate $PM_{2.5}$ and NO_x by 72% and 51%, respectively, when compared to EFs measured in this study. Total pollutant emitted (*TPE*) in the emission control area (ECA) was calculated and emission benefits were estimated as the VSR zone increased from 24 nmi

to 200 nmi. TPE_{CO2} and $TPE_{PM2.5}$ estimated for large container vessels showed benefits for CO_2 (2-26%) and $PM_{2.5}$ (4-57%) on reducing speeds from 15 to 12 knots whereas TPE_{CO2} and $TPE_{PM2.5}$ for small and medium container vessels were similar at 15 and 12 knots.

6.2. Introduction

Marine shipping is the most efficient mode of transporting goods with about 90% of the global merchandise transported by sea utilizing ~103,000 ocean-going vessels (OGVs).[1,2] However, OGVs are significant emitters of criteria pollutants and the greenhouse gas, carbon dioxide (CO_2). Criteria pollutants are those pollutants that are common and found all over United States. Criteria pollutants emitted by OGVs are nitrogen oxides (NO_x), sulfur oxides (SO_x), carbon monoxide (CO) and particulate matter ($PM_{2.5}$). In international waters, these vessels consume heavy fuel oil (HFO) with a sulfur content of up to 3.5% by weight, which upon combustion, produces large amounts of SO_x and $PM_{2.5}$.

OGVs navigate near coastlines as they follow the main shipping lanes. According to Corbett *et al.*,[3] 70% of ship related emissions occur within 216 nmi of the coastline. Oftedal[4] estimates that 74-83% of all vessels are within 200 nmi of land at any given time. Recent studies[29,30] have linked PM emissions from OGVs to an increased number of premature deaths. Thus, there is an interest in reducing emissions around coastlines and population centers. Towards that end, some port authorities have launched VSR programs; for example, the Los Angeles and Long Beach San Pedro Bay Ports have a voluntary VSR program in which vessels are slowed to 12 knots in VSR zones (20 and 40 nmi).[5] This voluntary program is based on the principle that the vessel speed is directly proportional to the cube of fuel

consumption. Hence, small reductions in speed will produce large reductions in fuel consumption and subsequently, CO_2 and criteria pollutants. Along with the port's voluntary VSR program, the California Air Resources Board (CARB) implemented a fuel regulation, effective from July 2009, which requires OGVs to use lower-sulfur marine distillates within 24 nmi of the California Coastline to curb SO_x and $PM_{2.5}$ emissions.[6] Moreover, the International Maritime Organization (IMO) designated the waterways off North American coasts as Emission Control Areas (ECA) where emissions of NO_x, SO_x and $PM_{2.5}$ mass from OGVs will be significantly reduced.[7] OGVs complying with ECA standards require progressive adaptation of new tiers of NO_x and fuel sulfur controls over the next decade.

Recently, several researchers have presented CO_2 reduction potentials with reduction in speed on the basis of fuel consumption. Psaraftis *et al.*[8] estimated reduction in fuel consumption and CO_2 emissions with reduction in vessel speed. Corbett *et al.*[9] also provided different speed reduction scenarios and estimated route-specific economically optimal speeds for maximum profits.

While container vessels account for less than 5% of the total OGV fleet, they emit more than 21% of the CO_2 from the international shipping industry.[10] It has been reported that around 32% of all containerized trade in the United States of America flows through the port of Los Angeles and Long Beach.[11] Approximately 60% of the total fleet arriving at the Los Angeles and Long Beach port in 2009 was container vessels. Therefore, emission measurements were made from two container vessels complying with the Port's voluntary VSR program. This study provides gaseous and particulate emission benefits for operating at reduced vessel speeds. It also provides comparisons between measured and calculated EFs at

low loads. Scenarios are presented to estimate total pollutant emitted (*TPE*) in ECA and emission benefits on extending the VSR zone from 24 nmi to 200 nmi in ECA.

6.3. Experimental Methods

6.3.1. Vessel and Engine Description

Emissions testing was performed on the main propulsion engines of two container vessels. The first vessel (Panamax class) with a capacity of 5,000 twenty-foot equivalent units (TEU) was tested twice and the second vessel (post-Panamax; up to 10,000 TEU) was tested once; hence, data from three trips are presented in this study. Emissions were measured from two 2-stroke slow speed marine engines- a Sulzer 9RTA84C, 36740 kW @ 102 rpm (Panamax) and a Hyundai B&W 11K 98ME7; 68530 kW @ 97 rpm (post-Panamax). Fuel consumption, engine load and vessel speed were monitored for all test modes from the engine computer and can be found in table 1.

Table 6-1: Main engine, fuel consumed, % load, vessel speed, type of emissions measured and location of measurements

Trip	Vessel	Engine	VSR measurements	Fuel	Engine Load	Vessel Speed	Gaseous/PM/EC-OC Measurements
1 (July 2009)	1	Sulzer 9RTA84C	Out of Long Beach Port	MGO	11	11	Yes/Yes/Yes
				MGO	21	15	Yes/Yes/Yes
			Into Oakland Port	HFO	10	12	Yes/Yes/Yes
2 (August 2009)	1	Sulzer 9RTA84C	Out of Long Beach Port	MGO	9	13	Yes/No/No
				MGO	18	14	Yes/Yes/No
			Into Oakland Port	MGO	17	14	Yes/No/No
3 (September 2010)	2	Hyundai B&W 11K 98ME7	Out of Long Beach Port	MGO	9	12	Yes/No/No
			Into Oakland Port	MGO	12	12	Yes/Yes/Yes
				MGO	23	15	Yes/Yes/Yes

6.3.2. Fuel Properties

Two different grades of fuel meeting ISO 8217 specifications were used for each trip. Marine gas oil (MGO) was used within regulated waters and HFO was used outside of regulated waters. Sulfur content varied significantly; for the MGO it was: 0.00065%, 0.00942% and 0.1657% and for the HFO it was 3.14%, 2.15% and 2.5% by weight, respectively for trips 1, 2 and 3.

6.3.3. Test procedures

Vessels complying with the VSR program reduced their speed to 12 knots or below within 24 nautical miles of the coastline. Each trip originated from the San Pedro Bay ports (CA, USA) and ended at the Port of Oakland, (CA, USA). Emission measurements were made when the vessels were operating within the VSR zone and in international waters.

6.3.4. Sampling and Analysis

Sampling and analysis of gases and $PM_{2.5}$ mass conformed to ISO 8178-2 requirements.[12] A partial flow dilution system with a single venturi was installed to conduct PM testing.[13,14] Although allowed by the ISO protocol, transfer lines were not used in any of the tests as earlier research showed that significant PM losses can occur in the lines.[13] Dilution ratios (DRs) were determined from raw and dilute CO_2 and NO_x exhaust concentrations and agreed within 5% for the two gases. A Horiba PG-250 Exhaust Gas Analyzer was used to measure CO, CO_2, and NO_x concentrations. SO_2 concentrations were calculated from fuel sulfur content per ISO 8178-1.[15]

$PM_{2.5}$ mass concentrations were determined gravimetrically on pre-weighed 47-mm diameter 2 μm pore Teflo® filters (Pall Gelman, Ann Arbor, MI). Loaded Teflo® filters were weighed using a Mettler Toledo UMX2 microbalance following the guidelines within the Code of Federal Regulations (CFR).[16] The Teflo® filters were subsequently extracted with HPLC grade water and isopropyl alcohol and analyzed for sulfate ions using a Dionex DX-120 ion chromatograph. Sulfate in $PM_{2.5}$ was assumed to be in hydrated form as $H_2SO_4.6H_2O$, as predicted using the aerosol thermodynamic model ISORROPIA.[26-28] Hence, a factor of 2.15 was applied to the mass of sulfate ions to determine its total contribution to the $PM_{2.5}$ mass.[13,17] The elemental carbon/organic carbon (EC/OC) analysis was performed on $PM_{2.5}$ collected on 2500 QAT-UP Tissuquartz Pall (Ann Arbor, MI) 47 mm filters, which were preconditioned at 600°C for a minimum of 5 hours. Analysis followed the NIOSH[18] method using a Sunset Laboratory (Forest Grove, OR) thermal/optical carbon aerosol analyzer.

6.4. Results and Discussion

Emission rates were calculated in kilogram/hour (kg/hr) and kg/nmi using measured concentration, calculated exhaust flow rate and vessel speed obtained from the engine computer. The carbon balance method[12] was used to calculate the exhaust flow rate. Percent reductions of pollutants are reported from emission rates in kg/hr and kg/nmi.

6.4.1. Gaseous Emissions

The speed of the vessel (V), at ~80% of engine load is considered to be cruise speed.[19,20] Therefore, the engine load considered for cruise speed in trip 1 (24 knots), trip 2 (24 knots)

and trip 3 (25 knots) were 81%, 83% and 75% respectively. Identical engine loads were not obtained due to practical constraints. Comparisons of greenhouse and criteria emissions were made when the vessels were running at cruise and at VSR speeds. The average percent reductions in gaseous emissions (CO_2 and NO_x) are presented in Figure 1 for V≤12 knots (Case 1) and 12<V≤15 knots (Case 2). The reductions in emissions are attributed to both lower sulfur fuel and reduced speed for both cases. Using lower sulfur fuel (MGO) does not affect CO_2 emissions significantly and therefore the CO_2 reductions observed are attributed to VSR; use of MGO compared with HFO is expected to decrease NO_x emissions by ~6-10% due to the lower nitrogen content in the MGO. On average, emissions (kg/nmi) reductions in CO_2 and NO_x for V > 12 and ≤ 15 knots were 57% and 60% respectively. Moreover, vessels operated at 12 knots or below showed similar reduction (61% and 56%) in CO_2 and NO_x. In this instance, it appears that a vessel speed of ≤15 knots is almost equally effective in reducing gaseous emissions within VSR zone for container OGVs. Gaseous emissions at cruise and reduced speeds for all trips in kg/hr, kg/nmi and g/kW-hr are presented in Table B-1, B-2 and B-3, respectively. However, it is important to note that vessels speeding up to make up for lost time at the slower speeds in the VSR zone could have an overall increase in CO_2 and other emissions.

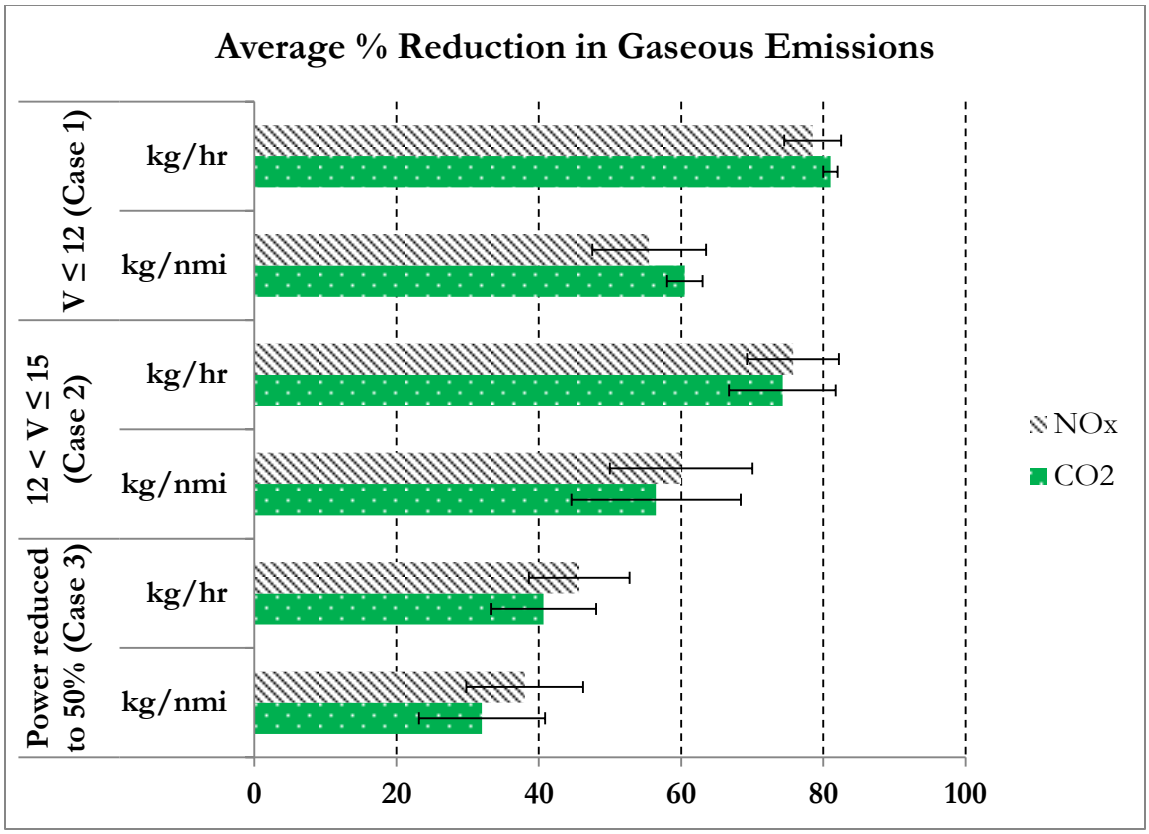

Figure 6-1: Average reduction in gaseous (NO_x and CO_2) emissions from all trips for vessel speed (V) equal to 12 knots or below (Case 1), 12< V ≤ 15 (Case 2) and at 50% engine load (Case 3). Reductions in NO_x and CO_2 for Case 1 and 2 are due to change in speed and fuel (HFO to MGO) whereas for Case 3 reductions are due to change in speed only

OGVs are mostly operated in international waters and can be subject to local, national, and international requirements. Currently, the IMO has only capped fuel sulfur content (≤3.5%) in international boundaries. These vessels typically run at cruising speed consuming tons of fuel with high sulfur content and consequently emit large quantities of carbon dioxide and criteria pollutants. However, when fuel prices are high and time is secondary, vessels sail at a speed closer to 50% engine load to save fuel. Therefore, emission measurements were also conducted at 50% engine load and were compared with loads at cruising speed. Vessel speed

at ~50% engine load for trip 1, 2 and 3 were 19.5, 19.5 and 21.8 knots, respectively. Case 3 in Figure 1 represents the CO_2 and NO_x benefits by reducing speed by between 13 and 19% (engine load ~50%) in international waters. On average, 32% and 38% reduction in CO_2 and NO_x emissions (kg/nmi) were observed. Hence on a global perspective, CO_2 and NO_x mitigation reduction may be possible by reducing the vessel speed by merely 3-6 knots from cruise speed.

6.4.2. Effect of ocean currents

This study also evaluated the impact of ocean currents on gaseous emissions which can be considerable when a vessel operates at low speed. Table 2 represents the gaseous emissions from Vessel 2 when it was moving out of the Long Beach port (along ocean current) and against ocean current into the Oakland port at the speed of 12 knots. Even though the vessel was moving at the same speed at both locations, both CO_2 and NO_x were increased significantly when moving against the current (21% and 10%, respectively). A 21% higher fuel consumption was also observed when the vessel moved against the ocean current compared to moving with the current. Thus, ocean currents are significant factors in determining actual engine load and hence, emissions from vessels moving at slow speeds in the VSR zone.

Table 6-2: Gaseous emissions from vessel 2 in moving against and along ocean current at the same speed

Emissions (kg/nmi) from Vessel 2 at 12 Knots			
Gases	**Against Ocean Current**	**Along Ocean Current**	**% Reduction in Emissions**
CO_2	516±28	406±3	21±4
NO_x	18.2±0.5	16.3±0.2	10±1
CO	0.27±0.02	0.52±0.01	-90±11

6.4.3. Particulate Emissions

Particulate measurements were also conducted at lower speeds with vessel operating on HFO and MGO during trip 1. Total particulate matter measured was observed to be primarily composed of hydrated sulfate, with moderate amounts of OC and small amounts of EC and ash, similar to previous studies.[13,21] Table 3 presents the emissions reduction in kg/hr and kg/nmi occurring due to vessel speed reduction and fuel consumed. When the vessel was operated on HFO and its speed was reduced to 12 knots, an approximately 69% reduction in $PM_{2.5}$ (kg/nmi) was obtained. These reductions improved to a total of ~97%, when fuel was switched to MGO and operated at the reduced speed of 11 knots. Almost the entire hydrated sulfate was removed after switching to MGO, consistent with the low sulfur content in MGO (0.00065%) in comparison to HFO (3.14%). EC and OC emissions were reduced by 53% and 70% on reducing the vessel speed to 12 knots. Similar to $PM_{2.5}$, higher reductions (73% in EC and 87% in OC) were observed on switching to MGO with reduced speed. $PM_{2.5}$ emission benefits by reducing engine load from ~80% to ~50% in international waters where vessels consumed HFO led to reductions of 48%, 54% and 40% in $PM_{2.5}$ (kg/nmi) for trip 1, 2 and 3, respectively.

Table 6-3: Reduction in $PM_{2.5}$, $H_2SO_4 \cdot 6H_2O$, Organic Carbon (OC), and Elemental Carbon (EC) from Trip 1

Trip 1 : Particulate emissions (kg/hr) reduction due to change in speed and fuel					
Units	(kg/hr)			% reduction	
Fuel	HFO[1]	HFO[2]	MGO[1]	HFO[a]	MGO[b]
Speed	24 knots	12 knots	11 knots	12 knots	11 knots
$PM_{2.5}$	65±1	10	0.99±0.15	85±0	98±0
$H_2SO_4.6H_2O$	61±2.5	7.7	0.07±0.02	87±1	100±0
EC	0.23±0.02	0.05	0.028±0.001	78±2	88±1
OC	7.1±0.3	1.1	0.41±0.05	84±1	94±0
Trip 1 : Particulate emissions (g/nmi) reduction due to change in speed and fuel					
Units	(g/nmi)			% reduction	
Fuel	HFO[1]	HFO[2]	MGO[1]	HFO[a]	MGO[b]
Speed	24 knots	12 knots	11 knots	12 knots	11 knots
$PM_{2.5}$	2708±42	833	90±14	69±0	97±1
$H_2SO_4.6H_2O$	2542±104	639	6.4±1.8	75±1	100±0
EC	9.6±0.8	4.5	2.5±0.1	56±4	73±1
OC	296±13	89	37±5	69±1	87±1
[1]Average and standard deviation calculated based on triplicate filter measurements; [2]Based on one filter measurement; [a]Represents emission reductions due to change in speed (cruise to 12 knots) while engine consumed HFO; [b]Represents emission reductions due to change in speed (cruise to 11 knots) and fuel (HFO to MGO)					

6.4.4. Comparison of measured and calculated EFs at ≤20% loads

Two-stroke slow marine diesel engines operate less efficiently when run at ≤20% loads and EFs are difficult to estimate at these loads. The Energy and Environmental Analysis, Inc. (EEIA)[22] developed a formula for EFs of vessels operating at engine loads ≤ 20%, such as those encountered during harbor maneuvering and when moving slowly at sea in VSR zones.

Their formula was established based on data from eleven vessels, two of which were container vessels. Their formula for low load EF is being used in the development of emission inventories for USEPA[20] and CARB[19] and is based upon the concept that the brake specific fuel consumption (BSFC) increases as load decreases below about 20% engine load.

The current practice of determining fractional load relies upon propeller law which states the propulsion engine load varies with the cube of vessel speed. Hence, at a given speed, propulsion engine fractional load (Eqn. 1) is estimated by the ratio of cube of actual speed (*AS*) and maximum speed (*MS*).

$$fractional\ load = (AS/MS)^3 \quad (1)$$

EEIA formula (Eqn. 2) to generate EFs (*y*) for the range of load factors from 2% to 20% for selected pollutants is:

$$y\ (\text{g/kW-hr}) = a(fractional\ load)^{-x} + b \quad (2)$$

Values of *a*, *b* and *x* are different for different pollutants (Table 4).

Table 6-4: Low-load EF regression variables

Pollutant	Exponent (x)	Intercept (b)	Coefficient (a)
NO_x	1.5	10.4496	0.1255
$PM_{2.5}$	1.5	0.2551	0.0059
CO_2	1	648.6	44.1
CO	1	0.1458	0.8378

The calculated $EF_{PM2.5}$, EF_{NOx}, EF_{CO} and EF_{CO2} using the EEIA formula are compared with the measured EFs for loads equal or below 20% (Figure 2). Equation 2 is derived from data

obtained from vessels operated on HFO. However, at low loads, our measured EFs are mostly based on MGO except for trip 1 where vessel was also operated at 12 knots on HFO (Table 1). Therefore, calculated EFs are corrected for fuel. Fuel correction factors applied in this study (UCR) are shown in Table 5. Correction factors of 0.94, 1 and 1 are applied for NO_x, CO_2 and CO, respectively, which are consistent with CARB's emission estimations methodology for ocean-going vessels.[34-35] Approximately 90% of the $PM_{2.5}$ was reduced in trip 1 on switching from HFO (3.14% S, V = 12 knots) to MGO (0.00065% S, V = 11 knots). Therefore, a correction factor of 0.10 was applied to the calculated $PM_{2.5}$ for sulfur content of 0.00065% and 0.00942%. The percentage error, which is equal to the ratio of calculated minus measured EF and the measured EF is obtained for each pollutant.

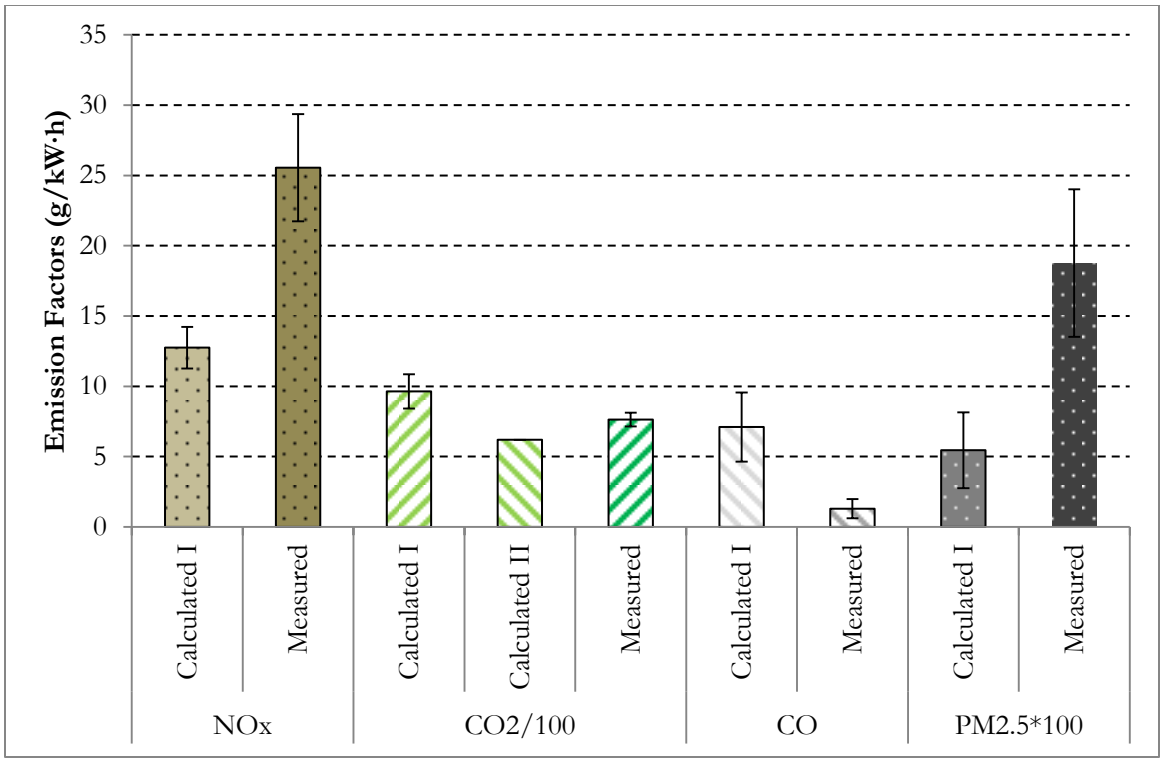

Figure 6-2: Comparison of calculated and measured EFs (g/kW-h) for vessels operating at low loads (2-20%) on MGO. Calculated I and II are EPA and CARB methodology, respectively. Note EF_{CO2} and $EF_{PM2.5}$ are divided and multiplied by a factor of 100, respectively

Table 6-5: Fuel correction factors from EPA, CARB and UCR (this study)

Trips	Sulfur Content (%)	Fuel Type	Fuel Correction Factors											
			CO_2			CO			NO_x			$PM_{2.5}$		
			EPA	CARB	UCR	EPA	CARB	UCR	EPA	CARB	UCR	EPA	CARB	UCR
Trip 1	3.14	HFO	-	-	1	-	-	1	-	-	1	-	-	1
Reference	2.7	HFO	1	1	1	1	1	1	1	1	1	1	1	1
Reference	0.2	MGO	-	1	1	-	1	1	-	0.94	0.94	-	0.19	0.19
Trip 3	0.1657	MGO	-	-	1	-	-	1	-	-	0.94	-	-	0.18†
Reference	0.1	MGO	0.95	1	1	1	1	1	0.94	0.94	0.94	0.13	0.17	0.17
Trip 2	0.00942	MGO	-	-	1	-	-	1	-	-	0.94	-	-	0.10
Trip 1	0.00065	MGO	-	-	1	-	-	1	-	-	0.94	-	-	0.10

†Calculated using interpolation

On average, percentage errors for $PM_{2.5}$, NO_x and CO are -72%, -51% and 669%, respectively (Table S4). Based on data from this study, $EF_{PM2.5}$ and EF_{NOx} are highly underestimated whereas EF_{CO} are overestimated by the EEIA formula. The US EPA uses the EEIA formula to calculate EF_{CO2} at low loads and CARB assumes it to be constant (620 g/kW-hr). The average percentage error for the US EPA and CARB estimates are 20% and -20%, respectively (Table S4). Thus, EF_{CO2} is overestimated by the US EPA method while underestimated by the CARB method. Hence, the comparison shows that the current calculation methodology for predicting EFs at low loads is inconsistent with measured EFs at the low loads in this study. Agarwal *et al.*[14] had also showed that their $EF_{PM2.5}$ measurements from a tanker OGV at 13% engine load were underestimated by ~49% when calculated using EEIA methodology. If the results of the current study are confirmed by further measurements than the underestimation of key pollutant levels of $PM_{2.5}$ and NO_x, within the regulated zone will lead to an under appreciation of the potential increased health risk for people living near ports.

6.5. Calculating the effect of the control distance

The current control distance for the ECA is 200 nautical miles from territorial sea baseline. In this section, scenarios were developed using the measured EFs and selected control distances to estimate the emission benefits of VSR zones with sulfur control. A total of 5 VSR distances (24, 40, 100, 150 and 200 nmi) were selected. Outside the VSR zone, a vessel is assumed to be operating at cruise speed (~80% engine load) and inside the VSR zone, a vessel speed is 12 or 15 knots. Equations 3 to 5 are used to calculate the *Total Pollutant Emitted (TPE)* in tonnes per year (tpy) within ECA.

$$\mathrm{PEV} = \frac{\mathrm{PEF} \times \mathrm{VD}}{\mathrm{VRS}} \quad (3)$$

$$\mathrm{PERE} = \frac{\mathrm{PEF} \times \mathrm{RED}}{\mathrm{VCS}} \quad (4)$$

$$\mathrm{TPE} = \frac{[2 \times \mathrm{V} \times (\mathrm{PEV} + \mathrm{PERE})]}{1000} \quad (5)$$

Where:

PEV = Pollutant emitted in VSR zone (kg), PEF = Pollutant emission factor (kg/hr), VD = VSR distance (nmi), VRS = Vessel reduced speed (12 or 15 knots), PERE = Pollutant emitted in rest of ECA (kg), RED =Rest of ECA distance (nmi), VCS = Vessel cruise speed (knots), TPE = Total pollutant emitted (tpy) and V =Total number of vessels

Looking at the Ports of Long Beach and Los Angeles as a case study, a total of 2,487 container vessels arrived in 2009.[11,23] Container vessels that arrived at both ports were divided into different classes according to vessels type (Table S5). Scenarios have been presented for two categories. Category A includes all vessels with average maximum power of the main engine ~41.7 MW and category B includes vessels with large main engine (average maximum power ~65.2 MW). Therefore, EFs of Vessel 1 (~36.7 MW) and Vessel 3 (~68.5 MW) are applied to categories A and B, respectively.

Category A and B vessels show significantly low TPE_{CO2}, TPE_{NOx} and $TPE_{PM2.5}$ when VSR zone is introduced in the ECA with *TPE* decreasing linearly with an increase in the VSR boundary (Figure 3 and 4). Figure 3 reveals that emission benefits are almost same with vessel speed of 12 and 15 knots except for CO, which has higher TPE_{CO} at 15 knots than cruise speed and 12 knots. *TPE* is directly proportional to emission rate (kg/hr) and time

taken by vessels to complete 200 nmi. For this particular vessel, percent reduction in emission rate of CO on reducing speed is less than percent increase in time taken to complete 200 nmi. Therefore, TPE_{CO} at 15 knots were higher than cruise speed. Even though engines are inefficient at low loads, CO emissions are low across all loads. Please note that the TPE_{CO} was less than 1% of TPE_{CO2} for category A. Contrary to category A, category B TPE_{CO2} (Figure 4a) decreased more with 12 knots (7-58%) in comparison to 15 knots (5-43%). Category B $TPE_{PM2.5}$ reduction almost doubled on reducing vessel speed from 15 knots (5-38%) to 12 knots (9-73%). The reduction in category B TPE_{NOx} are similar for both reduced speeds which was expected as NO_x formation in diesel combustion is dominated by the oxidation of nitrogen in the combustion chamber and has <10% dependence on fuel-bound nitrogen[24,25] and suggests that the combustion temperature inside the engine cylinder did not change significantly between 12 and 15 knots speed of the vessel. Category B TPE_{CO} shows similar trend as of category A TPE_{CO}.

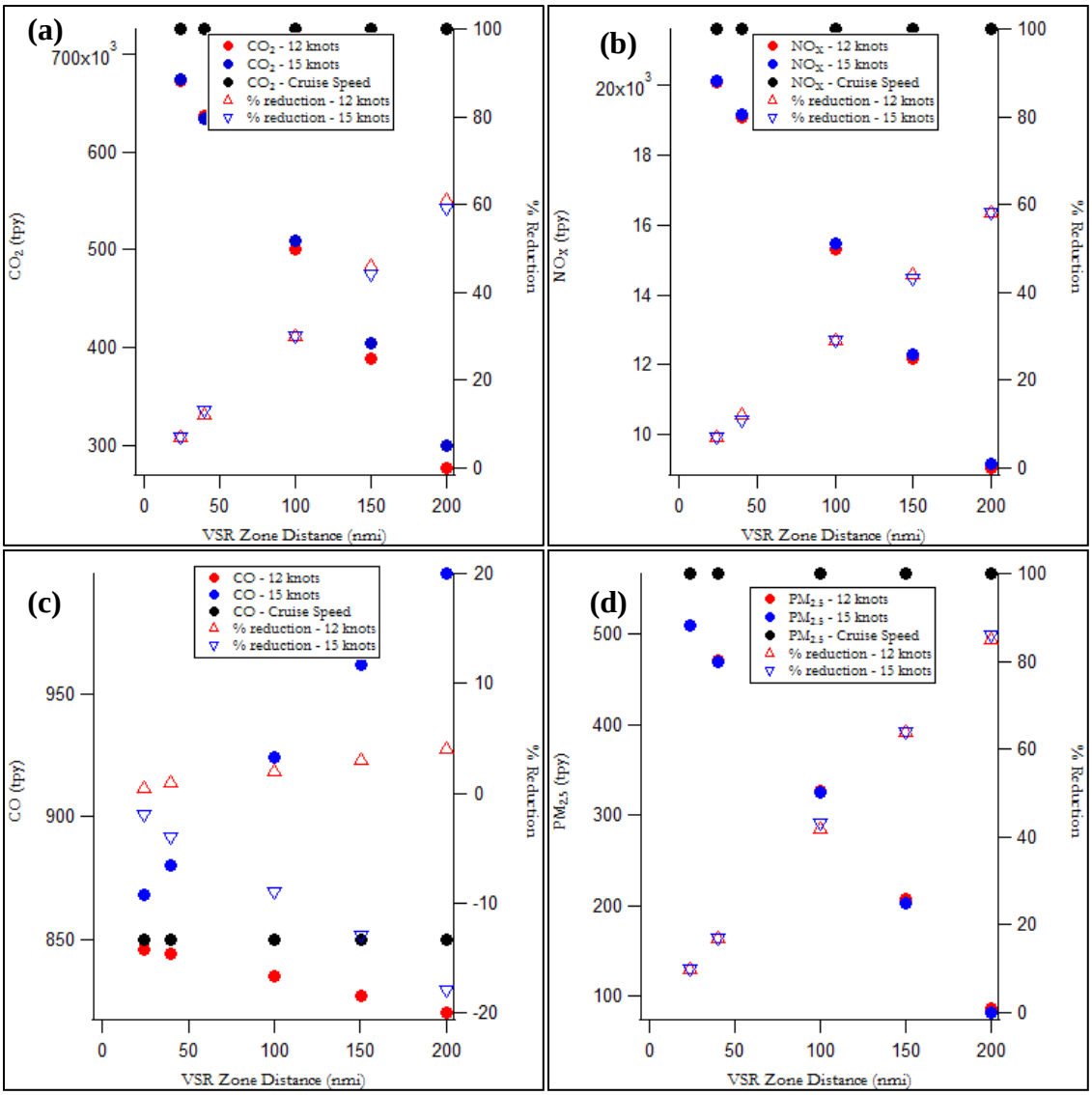

Figure 6-3: Estimated emission scenarios for (a) CO_2, (b) NO_x, (c) CO, (d) $PM_{2.5}$ when VSR boundary is extended to 24, 40, 100, 150 and 200 nautical miles from coastline and vessels are operated on MGO and running at reduced speed of 12 and 15 knots. Total number of container vessels (category – A) arrived at port of Los Angeles and Long Beach in 2009 are used to calculate emissions emitted in tonnes per year (tpy). The percent reductions are calculated for both reduced speeds from the baseline (cruise speed)

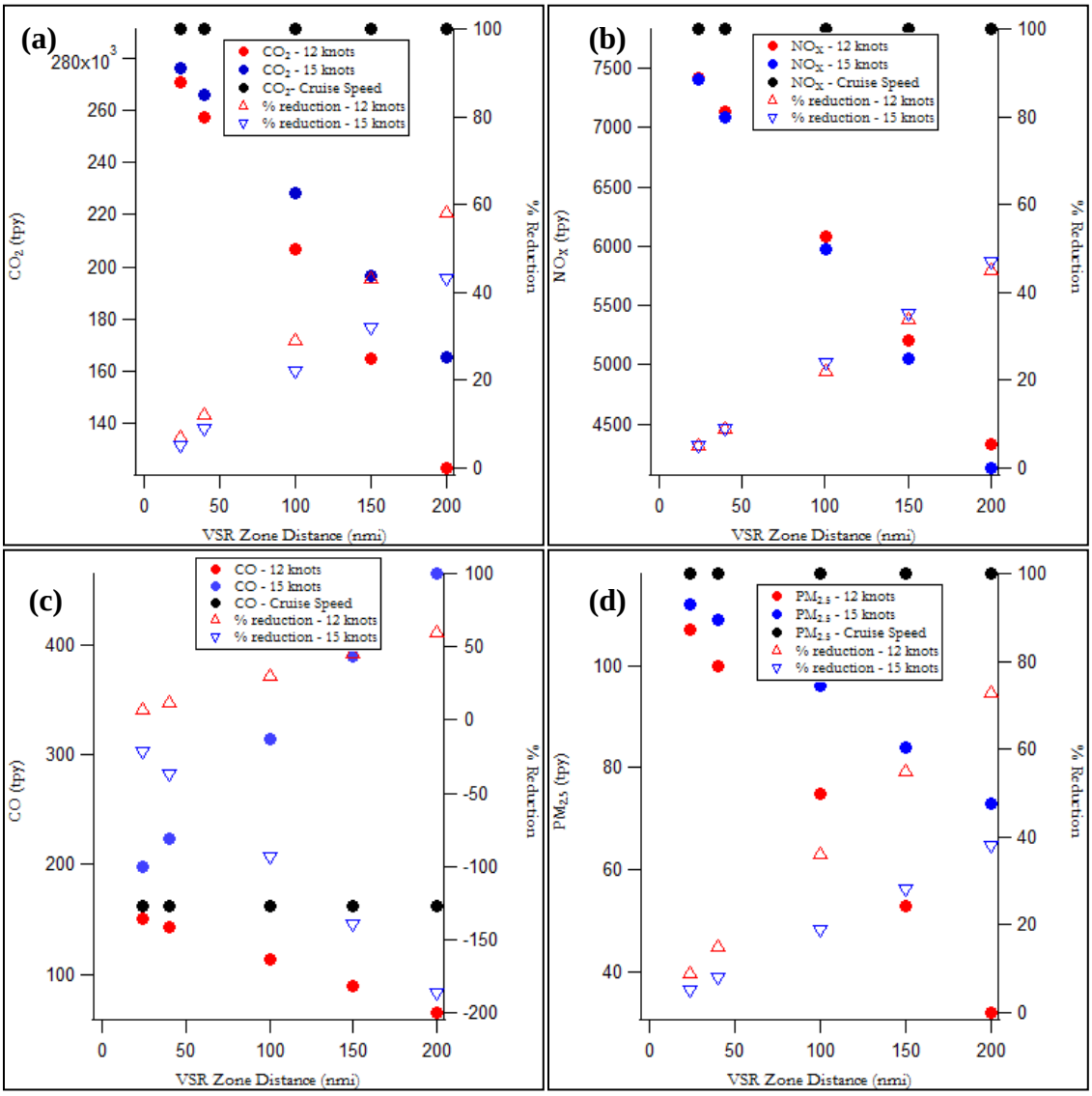

Figure 6-4: Estimated emission scenarios for (a) CO_2, (b) NO_X, (c) CO, (d) $PM_{2.5}$ when VSR boundary is extended to 24, 40, 100, 150 and 200 nautical miles from coastline and vessels are operated on MGO and running at reduced speed of 12 and 15 knots. Total number of large container vessels (category – B) arrived at port of Los Angeles and Long Beach in 2009 are used to calculate emissions emitted in tonnes per year (tpy). The percent reductions are calculated for both reduced speeds from the baseline (cruise speed)

Similarly, *TPE* from Suezmax class tankers[14] are estimated for CO_2, NO_x, $PM_{2.5}$ and CO and presented in Appendix B (Figure B-1). These tankers represented 11% of the total tankers arriving at the San Pedro ports in 2009. In the case of Suezmax class tankers, only 12 knots (~50% engine load) is considered as reduced speed because ~16 knots (~ 84% engine load) is cruise speed. Overall, emission reductions of 6-10% are estimated when the VSR zone is extended up to 40 nmi for CO_2, NO_x and $PM_{2.5}$. These emission benefits further increases linearly with increasing the VSR boundary. Decreasing tanker speed shows higher TPE_{CO} at 12 knots than at cruise speed. This analysis suggests that reducing speed of large container and Suezmax class tankers to 12 knots would result in emission benefits whereas small and medium container vessels may give similar emission benefits at 15 knots as 12 knots. One should note that the slowing the vessel would results in emission benefits from propulsion engine and increase in emissions from auxiliary engine due to additional operating time at sea, however, this would slightly mitigate the actual benefits achieved through VSR due to relatively large difference in output power of propulsion and auxiliary engines.

6.6. Acknowledgements

This study would have not been possible without the support of anonymous shipping companies, the funding from the California Air Resources Board and United States Environmental Protection Agency, the analytical support from Ms. Kathy Cocker and the generous helping hands of the crew on the both vessel. We would also like to thanks Dr. Varalakshmi Jayaram, Mr. Charles Bufalino for test preparation and Mr. James Gutierrez, Ms. Poornima Dixit, Mr. David Torres, Mr. Charles Wardle for their support in analyses of the sample media.

6.7. Literature Cited

1. UNCTAD 2010. *United Nation Conference of Trade and Development*. **2010**.
2. IMO. International Maritime Organization, Maritime Knowledge Centre. *International Shipping and World Trade Facts and Figures*. October **2009**.
3. Corbett, J.J., Fischbeck, P.S., Pandis, S.N. Global Nitrogen and Sulfur Emissions Inventories for Oceangoing Ships. *J. Geophys. Res.* **1999**, 104 (D3), 3457-3470.
4. Oftedal, S. Air Pollution from Sea Vessels, European Federation for Transport and Environment, Secretariat: Rue de la Victoira 26, 1060 Brussels, Belgium **1996**.
5. CARB. Public Workshop Vessel Speed Reduction for Ocean-Going Vessels. Sacramento.September,**2008**.http://www.arb.ca.gov/ports/marinevess/vsr/docs/090908speakingnotes.pdf.
6. Title 13 section 2299.3. *California Code of Regulations*.
7. EPA. Designation of North American Emission Control Area to Reduce Emissions from Ships: Regulatory Announcement, EPA-420-F-10-015, March **2010**. http://www.epa.gov/nonroad/marine/ci/420f10015.htm.
8. Psaraftis, H.N., Kontovas, C.A., Kakalis, M.P. Speed Reduction as an Emissions Reduction Measure for Fast Ships. *10th International Conference on Fast Sea Transportation*. Fast 2009, Athens, Greece, October **2009**.
9. Corbett, J.J., Wang, H., Winebrake, J.J. The Effectiveness and Costs of Speed Reductions on Emissions from International Shipping. *Transportation Research Part D* 14 (**2009**) 593-598.

10. IMO. Prevention of Air Pollution from Ships. Second IMO GHG Study, **2009**. http://www.shippingandco2.org/IMOGHGStudy-Second.pdf.
11. POLB. Emission inventory full report 2009 – Port of Long Beach. 2009. http://www.polb.com/civica/filebank/blobdload.asp?BloblD=7390.
12. ISO, ISO 8178-2, Reciprocating Internal Combustion Engines: Exhaust Emission Measurement. Part-2: Measurement of gaseous and particulate exhaust emissions at site. *International Organization of Standardization.* **1996**.
13. Agrawal, H., et al., In-use gaseous and particulate matter emissions from a modern ocean going container vessel. *Atmospheric Environment*, **2008**. 42(21): p. 5504-5510.
14. Agrawal, H., et al., Emission measurements from a crude oil tanker at sea. *Environmental Science & Technology*, **2008**. 42(19): p. 7098-7103.
15. *International Organization for Standardization.* **1996**. First edition(8178-4).
16. Protection of the environment. Title 40. Section 86 and 89. *Code of Federal Regulations.*
17. Petzold, A., et al., Physical Properties, Chemical Composition, and Cloud Forming Potential of Particulate Emissions from a Marine Diesel Engine at Various Load Conditions. *Environmental Science & Technology*, **2010**. 44(10): p. 3800-3805.
18. NIOSH, NIOSH Manual of Analytical Methods; National Institute of Occupational Safety and Health: Cincinnati, OH. **1996**.
19. California Air Resources Board. Emissions Estimation Methodology for Ocean-Going Vessels. October **2005** http://www.arb.ca.gov/regact/marine2005/appd.pdf.
20. U.S. Environmental Portection Agency. Current Methodologies and Best Practices in Preparing Port Emission Inventories: final report; April, **2009**;

http://www.epa.gov/sectors/sectorinfo/sectorprofiles/ports/ports-emission-inv-april09.pdf.

21. Agrawal, H., Welch, W.A., Henningsen, S., Miller, J.W., Cocker, D.R. Emissions from Main Propulsion Engine on Container Ship at Sea. *Journal of Geophysical Research*, vol 115, D23205, 7 PP., **2010**.
22. EEIA for Sierra Research, for EPA, Analysis of Commercial Marine Vessels Emissions and Fuel Consumption Data, Feburary **2000**. *Sierra Research Work Assignment No. 1-10*. EPA420-R-002.
23. The Port of Los Angeles. Port of Los Angeles Inventory of Air Emissions-**2009**. http://www.portoflosangeles.org/DOC/REPORT_Air_Emissions_Inventory_2009.pdf.
24. Bowman C. Kinetics of Pollutant Formation and Destruction in Combustion. *Progress in Energy and Combustion Science* **1975**;1:33-45.
25. Heywood J. Pollutant Formation and Control in Internal Combustion Engine Fundamentals. New York: McGraw-Hill; **1988** pp 567-667.
26. Nenes, A., Pilinis, C., Pandis, S.N. (1998) ISORROPIA: A New Thermodynamic Model for Multiphase Multicomponent Inorganic Aerosols, Aquat. Geochem., 4, 123-152.
27. Fountoukis, C. and Nenes, A. (2007) ISORROPIA II: A Computationally Efficient Aerosol Thermodynamic Equilibrium Model for K+ - Ca2+ - Mg2+ - NH4+ - SO42- - NO3- - - Cl- - H2O Aerosols, Atmos. Chem. Phys., 7, 4639-4659.
28. ISORROPIA. http://nenes.eas.gatech.edu/ISORROPIA.

29. Corbett, J.J., Winebrake, J.J., Green, E.H., Mortality from ship emissions: A global assessment. *Environ. Sci. Technol.* **2007**, 41 (24), 8512-8518.

30. Winebrake, J.J., Corbett, J.J., Green, E.H., Lauer, A., Mitigating the Health Impacts of Pollution from Oceangoing Shipping: An assessment of Low-Sulfur Fuel Mandates. *Environ. Sci. Technology*. **2009**, 43 (13), 4776-4782.

31. POLA. Port of Los Angeles-Inventory of Air Emissions 2009. http://www.portoflosangeles.org/DOC/REPORT_Air_Emissions_Inventory_2009.pdf

32. Khan, M.Y., Giordano, M., Gutierrez, J., Benefits of Two Mitigation Strategies for Container Vessels: Cleaner Engines and Cleaner Fuels. Environ. Sci. Technology. **2012**, 46, 5049-5056.

33. U.S. Environmental Protection Agency (USEPA). Current Methodologies in Preparing Mobile Source Port-Related Emission Inventories. Final Report. April 2009. http://www.epa.gov/cleandiesel/documents/ports-emission-inv-april09.pdf

34. CARB. http://www.arb.ca.gov/regact/2008/fuelogv08/fuelogv08.htm; Appendix D, Table II-6 to II-8

35. Port of Los Angeles Inventory of Air Emissions-2010. http://www.portoflosangeles.org/pdf/2010_Air_Emissions_Inventory.pdf

Chapter Seven: Evaluation of Hybrid Retrofit System for a Tugboat

7.1. Abstract

Emissions from harbor craft are a significant source of greenhouse gases and criteria pollutants associated with port activities. In this study, emissions of criteria pollutants and greenhouse gases are reduced by retrofitting the drive train with a hybrid configuration, replacing one auxiliary engine with a larger, low emission engine and adding batteries. The project involved three phases. The first phase of the study was to measure emissions from the main and auxiliary engine on the conventional tug using ISO 8178 guidelines and to ensure that these engines are representative of engines in their category and emissions are within certification limits. The second phase of the study was to confirm that the emissions from the new auxiliary engine were within certification limits and to establish weighing factors for the operating modes of the hybrid tug. The weighting factors were determined by logging engine load, rpm, fuel consumption rate and other parameters from all four engines and current and voltage from batteries for a period of 45 days. The weighting factors were found to be 0.13 for Shore Power, 0.38 for Stop, 0.02 for Idle, 0.14 for Transit (includes Transit 1& Transit 2) and 0.33 for Assist (includes barge move). The third phase of this study involved combining the activity and emissions data to calculate the overall in-use

emissions from tug prior and after retrofit. Emission reductions with the hybrid technology were 29% for $PM_{2.5}$, 31% for NOx and 30% for CO_2.

7.2. Introduction

As harbor craft operate within the ports and near populated communities, their emissions can have a significant impact on the health of people living there. Furthermore, most of the harbor craft operate with diesel engines and diesel exhaust is classified as a toxic by the Air Resources Board and a carcinogen by the United Nation's health agency. Recent regulation has reduced diesel PM by repowering tugs with engines having lower emissions and mandating the use of low-sulfur fuel.

Recently, another prevalent solution to reduce emissions is the use of two or more propulsion sources, commonly known as the hybrid technology, was evaluated. In an earlier project significant emission reductions up to 73 % for $PM_{2.5}$, 51% for NO_x and 27% for CO_2 were observed when a conventional and new built hybrid tug boat were compared. The goal of this study was to evaluate the criteria emissions reduction and fuel economy benefits by retrofitting an existing tug, the *Campbell Foss* with hybrid technology.

This research project was conducted in three phases. In the first phase emissions were measured for the main engines (ME) and auxiliary engines (AE) of the *Campbell Foss* prior to the retrofit to a hybrid. The next phase involves the development of the activity of the hybrid *Campbell Foss* and emissions testing of the new retrofit AE engine according to ISO 8178 D2 and in-use testing based on activity data. A data-logging system, capable of simultaneously monitoring and reporting the status of the power sources was installed for a

period of over one month. Four gigabytes of data were analyzed to determine the weighting factors, i.e., the fraction of time spent by the tug in the six discrete operating modes shore power, stop, idle, transit 1, transit 2 and assist. Further engine histograms for all four engines on the tug at these operating modes were established. The third and final phase of the work involved retesting of new retrofit engine at 1000 hours of operation to ensure durability of emissions profile and combining the activity and emissions data to calculate the overall in-use emissions from the tug prior and after retrofit.

7.3. Approach

The emission benefits of a hybrid tug can be calculated as follows

$$Emission\ Reduction\ \% = \frac{TE_c - TE_h}{TE_c} \times 100 \quad (1)$$

where,

$\boldsymbol{TE_c}$ total in-use emissions for conventional tugboat in g/hr

$\boldsymbol{TE_h}$ total in-use emissions for hybrid tugboat in g/hr

The total in-use emissions of any gaseous or particulate matter species, is determined using the following equation:

$$\boldsymbol{TE} = \sum_{i=1}^{n}[W_i \sum_{j=1}^{m}(E_{ij})] \quad (2)$$

where,

$\boldsymbol{TE}$ total in-use emissions in g/hr

$\boldsymbol{n}$ total number of operating modes

$\boldsymbol{m}$ the total number of power sources on the tug

$\boldsymbol{W_i}$ weighting factor for i^{th} operating mode (See Equation 3)

$\boldsymbol{E_{ij}}$ total in-use emissions in g/hr from the j^{th} power source for the i^{th} operating mode (See Equation 4)

The weighing factors for each operating mode are calculated as follows:

$$\boldsymbol{W_i = \frac{t_i}{t_{total}}} \quad (3)$$

where,

$\boldsymbol{W_i}$ weighting factor for the i^{th} operating mode

$\boldsymbol{t_i}$ time spent by the tug in the i^{th} operating mode

$\boldsymbol{t_{total}}$ total sample time for the tug

As mentioned earlier, tugboats typically have four engines, two for propulsion and two auxiliary generators. To determine the total in-use emissions from each of these engines/power sources the following equation can be used:

$$\boldsymbol{E_{ij} = \sum_{k=1}^{p}[WL_{ijk}\, EL_{jk})]} \quad (4)$$

where,

$\boldsymbol{E_{ij}}$ total in-use emissions in g/hr from the j^{th} power source/engine for the i^{th} operating mode

$\boldsymbol{p}$ total number of operating modes for the j^{th} power source (marine diesel engine). there are twelve operating modes for the engine based on the percentage of maximum engine load: off, 0 to <10%, 10% to <20%, 20% to <30%, and so on until 90% to <100% and 100%.

$\boldsymbol{WL_{ijk}}$ fraction of time spent by the j^{th} power source/engine at its k^{th} operating mode during the i^{th} tug boat operating mode. This value can be obtained from the engine histograms

$\boldsymbol{EL_{jk}}$ emissions in g/hr for the j^{th} power source/engine at its k^{th} operating mode

While developing engine histograms for the hybrid tugboat it is important to ensure that the state of charge of the battery at the start and end time of each sample period chosen for the calculation of the engine histogram are the same. This would eliminate any biases in emissions resulting from operation of the auxiliary generators for charging the batteries. The protocol was adopted after reviewing the hybrid testing protocol adopted by the Society of Automotive Engineers[1](SAE) and California Air Resources Board[2] (CARB) for testing hybrid electric vehicles.

7.4. Test Tugboat

The primary objective of this project was to determine emission benefits of using a hybrid retrofit system on a tugboat. For this purpose, one of the tugboats (*Campbell Foss*) belonging

to Foss' fleet operating in the Port of Los Angeles and Long Beach was retrofitted with hybrid components in addition to the repowering one of the auxiliary engines. Originally, *Campbell Foss* was equipped with EPA Tier 1 marine main and auxiliary diesel engines. During the hybrid retrofit process, one of the auxiliary engines was replaced by an EPA Tier 2 marine auxiliary engine. Details of power sources on the *Campbell Foss* tugboat are described below.

The conventional *Campbell Foss* was powered by two 1902 kW CAT 3512C main engines and two 125 kW John Deere 6081 auxiliary engines (Table 7-1). This tugboat has two Azimuthing stern drives (ASD) for propulsion units. Each main engine was connected through a mechanical drive shaft to each ASD.

Table 7-1: Engine Specifications for *Campbell Foss*

	Main Engine (ME)	**Auxiliary Engine (AE)**
Manufacturer /Model	CAT 3512	John Deere 6081
Manufacture Year	2005	2005
Certification Standard	Tier 1	
Technology	4-Stroke Diesel	4-Stroke Diesel
Max. Power Rating	1902 kW	125 kW
Rated Speed	1800 Rpm	1800 Rpm
# of Cylinders	8	8
Displacement	58.6 liters	8.1 liters

The retrofit hybrid *Campbell Foss* is powered by the original MEs and one of the two original AEs. The other AE was repowered with a new Tier 2 engine (Table 7-2). It also has 10

Lithium Polymer batteries providing a total of 65 kW-hr of energy in a single bank. The batteries are typically charged by the AEs but can be charged from shore power.

Table 7-2: Repowered AE engine Specifications for *Campbell Foss*

	Auxiliary Engine (AE)
Manufacturer /Model	MTU/Detroit Diesel Series 60
Manufacture Year	2011
Technology	4-Stroke Diesel
Certification Standard	Tier 2
Max. Power Rating	350 kW
Rated Speed	1800 rpm
# of Cylinders	6
Displacement	14 liter

In the case of the conventional *Campbell Foss* the main engines were linked mechanically to the propellers through a drive shaft. Therefore both main engines had to be operated for moving and maneuvering the boat. The auxiliary engines were only used for hoteling, lighting, air conditioning and operating the winch motor. However, in case of the hybrid retrofit *Campbell Foss*, there is a motor-generator unit mounted in the shaft line between each engine and ASD. An additional clutch was also fitted between the main engine and motor-generator. With the clutch open, the motor-generator uses electrical power from the batteries and auxiliary engines to drive the shaft for propelling the boat.

With the clutch engaged, the motor-generator is able to produce from the shaft using the main engines or freewheeling propeller (regenerative power). This power is used for charging

the batteries, driving the winch and other hoteling activities of the tug. This means that AE's are not required to be running when the main engines are providing propulsion.

The batteries on the *Campbell Foss* are predominately charged using the power from the auxiliary engines drawn through the DC bus. In the previous ARB[4] study, auxiliary engines in the hybrid tugboat were of higher power rating than conventional tugboat so that they can be used for charging batteries and propelling the tugboat. Therefore, in *Campbell Foss*, one of the JD 6081's was replaced by an engine with a higher power rating.

The hybrid *Campbell Foss* is equipped with an energy management system that manages the power sources and the drive train. A Schematic of the diesel electric drive train is shown in Figure 7-1. The captain on the hybrid tug uses a switch in the wheelhouse to communicate the desired operating mode of the tug to the energy management system. The signal from this wheelhouse switch helps the energy management system in making decisions regarding the number of power sources required to operate the tug.

7.5. Test Schedule

The testing program was conducted over the period of 13 months which included data logging for approximately 37 days to determine the activity of the hybrid tugboat and emissions measurement from main and auxiliary engines.

According to the test plan, activity of the tugboat was to be logged for at least continuous 30 days. However, due to technical issues with the Hybrid tugboat and data logger, data was obtained intermittently for nine to nineteen days period. Thus, activity data was logged for more than 30 days to ensure that the logged activity is representative of tugboat operation.

Table 7-3 shows the schedule for data logging on the Hybrid tugboat. Details of the data logging procedure and analysis to determine the tugboat activity are provided in section 7.6.

Table 7-3: Data Logging Test Schedule

Tugboat	Start Date	Stop Date
Hybrid Campbell	5/25/2012	6/6/2012
	6/9/2012	6/17/2012
	6/21/2012	7/9/2012

Emissions testing of main and auxiliary engines were performed in three phases. A brief description of these phases is provided below. Test schedules for Phase *I*, *II* and *III* are provided in Table 7-4. Further details on emissions testing and analysis are presented in section 7.7.

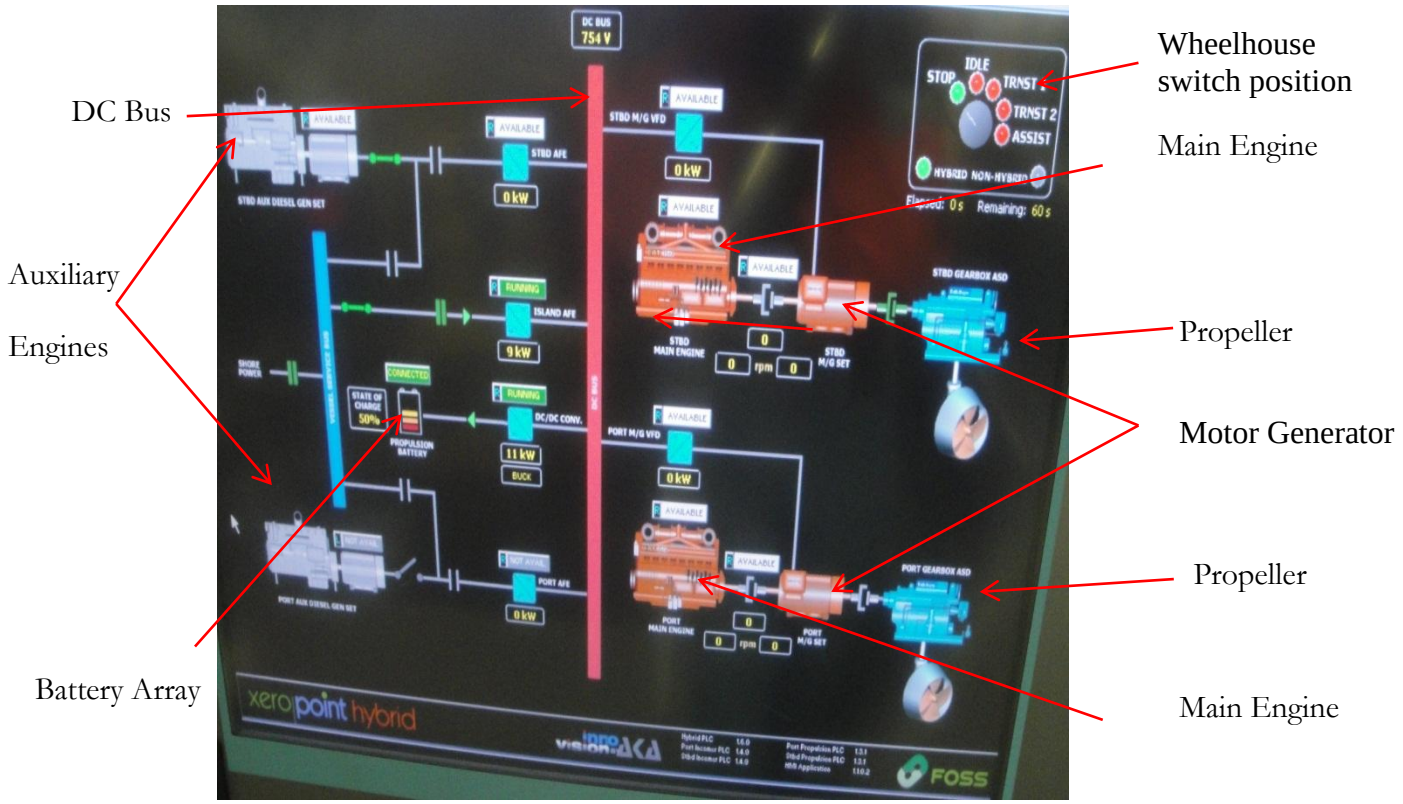

Figure 7-1: Diesel Electric Drive Train on the Hybrid *Campbell Foss*

Phase I involves testing one ME and one AE from the *Campbell Foss* tug prior to retrofit following the load points in the ISO 8178 E3 (ME), ISO 8178 D2 (AE) and the in-use load points determined in the previous ARB report[4].

Phase II involves the testing of the new retrofit AE engine according to ISO 8178 D2 and in-use load points.

Table 7-4**:** Test Schedules for Emissions Testing *Phase I*, *II* and *III*

Phase	Tugboat	Engine	Date
I	Conventional	CAT 3512C	6/27/2011
		JD 6081	6/28/2011
II	Hybrid	MTU/Detroit Series 60	3/21/2012
III	Hybrid	MTU/Detroit Series 60	7/12/2012

Phase III involves retesting the new retrofit AE engine after the 1000 hour operation according to ISO 8178 D2 test cycle and in-use load points. This test was required to show the durability of the new engine over time.

7.6. Determining Tugboat Activity

The following sections describe the typical operating modes of the tug boat, procedure for data collection and analysis to establish the weighing factors for each operating mode as well as development of engine histograms for all four engines on the tugboat.

7.6.1. Tug Operating Modes

There are five operating modes pre-determined for the hybrid *Campbell Foss*. These operating modes are *Stop*, *Idle*, *Transit 1*, *Transit 2* and *Assist*. In addition to these modes, *Shore Power* was determined from in-use activity data.

Shore Power: The tug is at the dock plugged into shore power for its utilities. None of the engines are operating during this mode. The hybrid boat spends considerable amount of time plugged into shore power. The conventional boat also spends similar amount of time plugged into shore power when at dock. During this time, batteries can be charged.

Stop: During this operation the tug boat is at the dock (shore power is unavailable) with batteries or one auxiliary engine supplying power for the lights and air-conditioning on the boat. On the conventional tug one auxiliary engine is always on at *Stop*. The hybrid tug switches between one auxiliary engine and batteries during this mode. If the state of charge (SOC) of the battery arrays reduce to 20% the 125 kW auxiliary engine will turn on to charge the batteries and provide hoteling power for the tug. As soon as the batteries are charged to a SOC of 95% the engine turns off and the batteries discharge providing hoteling power.

Idle: In this mode the tug is idling at sea waiting for a vessel to arrive or a call from the dispatch office to start or transit to a job. The conventional tug operates two main propulsion engines and one auxiliary generator during *Idle*. As in the case of *Stop* the hybrid tug switches between the batteries and one auxiliary engine.

Transit 1: The mode refers to the movement of the tug between jobs and to and from different docks. The conventional tug boat operates two main engines and one auxiliary

engine during transit. The hybrid boat operates its 350 kW auxiliary engine for transit at <6.0 knots within the port. The auxiliary engine also provides power for battery charging and hotel loads.

Transit 2: This mode is available to provide transit speeds up to approximately 7.5 knots. In this mode the 350 kW and 125 kW auxiliary engines provide power for propulsion, battery charging and hotel load. Main engines are rarely operated during *Transit 2* in the hybrid tugboat.

Assist: Tug boats typically perform two kinds of jobs in the ports – a) assisting ships from berth to sea and vice-versa b) moving barges from one location to another. In this study, both jobs are considered under *Assist* as both main engines are operating irrespective of job nature. The conventional tug operates two main engines and one auxiliary engine during this mode. The hybrid boat operates both main engines. A 350 kW auxiliary engine rarely operates during *Assist*.

Tables 7-5 and 7-6 show the operating details for the conventional and hybrid tug boats during each mode.

Table 7-5: Operating modes of conventional tugboat

Operational Modes	ME#1 CAT 3512C	ME#2 CAT 3512C	AE#1 JD 6081	AE#2 JD 6081
Shore Power	Off	Off	Off	Off
Stop	Off	Off	On	Off
Idle	On	On	On	Off
Transit 1	On	On	On	Off
Transit 2	On	On	On	Off
Assist	On	On	On	Off

Table 7-6**:** Operating modes of hybrid tugboat. ME: *Main Engine*; AE: *Auxiliary Engine*

Operational Modes	ME#1 CAT 3512C	ME#2 CAT 3512C	AE#1 DETROIT	AE#2 JD 6081	Battery
Shore Power	Off	Off	Off	Off	Off
Stop	Off	Off	Off	On (as needed)	On
Idle	Off	Off	Off	On (as needed)	On
Transit 1	Off	Off	On	Off	Off (Charging)
Transit 2	Off	Off	On	On	Off (Charging)
Assist	On	On	Off	Off	On (as needed)

To determine the activity of the hybrid tug GPS, engine and battery data had to be logged continuously for a period of over one month. For this purpose, a Labview program was developed that was capable of interfacing with four engine electronic control modules (ECMs), a GPS and batteries to retrieve the required information continuously on a second by second basis and write it into a comma separated value (CSV) file. Each line in the CSV file generated by the code represents one second. The program automatically creates a new file after 65500 seconds thereby ensuring that the CSV file is not too large for Microsoft Excel to handle. This Labview program was installed and operated on the data-logger which is a computer with Windows XP operating system. The Labview program was incapable of logging ECM signals from two different protocols. Therefore, MTU/Detroit diesel engine which was sending 1708 signals was recorded separately on the laptop with the same Labview program. Table 7-7 lists all the parameters that were logged from the tugboat along with the devices used for interfacing between the power sources and the data-logger.

Schematic of the data-logger set up on the hybrid tugboat is provided in Figures 7-2. The data-logger and the laptop were placed on the workbench in the engine room of tug boat.

Data from the ECMs on the two main propulsion engines and the two auxiliary engines were obtained using four Dearborn Protocol Adapters that convert the J1939 and 1807 signals to serial/RS-232 signals. Power for the Dearborn adapters was obtained from the batteries used for engine startup.

A Garmin GPS that provides data on location, speed and course of the tug at any second during the sample time was placed at the top of the mast on the tug boat to ensure that it receives a clear signal. Serial cables were run from GPS to the data-logger.

The hybrid tug has a switch in the wheelhouse that used by the captains for operating the boat. This wheelhouse switch communicates with an energy management system to determine how many power sources will be required for that operation. The wheelhouse switch has five positions which indicate the mode of operation of the tug. These are listed below:

1 - Stop Tug switches between the batteries and one auxiliary engine.

2 - Idle Tug switches between the batteries and one auxiliary engine.

3 - Transit 1 Tug uses one auxiliary engine (JD 6081 – 125kW).

4 – Transit 2 Tug uses both auxiliary engines.

5 - Assist Tug uses both main and the batteries (if needed) for a job.

AKA provided us with five digital signals, indicating the operating mode of the hybrid tugboat. They also provided us with three analog signals that give information on the operation of the battery array

1 - State of Charge of Battery Array

2 - Voltage of Battery Array

3 - Current for Battery Array

The wireless network on the boat was not strong enough for file transfer. Therefore the port engineer uploaded the CSV files on a weekly basis to a file transfer protocol (FTP) site.

	HT	Devices Used	Parameters Logged
GPS	√	Garmin GPS 18 PC receives wireless signal from satellite and transmits it through a serial port to the data-logger	Date, time, latitude, longitude, speed and course
Two main propulsion engines and two auxiliary engines	√	4 Dearborn Protocol Adapters Model DG-DPAIII/i that receive J1939 and 1708 signal from engine electronic control modules (ECM) 4 Dearborn Protocol Adapter cables (DG-J1939-04-CABLE) that convert the J1939 signal to serial/RS232 signal, One USB2-4COM-M that receives 4 serial signals and transmits them through one USB port to the data-logger	Engine speed (rpm), engine load (percentage of maximum load at the engine speed), instantaneous fuel flow rate (cc/min), inlet manifold temperature (°F) and pressure (kPa)
Wheelhouse Switch	√	5 Philmore 86-124 (24 vDC, 10 A) SPDT relays convert the signals from wheelhouse switch to digital voltage signals. Omega's USB-1608FS box receives these five digital signals from the relays and transmits them through a single USB cable to the data-logger.	Operating Modes: Stop, Idle, Transit 1, Transit 2 and Assist
Battery Array	√	Omega's USB-1608FS box that receives three analog signals from the battery array and transmits them through a single USB cable to the data-logger.	State of charge, voltage in volts and current in amps from battery array.

Table 7-7: Details of Data-Logger

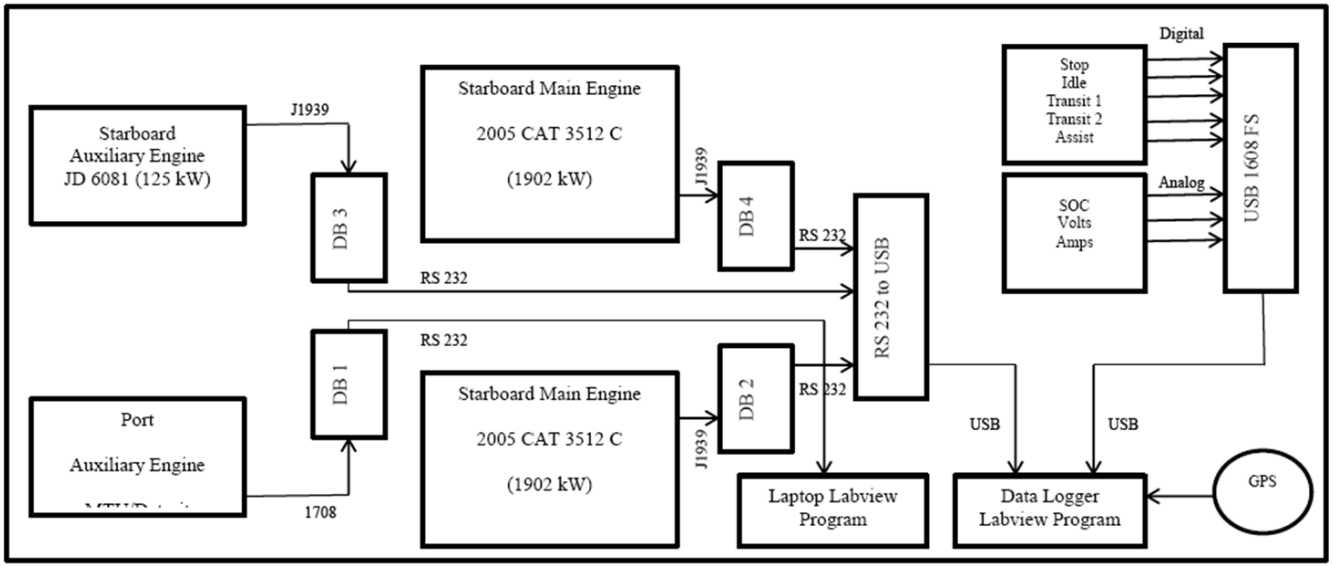

Figure 7-2: Schematic of Data-Logging system on a Hybrid Tugboat

7.6.2. Establishing Weighting Factors for Tugboat Operating Modes

The weighing factor for each operating mode was calculated as the ratio of the time spent by the tug in that mode to the total sample time (Equation 3). The CVS files obtained from data logger have five columns which represent five (*Stop*, *Idle*, *Transit 1*, *Transit 2*, *Assist*) operating modes of the tugboat. Depending upon the mode, tugboat is involved in; digital signals from Energy Management System will feed a value "1" to the data logger and "0" for rest of the operating modes. For example, when tugboat is in *Assist* mode, *Assist* column in the CVS file will be represented by "1" and rest of modes will be represented by "0". Therefore, in each CVS file, sum of individual operating modes represents the time spent by tug in those operating modes. Hence, weighting factor for each operating mode was obtained as the ratio of the time spent by the tug in that mode to the total sample time. Please note that the weighting factors for the conventional tugboat (prior to retrofit) are assumed to be same as hybrid tugboat.

7.6.3. Developing Engine Histograms

Engine histograms are basically graphs showing the amount of time the engine spends at different loads. In this project engine histograms have to be developed for all four engines for each tug operating mode. During the data logging procedure the engine speed in rpm and engine load as a percentage of the maximum load at that speed were retrieved from the engines' ECMs and written into the CSV files. For the auxiliary engines which are constant speed diesel generators, the percent load from the ECM has to be multiplied by the

maximum rated load of the engine in kW to get the load on the engine. The main propulsion engines are variable speed engines. Therefore, at any given speed the maximum attainable load in kW was obtained from the engines' lug curve and multiplied by the percent load retrieved from the ECM to determine the load on the engine. The Lug Curve for the main engine was obtained from the ARB[4] study.

The ratio of the carbon-dioxide emissions to the load on the engine is an indication of its thermal efficiency. This efficiency tends to be relatively constant across the entire range of engine operation. Therefore we would expect a straight line relationship between the engine load and the CO_2 emissions in kg/hr. Any significant deviation from the straight line relationship will indicate an error in the load readings provided by the ECM. Figure 7-3 to 7-5 shows plots of ECM load versus the measured CO_2 emissions in kg/hr for the main engine and auxiliary engines tested for emissions.

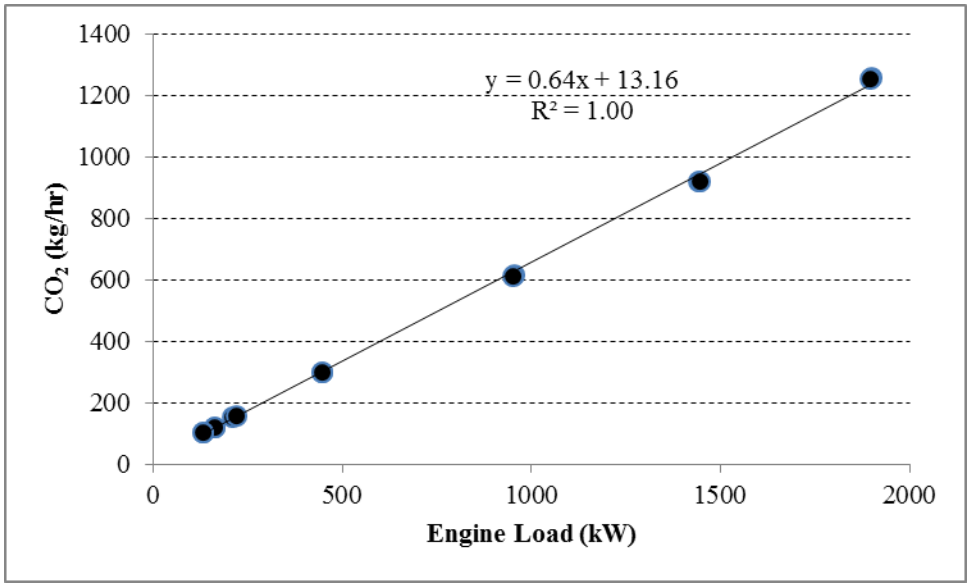

Figure 7-3: ECM load versus CO_2 emissions for the main engine (CAT 3512 C)

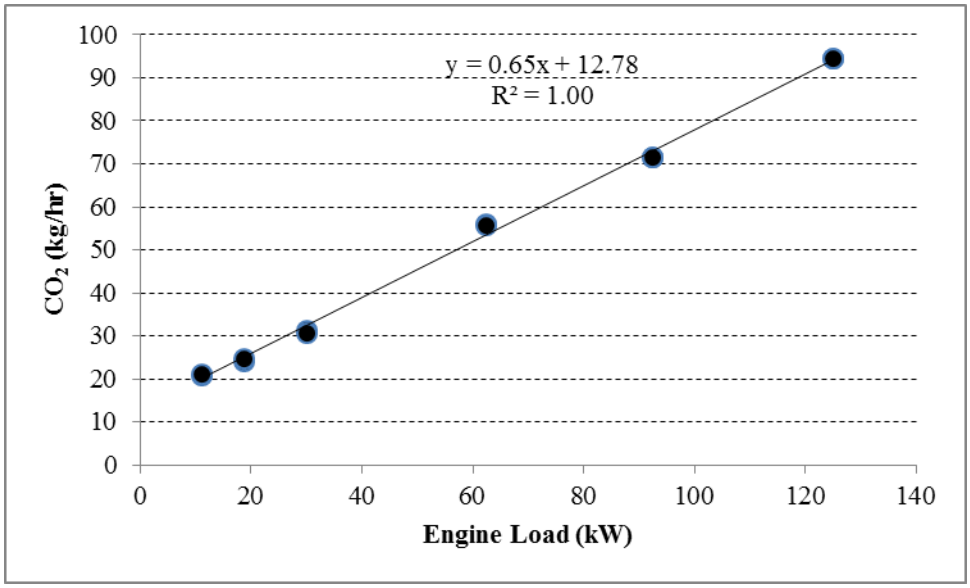

Figure 7-4: ECM load versus CO_2 emissions for the auxiliary engine (JD 6081)

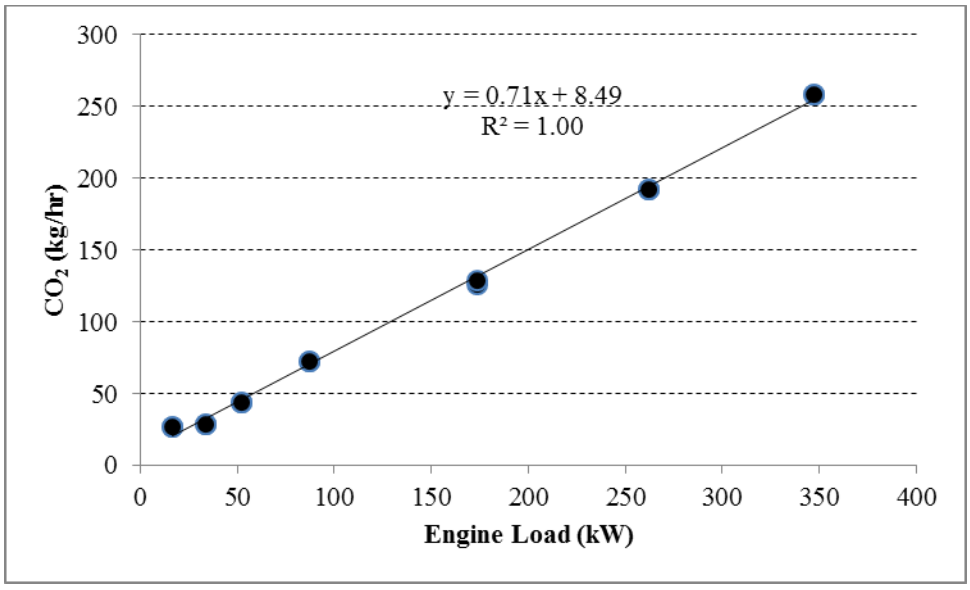

Figure 7-5: ECM load versus CO_2 emissions for the auxiliary engine (MTU/Detroit)

Within each CVS file, five more spreadsheets were added to represent five operating modes of the tugboat. Based on the digital value of "1" obtained from energy management system to indicate the engaged operating mode, data in CVS file was filtered and added to the respective operating mode spreadsheet. Within each operating mode spreadsheets, engine loads were split into twelve bins for all four engines:

Bin	load range	no. of data points in each Bin
Bin 0	0%	Bin 0
Bin 1	<10%	Bin 1- Bin 0
Bin 2	10% to <20%	Bin 2- Bin 1
Bin 3	20% to <30%	Bin 3- Bin 2
Bin 4	30% to <40%	Bin 4- Bin 3
Bin 5	40% to <50%	Bin 5- Bin 4
Bin 6	50% to <60%	Bin 6- Bin 5
Bin 7	60% to <70%	Bin 7- Bin 6
Bin 8	70% to <80%	Bin 8- Bin7
Bin 9	80% to <90%	Bin 9- Bin 8
Bin 10	90% to <100%	Bin 10- Bin 9
Bin 11	<101%	Bin 11- Bin 10

Using this data the fraction of time spent by the engine in any bin for a particular operating mode was calculated. This was then plotted in the form of engine histograms. The engine histograms developed from the CSV files are used to calculate the total emissions from a tug. Therefore it is important to ensure that the state of charge of the battery at the start and end

time of each sample period chosen for the calculation of the engine histogram are the same. This would eliminate any biases in emissions resulting from the use of the auxiliary engine for charging the batteries. This protocol was adopted based on the guidelines in the SAE[1] and CARB[2] testing protocols for hybrid electric vehicles.

7.7. Emissions Testing Procedure

7.7.1. Test Engines

Conventional *Campbell Foss* was powered by two main propulsion engines and two auxiliary engines/generators. The main engines (ME) CAT 3512 Tier 1 marine diesel engines while the auxiliary engines (AE) John Deere 6081 diesel engines (Table 7-8). The MEs were used for propulsion and the AEs were used for hoteling, lighting, air conditioning and to operate the winch motor.

Table 7-8: Engine Specifications for Conventional *Campbell Foss*

	Main Engine (ME)	**Auxiliary Engine (AE)**
Manufacturer /Model	CAT 3512	John Deere 6081
Manufacture Year	2005	2005
Certification Standard	Tier 1	
Technology	4-Stroke Diesel	4-Stroke Diesel
Max. Power Rating	1902 kW	125 kW
Rated Speed	1800 Rpm	1800 Rpm
# of Cylinders	8	8
Displacement	58.6 liters	8.1 liters

The retrofit hybrid *Campbell Foss* is powered by the original MEs and one of the two original AEs. The other AE was repowered with a new Tier 2 engine (Table 7-9).

Table 7-9: Engine specifications of new Auxiliary Engine

	Auxiliary Engine (AE)
Manufacturer /Model	MTU/Detroit Diesel Series 60
Manufacture Year	2011
Technology	4-Stroke Diesel
Certification Standard	Tier 2
Max. Power Rating	350 kW
Rated Speed	1800 rpm
# of Cylinders	6
Displacement	14 liter

7.7.2. Fuels

The project used commercial #2 diesel fuel meeting specification requirements of the California Air Resources Board and the ASTM 975. Typically, the sulfur content in the fuel is < 10ppmw.

7.7.3. Test Cycle and Operating Conditions

Phase I: The primary goal of this phase of the testing program was to establish if the test engines meet their certification standards when in-use. Gaseous and $PM_{2.5}$ emission measurements on these engines were made based on the ISO 8178-1 protocol.[3] Briefly, a partial dilution system with a venturi was used for $PM_{2.5}$ sampling. Carbon dioxide, nitrogen oxides and carbon monoxide were measured in both the raw and the dilute exhaust. The

ratio of the concentration of carbon dioxide in the raw to the in the dilute was used to determine the dilution ratio for $PM_{2.5}$ sampling.

The main propulsion engines were tested following the steady state load points in the ISO 8178-4 E3 cycle.[5] It has been found in the previous study that main engine spent significant amount of time at loads below 25%. Also, engine histogram (Figure 7-6) obtained from ECM clearly indicated that main engine was operated under 25% load for approximately 80% of its time. Therefore, an additional measurement was made at the 15% and 10% of engine load. The auxiliary engines were operated at the steady state load points in the ISO 8178-4 D2 cycle and at 15% engine load. Details of the test cycles are provided in Appendix B.

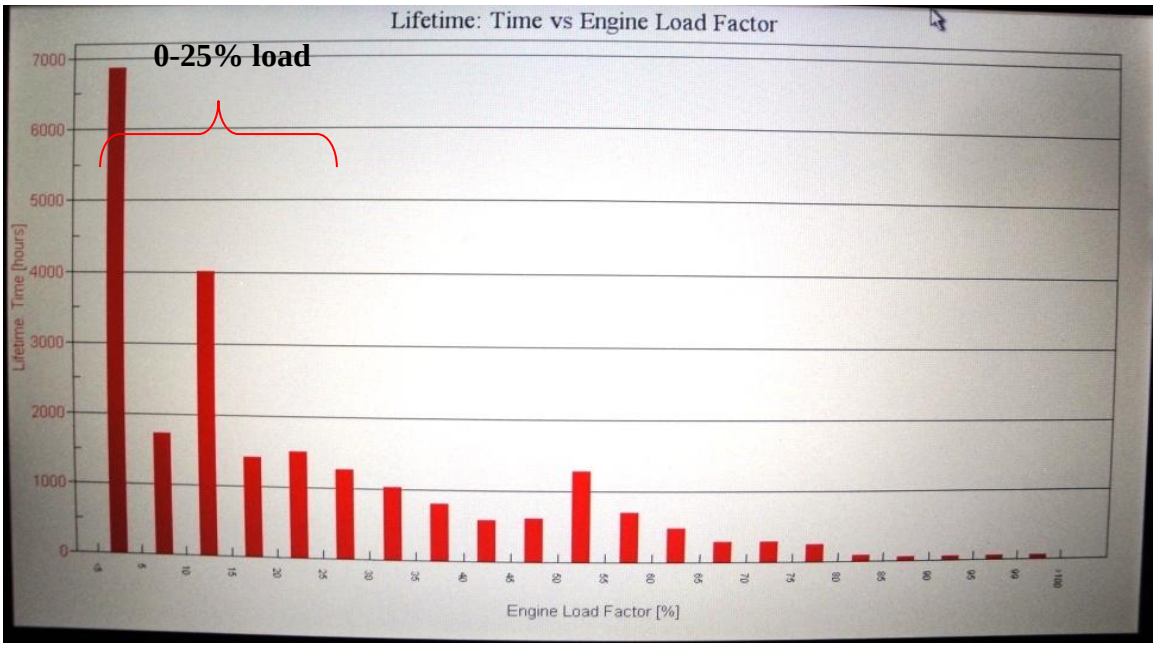

Figure 7-6: Engine Histogram Obtained from the ECM of the Main Engine on the *Campbell Foss*

The steady state load points on the main engine of the conventional tug were achieved while the tug pushed against the pier. Since the auxiliary generator on the conventional tug is not used for propulsion and the typical steady state load on this engine is 12% of its maximum load, a load bank had to be used to achieve the higher load points. Due to practical considerations, the actual engine load at each test mode on all four engines could differ by a factor of ±5% from the ISO target load. Table 7-10 lists the test matrix for Phase *I* of emissions testing.

Table 7-10: Test matrix of emissions testing of *Phase I*

Tug Boat	Engine	DATE	Engine Loads
Campbell	CAT 3512 C	6/27/2011	RT & ISO: 100%, 75%, 50%, 25%, 15%, 10%
Conventional	JD 6081	6/28/2011	RT & ISO: 100%, 75%, 50%, 25%, 15%, 10%

RT: Real Time Monitoring and Recording of Gaseous Emissions; ISO: Filter Samples taken in accordance with ISO 8178-4 E3/D2 cycles

At each steady state test mode the protocol requires the following:

1. Allowing the gaseous emissions to stabilize before measurement at each test mode.
2. Measuring gaseous and $PM_{2.5}$ concentrations for a time period long enough to get measurable filter mass
3. Recording engine speed (rpm), displacement, boost pressure and intake manifold temperature in order to calculate the mass flow rate of the exhaust.

Phase II: It involves the emissions testing of new retrofit AE engine according to ISO 8178 D2 and in-use load points. Test matrix for *Phase II* is shown in Table 7-11.

Phase III: involves retesting the new retrofit AE engine after the 1000 hour operation at the harbor according to ISO 8178 D2 test cycle and in-use load points. This test was required to

show the durability of the new engine over time. Test matrix for *Phase III* is shown in Table 7-11.

Table 7-11: Test matrix of emissions testing of *Phase II* and *III*

Phase	Tugboat	Engine	Date	Engine Loads
II	Hybrid	MTU/Detroit	3/21/2012	RT &ISO: 100%, 75%, 50%, 25%, 15%, 10%, 5%
III	Campbell	MTU/Detroit	7/12/2012	RT &ISO: 100%, 75%, 50%, 25%, 15%, 10%, 5%

RT: Real Time Monitoring and Recording of Gaseous Emissions; ISO: Filter Samples taken in accordance with ISO 8178-4 E3/D2 cycles

7.7.4. Sampling Ports

Only one sample port was available in the stack of each engine. A T- joint was installed at the end of the sample probe to provide raw gas sample for gaseous measurements and dilution for $PM_{2.5}$ sampling. Sample ports on both main and auxiliary engines were located before the muffler. For the main propulsion engines, the sample port was located just a few inches above the exhaust manifold while on the auxiliary engines it as several feet away from the manifold. The sampling probes used for emissions testing were $3/8^{th}$ inch stainless steel tubing. These probes were inserted five inches into the main engine stacks (stack diameter: fourteen inches) and two in into the auxiliary engine stack (stack diameter: six inches). These distances were sufficiently away from any effects found near the stack walls. Figure 7-7 and Figure 7-8 show pictures of installed setup for sampling gaseous and particulate emissions from auxiliary and main engines of the conventional *Campbell Foss* tug.

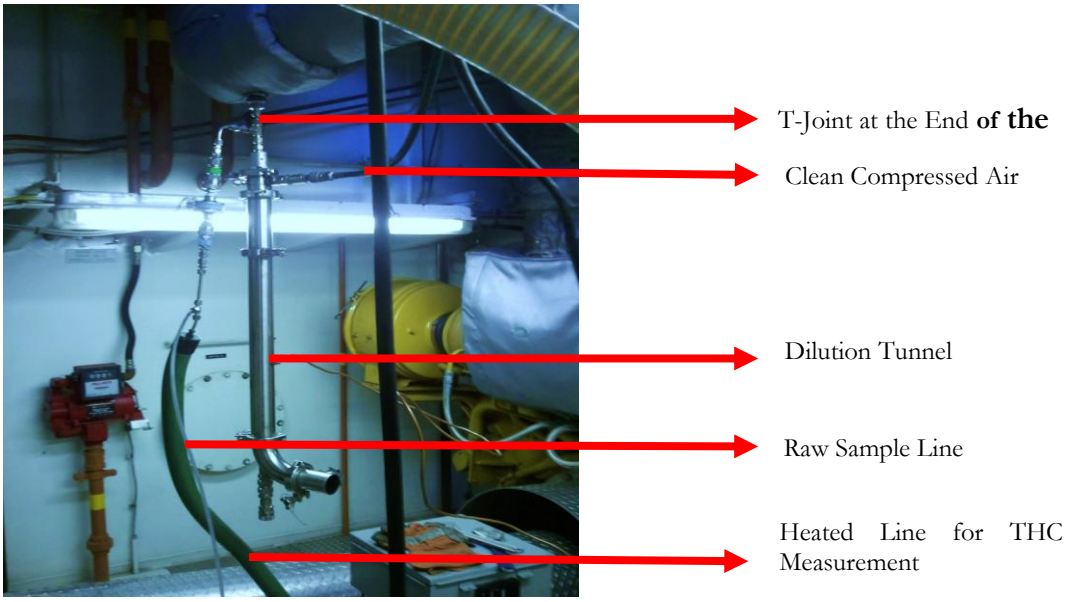

Figure 7-7 Sampling port for Auxiliary engine on conventional *Campbell Foss* tug boat

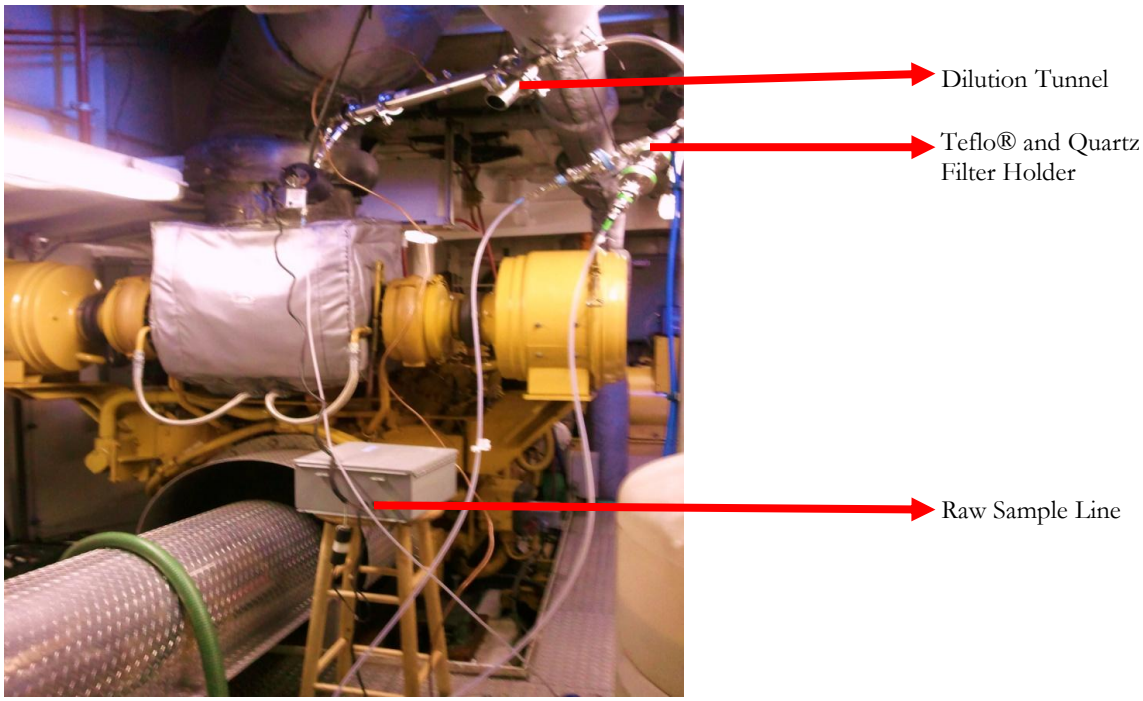

Figure 7-8 Sampling port for Main engine on conventional *Campbell Foss* tug boat

7.7.5. Measuring Gases and $PM_{2.5}$ emissions

The concentrations of carbon dioxide (CO_2), nitrogen oxides (NO_x) and carbon monoxide (CO) were measured both in the raw exhaust and the dilution tunnel with a Horiba PG-250 portable multi-gas analyzer. During Phase I particulate matter ($PM_{2.5}$) was sampled from the dilution tunnel on Teflo® and Tissuquartz filters. These filters were analyzed to determine the total and speciated $PM_{2.5}$ mass emissions.

7.7.6. Calculating Exhaust Flow Rates

Carbon Balance Method: The calculated emission factor is strongly dependent on the mass flow of the exhaust. Two methods for calculating the exhaust gas mass flow and/or the combustion air consumption are described in ISO 8178-1. Both methods are based on the measured exhaust gas concentrations and fuel consumption rate. The two ISO methods are described below.

Method 1, Carbon Balance, calculates the exhaust mass flow based on the measurement of fuel consumption and the exhaust gas concentrations with regard to the fuel characteristics (carbon balance method). The method is only valid for fuels without oxygen and nitrogen content, based on procedures used for EPA and ECE calculations.

Method 2, Universal, Carbon/Oxygen-balance, is used for the calculation of the exhaust mass flow. This method is applicable for fuels containing H, C, S, O and N in known proportions and does not apply here since the fuel contains only carbon and hydrogen.

The carbon balance methods may be used to calculate exhaust flow rate when the fuel consumption is measured and the concentrations of the exhaust components are known. In these methods, flow rate is determined by balancing carbon content in the fuel to the measured carbon dioxide in the exhaust. This method can only be used when the fuel consumption data are available.

For both main and auxiliary engine on the tug, fuel consumption rate was recorded from ECM. It was used in calculating exhaust flow rate by carbon balance method. Intake manifold temperature and boost pressure readings were obtained from the main engine ECM. These were used for the exhaust flow calculation based on the intake air method. Boost pressure was not retrievable from the auxiliary engine; therefore calculation based on the intake air method was not performed.

7.7.7. Calculation of Engine Load

The actual load on the engine at each test modes is required to calculate the modal and overall emission factors in g/kW-hr. The engine ECM provides engine speed and the percentage of the maximum engine load at that speed. For the main propulsion engines, this data was used along with the lug curve provided by the manufacturer for that engine family to determine the actual load in kW for each test mode. For the constant speed auxiliary engines the % of maximum engine load obtained from the engine ECM was multiplied by the engine's rated prime power to get the load on the engine in kW.

7.7.8. Calculation of Emissions in g/hr

Mass emissions of CO_2, NO_x and CO in g/hr were calculated using the calculated exhaust flows and the measured concentrations in the exhaust. For $PM_{2.5}$ mass emissions the concentration in the dilute exhaust was calculated as a ratio of the measured filter weight to the total sample flow through the filter. This was then converted to a concentration in the raw exhaust by multiplying with the dilution ratio. The raw $PM_{2.5}$ concentration was used along with the exhaust flow to determine the mass emissions in g/hr.

7.7.9. Calculation of Emission Factors in g/kW-hr

The emission factor at each mode is calculated as the ratio of the calculated mass flow (g/hr) in the exhaust to the reported engine load (kW).

An overall single emission factor representing the engine is determined by weighting the modal data according to the ISO 8178 E3 or ISO 8178 D2 cycle requirements and summing them. The equation used for the overall emission factor is as follows:

$$EF_{WM} = \frac{\sum_{i=1}^{n}(g_i \times WF_i)}{\sum_{i=1}^{n}(P_i \times WF_i)} \quad (5)$$

where:

$\boldsymbol{EF_{WM}}$ Overall weighted average emission factor in g/kW-hr

$\boldsymbol{n}$ Total number of modes in the ISO duty cycle

$\boldsymbol{g_i}$ Calculated mass flow in g/hr for the i^{th} operating mode

$\boldsymbol{WF_i}$ weighing factor for the i^{th} operating mode

$\boldsymbol{P_i}$ Engine load in kW for the i^{th} operating mode

7.8. Results and Discussions

7.8.1. Emissions Testing *Phase I*

The primary gaseous emissions measured during this test program include a greenhouse gas carbon dioxide (CO_2), and the criteria pollutants: nitrogen oxides (NO_x), carbon monoxide (CO). Each of these gaseous species was measured using the ISO standard instrumentation. In addition to gaseous emissions, the $PM_{2.5}$ mass emissions and the speciated $PM_{2.5}$ emissions as elemental carbon (EC) and organic carbon (OC) were measured. As described earlier, the PM mass in the raw exhaust was sampled using a partial dilution method and collected on filter media. A detailed list of the modal gaseous and $PM_{2.5}$ emissions in g/hr and g/kW-hr, for the two test engines are provided in Tables 7-12 and 7-13 respectively. In the previous study, activity data developed for the tug boat reflected that the tug spends significant amount of time while operating between 10-20% engine loads. Therefore, emissions at 15% load for auxiliary engine, and 10% and 15% for main engine were tested in addition to load specified in ISO 8178 for engine certification.

Duplicate measurements were made at steady state test mode. Each gaseous measurement was a three to seven minute average of one hertz data obtained from the instrument. The standard deviation of three to seven minute averages was <2% for CO_2. This indicates that the load on the engine while testing that mode was steady, thereby validating the measurement at each of those test modes. In the case of $PM_{2.5}$, each measurement refers to a

filter sample. The range across these duplicate measurements is shown as error bars in the Figures 7-9 and 7-10.

Modal emissions data represented in Table 7-13 are helpful in developing emission inventories of tugboat. High emission factors are observed at loads 25% or below for both engines. This is consistent with our observations and the fact that brake-specific fuel consumption increases significantly at these load points.

Table 3-2 also lists the overall weighted average emission factors for both of the test engines. It also shows the EPA Tier 1 standard for that each test engine family. The overall weighted average for auxiliary engine (JD 6081) is well below EPA Tier 1 standards for NO_x and $PM_{2.5}$. Moreover, EF_{CO} is comparatively very low which is typical of diesel engines. In case of Main engine (CAT 3512 C); overall weighted emission factors are also below EPA Tier 1 limit. $EF_{PM2.5}$ is significantly lower than standard which is similar to previous study. The speciated $PM_{2.5}$ data suggests that for both engines, organic fraction of total PM dominates at lower loads ($\leq$ 25%) and elemental carbon at loads above 25%.

Overall, *Phase I* study concludes that the both engines are well maintained; their emissions are within certification limits and are representative of engines in their category.

Table 7-12: Results for *Phase I* of Emissions Testing in g/hr

Load		NO_x	CO	CO_2	THC	$PM_{2.5}$	EC	OC
Target	**Actual**	**g/hr**						
Auxiliary Engine on Conventional Campbell Tug JD 6081								
10%	9%	242	42	20920	9.2	8.6	0.8	4.6
15%	15%	278	39	24463	13	8.6	1.3	5.2
25%	24%	366	44	30950	7.7	17	6.4	5.7
50%	50%	372	88	55781	12	23	19	5.7
75%	74%	519	137	71380	16	37	22	11
100%	100%	753	296	94530	20	45	28	11
Main Engine on Conventional Campbell Tug CAT 3512 C								
10%	8%	2299	166	121606	63	10	1.6	5.0
15%	11%	2922	195	155143	63	6.7	3.2	5.7
25%	24%	4860	1252	300463	116	32	18	11
50%	50%	8638	2574	615489	155	101	56	28
75%	76%	11728	2571	922501	207	190	76	66
100%	100%	14078	2481	1257418	224	207	81	81

Table 7-13: Emission Factors in g/kW-hr from *Phase I* of Testing

Load		NO_x	CO	CO_2	THC	$PM_{2.5}$	EC	OC
Target	**Actual**	**g/kW-hr**						
Auxiliary Engine on Conventional Campbell Tug JD 6081								
10%	9%	21.5	3.75	1860	0.82	0.76	0.07	0.41
15%	15%	14.8	2.09	1305	0.69	0.46	0.07	0.28
25%	24%	12.2	1.46	1032	0.26	0.55	0.21	0.19
50%	50%	5.9	1.41	892	0.20	0.37	0.31	0.09
75%	74%	5.6	1.49	772	0.17	0.40	0.24	0.12
100%	100%	6.0	2.37	756	0.16	0.36	0.22	0.09
Wt. Avg.		7.1	1.59	870	0.20	0.42	0.25	0.13
EPA Tier 1		9.2	11.4			0.54		
Main Engine on Conventional Campbell Tug CAT 3512 C								
10%	8%	14.3	1.03	755	0.39	0.06	0.01	0.03
15%	11%	13.6	0.91	722	0.29	0.03	0.01	0.03
25%	24%	10.9	2.8	671	0.26	0.07	0.04	0.02
50%	50%	9.1	2.7	647	0.16	0.11	0.06	0.03
75%	76%	8.1	1.8	639	0.14	0.13	0.05	0.05
100%	100%	7.4	1.3	663	0.12	0.11	0.04	0.04
Weighted Avg.		8.2	1.80	649	0.14	0.12	0.05	0.05
EPA Tier 1		9.2	11.4			0.54		

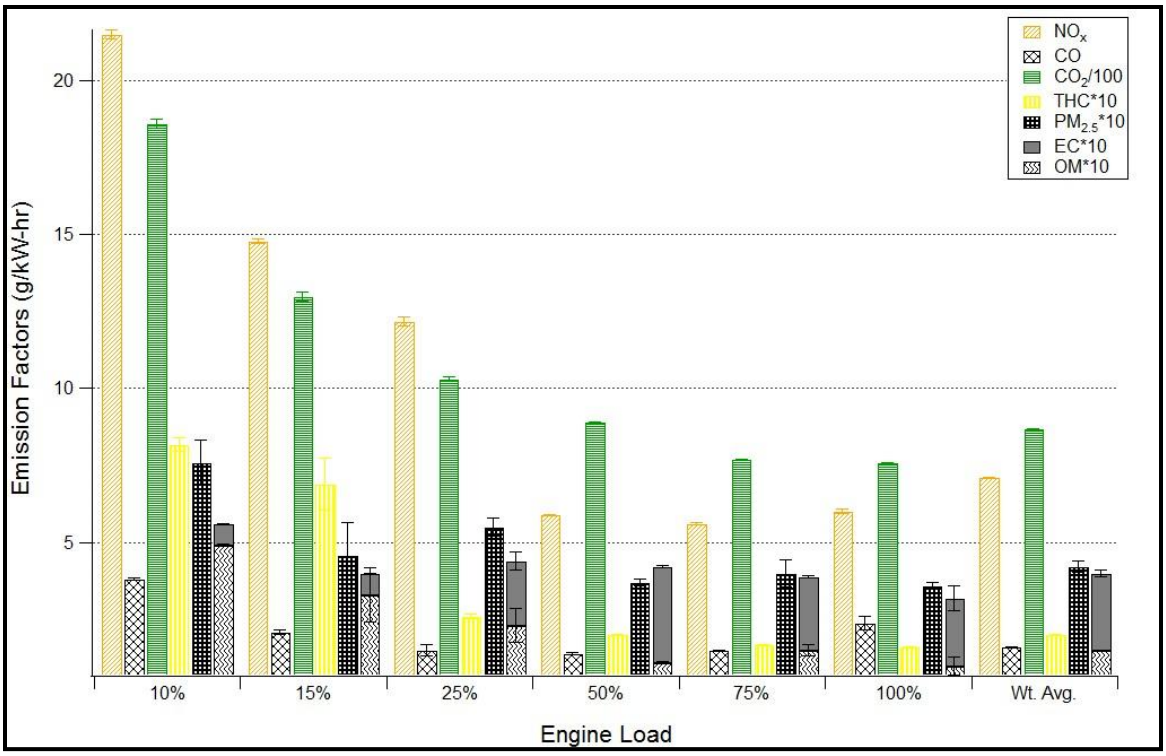

Figure 7-9: Modal Emission Factors for Auxiliary Engine on Conventional *Campbell Foss* Tug JD 6081

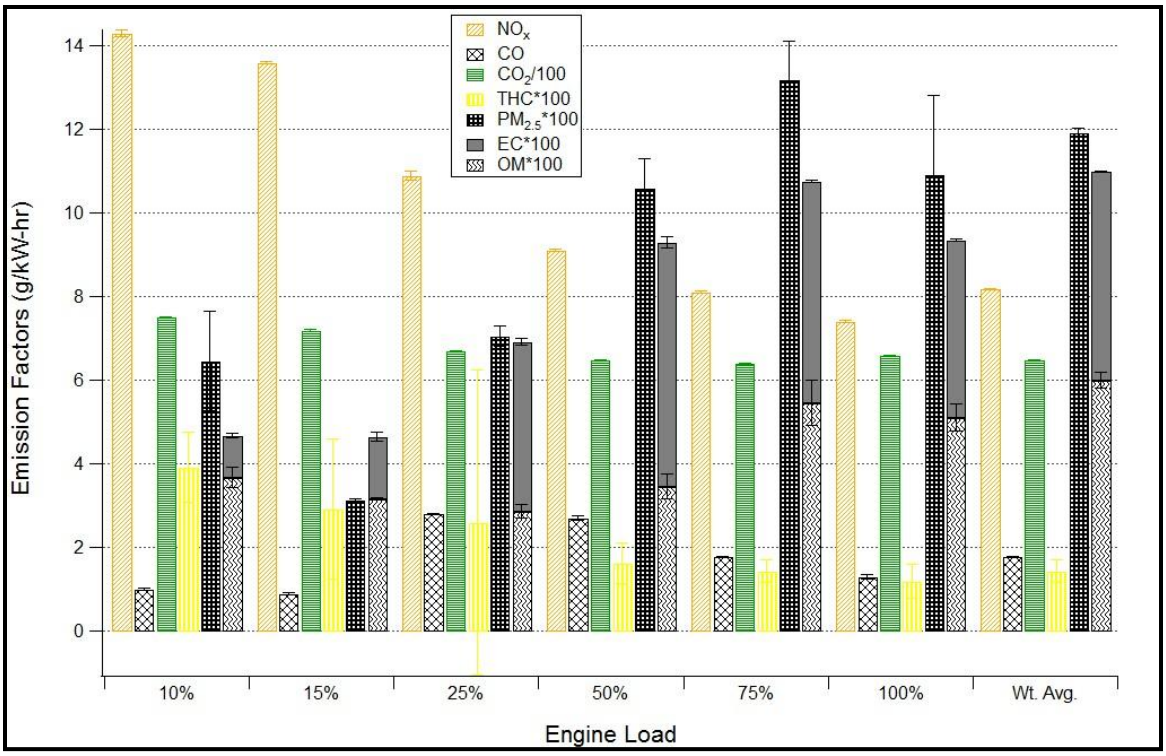

Figure 7-10: Modal Emission Factors for Main Engine on Conventional *Campbell Foss* Tug CAT 3512 C

Diesel particulate matter primarily consists of elemental and organic carbon. Figure 7-11 shows a plot of the $PM_{2.5}$ emissions in g/hr obtained from two separate methods – gravimetric measurements of $PM_{2.5}$ collected on Teflo® filters and total carbon analysis of $PM_{2.5}$ collected on parallel Tissuquartz filters by a thermal/optical carbon analyzer (±20% measurement uncertainty). Here, the total mass is represented as the sum of elemental carbon and organic mass. The organic mass is equal to the organic carbon multiplied by a factor of 1.2 to account for hydrogen and oxygen attached to the carbon in the total PM. Overall, good agreement is observed between two different PM measurement methods.

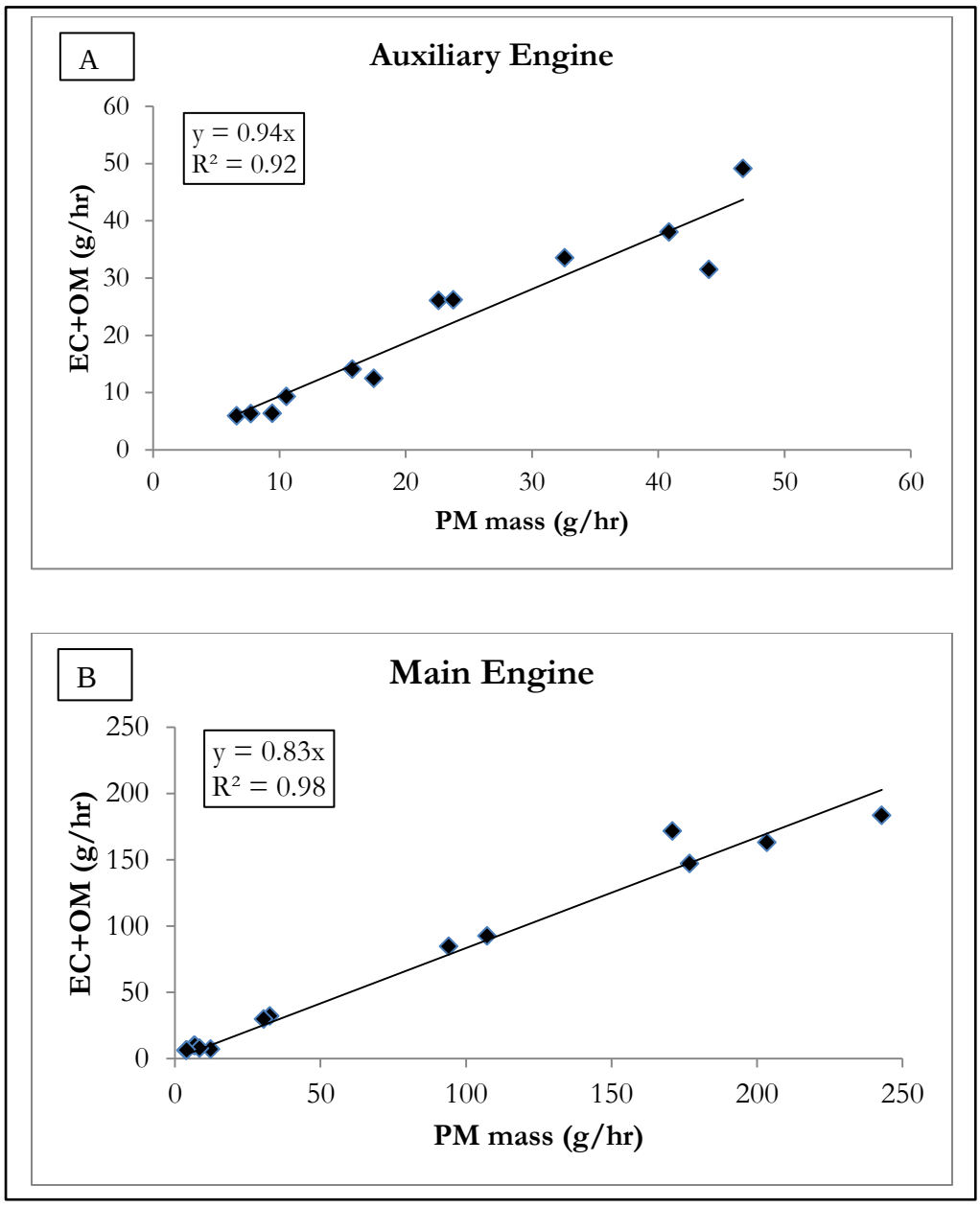

Figure 7-11: $PM_{2.5}$ Mass Balance for A) Auxiliary Engine JD 6081 and B) Main Engine CAT 3512C

7.8.2. Emissions Testing *Phase II* & *III*

Second and third phase of the emissions testing involved emission measurement from the new retrofit AE on the hybrid *Campbell Foss* at 0 hour and 1000 hours of operation, respectively. In both phases, emissions were measured at load points illustrated in ISO 8178 D2 test cycle and at 15% and 5% engine load where engine spends significant amount of time. Similar to *Phase I*, duplicate measurements were made at each load point. Table 7-14 and 7-15 shows gaseous and particulate emissions in g/hr and g/kW-hr, respectively.

Table 7-14: Emission Rates in g/hr for *Phase II* & *III* of Emissions Testing

Load (%)		NOx	CO	CO_2	THC	$PM_{2.5}$	EC	OC
Target	Actual	g/hr						
MTU/Detroit Series 60 (0 hour Emission Measurements)								
100	93	2507	116	259240	20.5	24.5	15.4	51.9
75	73	1879	73	194126	13.1	12.6	6.6	3.9
50	51	1075	63	129138	11.1	15.4	9.6	3.1
25	25	506	63	77094	11.8	10.9	6.0	3.9
15	15	305	71	48804	12.8	7.7	3.0	3.5
10	10	174	60	29843	11.7	6.0	1.6	3.7
5	5	144	73	26111	15.4	6.2	0.7	4.4
MTU/Detroit Series 60 (1000 hour Emission Measurements)								
100	99	2155	293	258404	166	40.2	24.6	36.1
75	75	1813	129	192278	127	32.6	16.0	20.8
50	50	1001	111	127348	100	19.4	20.2	10.0
25	25	466	76	72713	102	14.3	12.9	4.8
15	15	272	85	43997	118	8.9	4.8	2.0
10	10	169	71	28879	117	6.5	2.5	1.6
5	5	131	142	26394	13	3.2	0.9	1.6

The primary objective of emission measurements from MTU engine was to ensure that the emissions are within the Tier 2 standards and the tested engine is the representative of engines in their class.

Table 7-15 also lists the overall weighted average emission factors for MTU engine from both phases of testing. It also shows the EPA Tier 2 standard for that each test engine family. The overall weighted averages for MTU AE at 0 & 1000 hours are below EPA Tier 2 standards for NO_x and $PM_{2.5}$. Moreover, EF_{CO} is comparatively very low which is typical of diesel engines. The percentage difference between EF_{NOx} and EF_{CO2} measured at 0 hour and 1000 hours emissions testing are 7.8% and 3.0%, respectively which reflects good durability of the engine and robust emission measurements. Note that the emissions measured at 1000 hours are used in calculating in-use emissions from MTU engine.

Table 7-15: Emission Factors in g/kW-hr for *Phase II* & *III* of Emissions Testing

Load (%)		NOx	NOx+NHMC	CO	CO_2	THC	$PM_{2.5}$	EC	OC
Target	Actual	g/kW-hr							
MTU/Detroit Series 60 (0 hour Emission Measurements)									
100	93	7.7	7.7	0.35	793	0.06	0.07	0.05	0.16
75	73	7.4	7.4	0.29	762	0.05	0.05	0.03	0.02
50	51	6.1	6.1	0.35	729	0.06	0.09	0.05	0.02
25	25	5.8	5.9	0.72	886	0.14	0.13	0.07	0.04
15	15	5.8	6.0	1.34	927	0.24	0.15	0.06	0.07
10	10	5.0	5.3	1.72	861	0.34	0.17	0.05	0.11
5	5	8.2	9.1	4.18	1492	0.88	0.35	0.04	0.25
Weighted Avg.		6.7	6.8	0.42	776	0.08	0.08	0.04	0.04
Tier 2		–	7.2	5.0	–	–	0.20	–	–
MTU/Detroit Series 60 (1000 hour Emission Measurements)									
100	99	6.2	6.7	0.84	745	0.48	0.12	0.07	0.10
75	75	6.9	7.4	0.49	734	0.48	0.12	0.06	0.08
50	50	5.8	6.3	0.64	732	0.58	0.11	0.12	0.06
25	25	5.4	6.5	0.87	836	1.17	0.16	0.15	0.05
15	15	5.3	7.5	1.55	846	2.27	0.13	0.09	0.04
10	10	5.0	8.4	2.08	849	3.45	0.19	0.07	0.05
5	5	8.7	9.4	8.47	1553	0.75	0.19	0.06	0.09
Weighted Avg.		6.2	6.9	0.67	753	0.68	0.13	0.09	0.07
Tier 2		–	7.2	5.0	–	–	0.20	–	–

The rates in g/hr as a function of engine load for gaseous and particulate emissions coupled to the engine histograms (section 7.6.) are used to calculate total emissions from each engine at the different tugboat operating modes.

7.8.3. Activity

7.8.3.1. Weighting Factors for Tug Operating Modes

Figure 3-4 shows the overall weighting factors for the hybrid tugboat. Total sample times used for the determined these weighing factors were ~37 days for the hybrid tugboat. The figure shows that the dolphin class tug spends about ~51% of its total operating time at Stop (includes shore power), ~2% in Idle ~14% in Transit (Transit 1 and Transit 2), and ~33% in Assist (includes barge moves). Note that the overall weighting factors for the conventional *Campbell Foss* are assumed to be same as hybrid *Campbell Foss*.

Overall, 37 days of activity data was collected in three intervals of time period. Table 7-12 represents weighting factors for these three intervals. Clearly, no significant variation in operating modes was observed between three intervals.

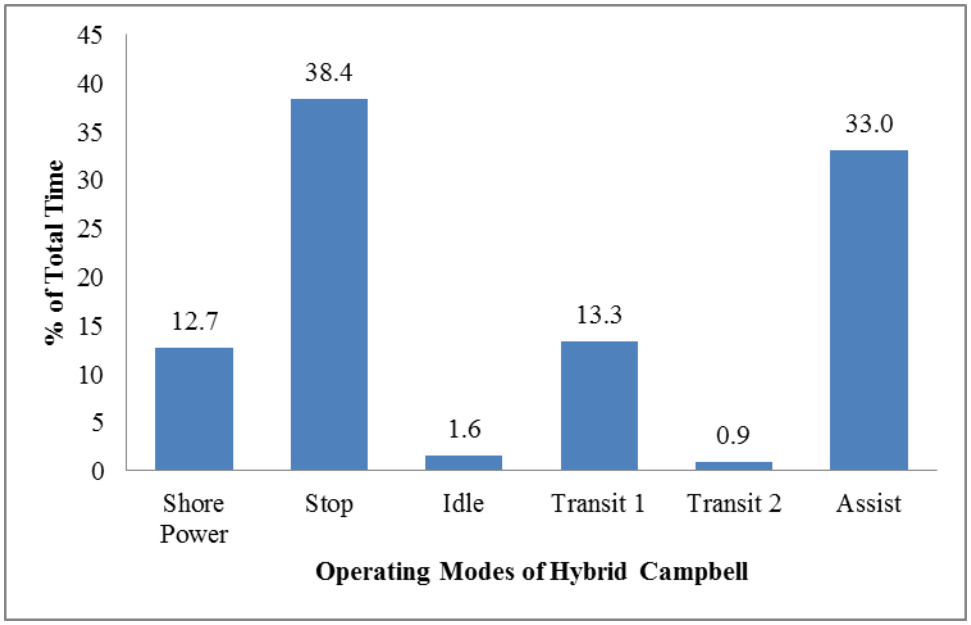

Figure 7-12: Overall Weighing Factors for Hybrid Tugboat Operating Modes

Table 7-16: Weighting factors for small intervals of time period

Time Period	Stop	Idle	Transit 1	Transit 2	Assist
05/25/12-06/06/12	50.6%	2.1%	14.8%	0.7%	31.7%
06/09/12-06/17/12	48.7%	3.7%	15.1%	1.2%	31.3%
06/21/12-09/07/12	52.2%	0.6%	11.7%	1.0%	34.5%

Tugboat operations in the port of Los Angeles and Long Beach harbor consist primarily of docking and undocking ocean going vessels such as containerships and bulkers providing tanker escorts and moving bunkering barges in the harbor. The barge movements provide bunker fuel to ocean going vessels while they are berthed at various facilities in the Long Beach and Los Angeles ports.

The bunker barges are loaded at the Vopak fueling facility at Berth 187 in Los Angeles and Foss tugs are berthed at Pier D Berth 49.In between Long Beach Berth 49 and Los Angeles Berth 187 there is the Schuyler Heim drawbridge over the Cerritos Channel. Until January 2012 the horizontal clearance under this bridge was 142 feet which meant the tugs moving barges could move freely under this drawbridge. However, there is currently a Caltrans project underway to replace the aging Schuyler Heim drawbridge for seismic upgrades. In January 2012, two trestles were constructed adjacent to the existing bridge, which resulted in a horizontal restriction of 75 feet between the trestles. The Foss bunker barges are 290 feet in length, 62 feet in breadth with a molded depth of 18.5 feet. The tugs which are secured alongside the barge are 34 to 40 feet in breadth with an additional three feet of fenders between the tug and barge. This tug barge combination cannot physically navigate through this newly restricted channel. This construction project is expected to continue for five years at which point the trestles will be removed and the horizontal clearance will return to pre-construction clearance.

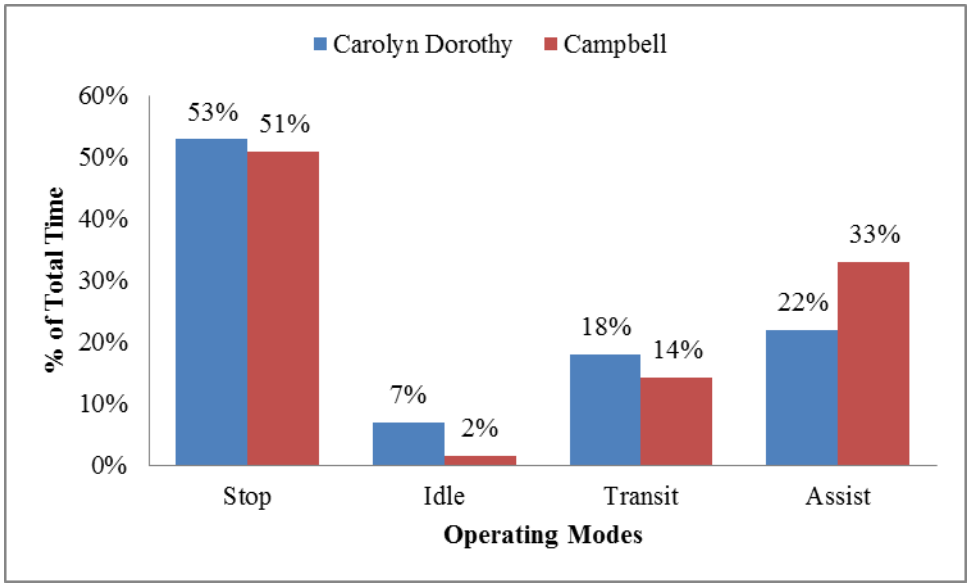

Figure 7-13: Comparison of Overall Weighting Factors for Hybrid *Carolyn Dorothy* and *Campbell Foss*

The practical result of this restricted waterway is that to service customers located at the majority of the terminals in the Port of Long Beach, Foss tugs with barges must now travel all the way through the Port of Los Angeles and enter the Port of Long Beach from the Outer Harbor instead of staying within the Inner Harbor of the Port of Long Beach. Between February and mid-November 2012 Foss tugs with barges have diverted over 1,800 miles due to this bridge construction project.

The ARB[4] study conducted in 2010, developed a duty cycle analysis for the Foss tugs *Carolyn Dorothy* (CD) and *Alta June* (AJ), sister vessels to the *Campbell Foss.* All three vessels operate from Long Beach Berth 49 and typically do the same mix of work in the ports of Los Angeles and Long Beach. The 2010 report showed both the *Carolyn Dorothy* and *Alta June* spent 22% of their time in "Assist" mode doing either ship assist or barge moves. The 2012

study of the *Campbell Foss* which was conducted between May and July of 2012 (after the channel restriction) showed this vessel spent 33% of its time in the "Assist" mode (Figure 7-15). One explanation for this variance is that this channel restriction and attendant navigational deviation means the *Campbell Foss* spent more time in the Assist mode because of the more time spent in moving barges for greater distance.

7.8.3.2. Engine Histogram for Conventional Campbell Foss

Alta June and *Campbell Foss* belongs to the same class of tugboats. Prior to the hybrid retrofit for *Campbell Foss*, both tugs had same MEs and AEs. Therefore, engine histograms obtained for *Alta June* in CARB study are assumed to be same for the conventional *Campbell Foss*.

The conventional *Campbell Foss* had only one of the two auxiliary engines working for all tug operating modes, except shore power. This auxiliary engine always operated at 10-12% of its maximum load. Therefore an engine histogram of the auxiliary engine would show a 100% bar at the 10-12% load with no bars at all other load points. The main engines on the conventional tug are off when the tug is at Stop or plugged into Shore Power. During the Idle mode these engines are idling with an engine load of about 5-7% of the maximum rated power. Figure 7-14 and 7-15 shows engine histograms for both main engines on the conventional *Campbell Foss* for transit and ship assist operating modes.

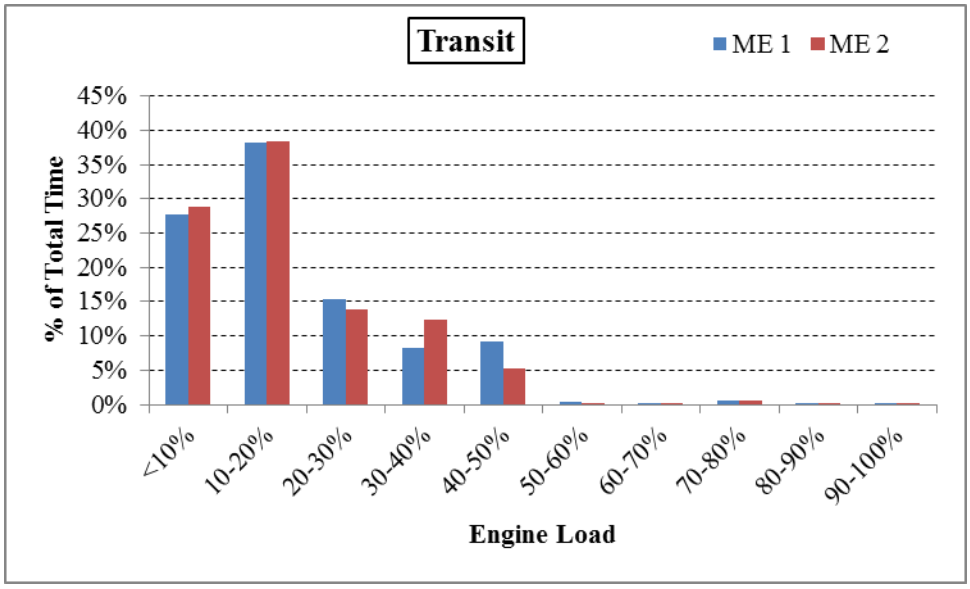

Figure 7-14: Main Engine Histogram during Transit Mode for Conventional *Campbell Foss*

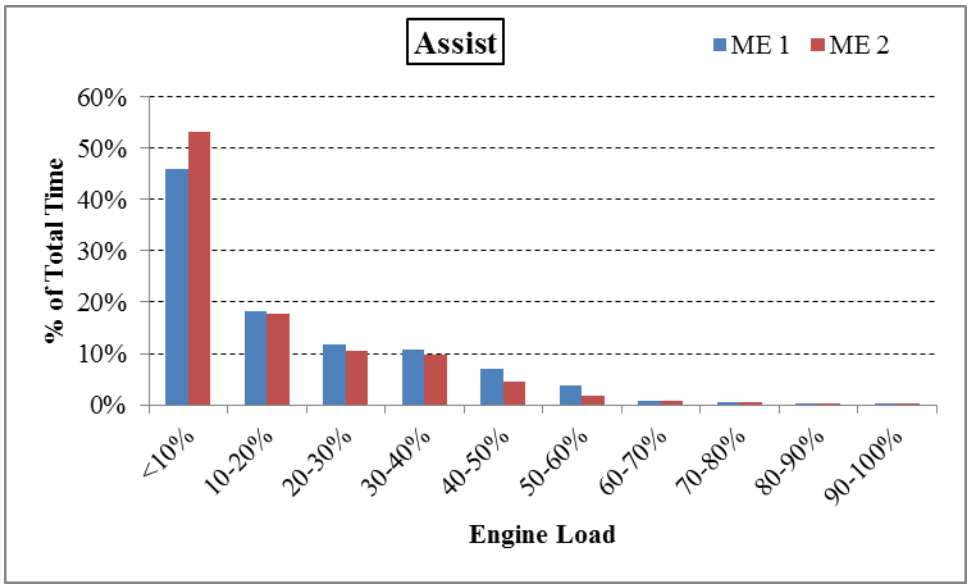

Figure 7-15: Main Engine Histogram during Assist Mode for Conventional *Campbell Foss*

7.8.3.3. Engine Histograms for Hybrid Campbell Foss

Engine histograms for hybrid *Campbell Foss* was obtained from the activity logged for 37 days during this study.

Stop Mode: In this mode, both main engines are off similar to conventional *Campbell Foss*. Energy required for hoteling purposes are either extracted from the JD AE or batteries. The MTU AE is rarely operated during Stop mode as shown in Figure 7-16. For the case of the conventional *Campbell Foss*, only one AE was always operated at 10-12% engine load. Therefore, some emissions benefits are expected on using hybrid tugboat during Stop mode.

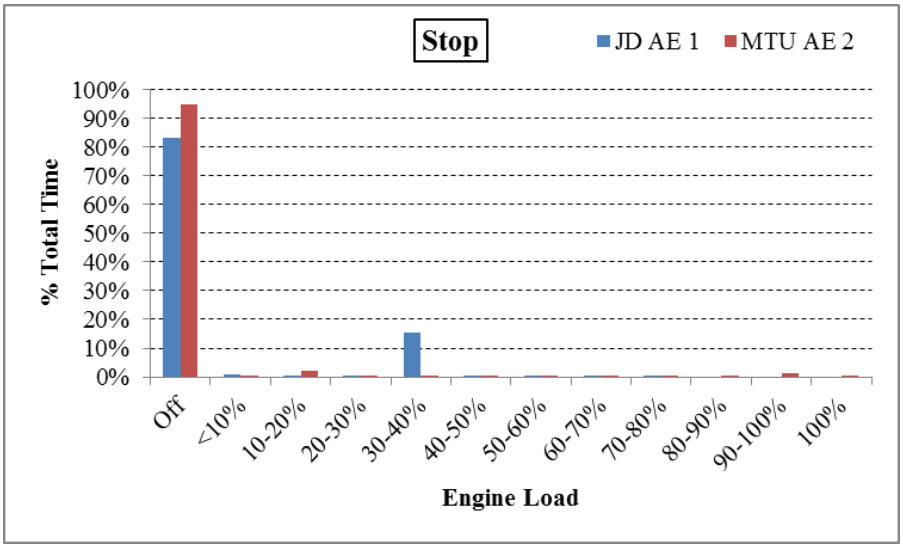

Figure 7-16: AEs histogram during Stop mode for Hybrid *Campbell Foss*

Idle Mode: In this mode, both main engines are off in the hybrid design, whereas in the case of the conventional *Campbell Foss*, main engines are always operated (95% of total time) at 5% engine load. Both AEs and batteries switched between each other during Idle mode. AEs histogram for hybrid *Campbell Foss* is shown in Figure 7-17. Only one AE was always

operated at 10-12% of maximum engine rated power in conventional *Campbell Foss*. Due to above differences in MEs and AEs operation, emission benefits are expected on using hybrid tugboat during Idle mode.

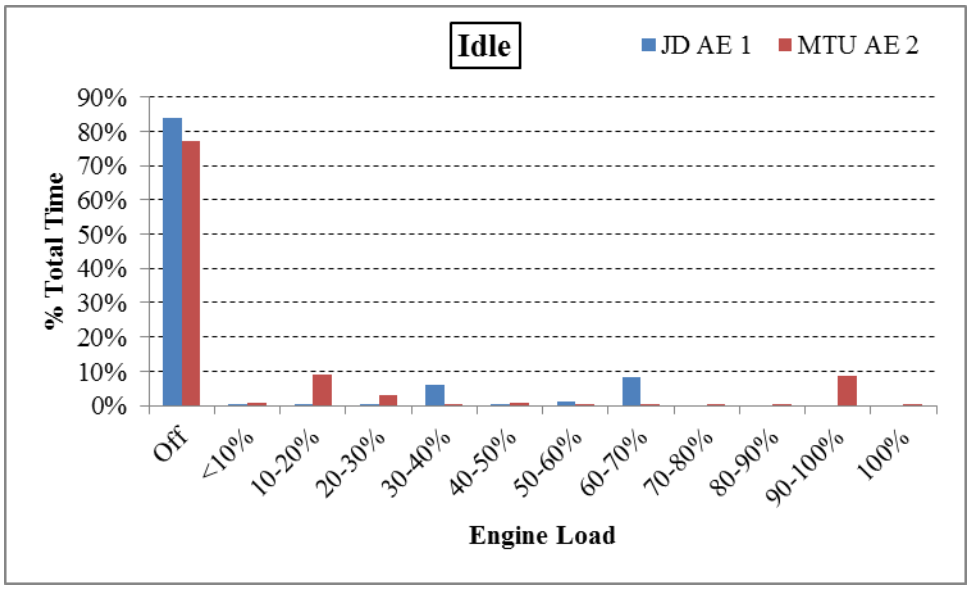

Figure 7-17: AEs histogram during Idle mode for Hybrid *Campbell Foss*

Transit Mode: This mode is the combination of Transit 1 and Transit 2 mode of the hybrid tugboat. MEs are rarely operated during Transit mode in hybrid tugboat. However, MEs in the conventional *Campbell Foss* were always operating during this mode (Figure 7-18). In the hybrid *Campbell Foss*, either one AE or both AEs are operated in Transit mode depending upon the speed requirement. Conventional *Campbell Foss* utilized one AE for hoteling purposes during Transit mode. As hybrid *Campbell Foss* are propelled by AEs instead of MEs (which are much higher in power), significant emission benefits are expected during Transit mode on operating hybrid *Campbell Foss*.

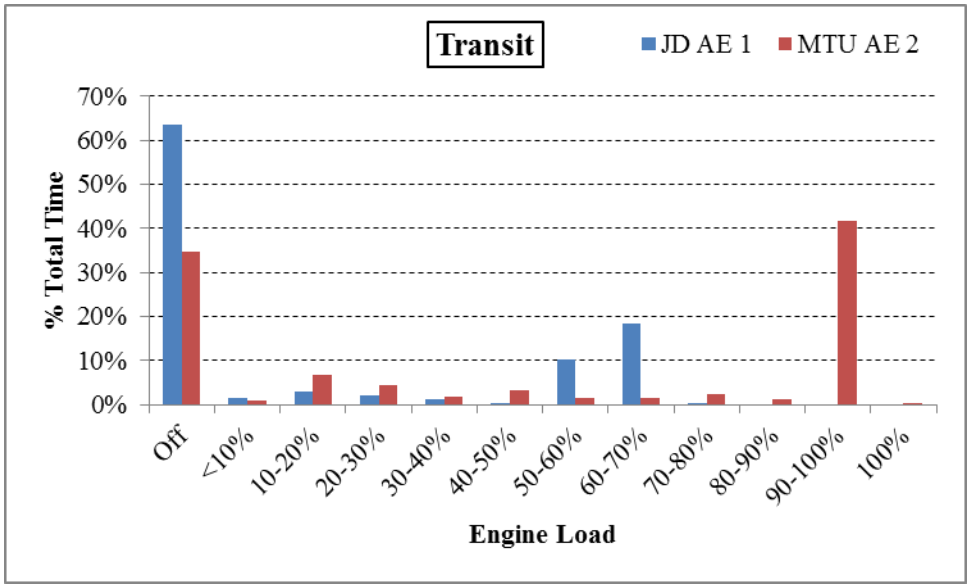

Figure 7-18: AEs histogram during Transit mode for Hybrid

Assist Mode: Both MEs are in operation for conventional and hybrid *Campbell Foss* during Assist mode. MEs histogram during Assist mode is shown in Figure 7-19. AEs in the hybrid *Campbell Foss* are rarely operated whereas one AE was always in operation for conventional *Campbell Foss* during Assist mode.

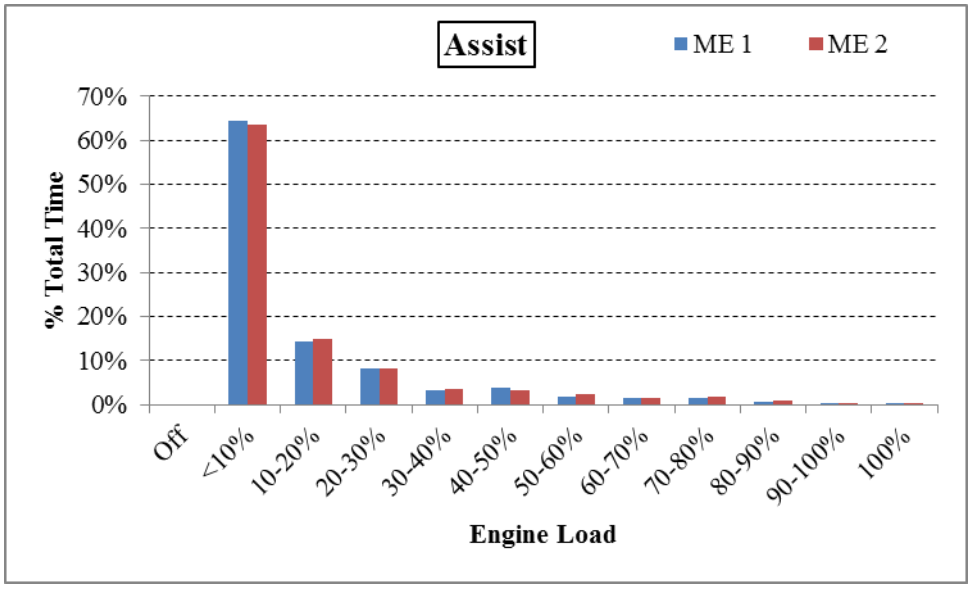

Figure 7-19: MEs histogram during Assist mode for Hybrid *Campbell Foss*

7.9. Total In-use Emissions

The total in-use emission form each tug configuration was calculated using the equations stated in Section 2.2. Emissions from each tug at a particular operating mode were calculated using engine histograms and engine emission profile data. Energy consumed when tug is plugged into shore power is assumed to be same for hybrid and conventional *Campbell Foss*. To determine the emissions for the shore power mode, the average load during shore power was multiplied by the emission factors of a conventional natural gas fired steam plants with selective catalyst reduction (SCR) for NOx control and with no CO catalyst (Table 7-17).

Table 7-17: Emission Factors for Shore Power[6,7]

	Emission Factor		
	lbs/10^6scf	lbs/MW-hr[a]	g/kW-hr
$PM_{2.5}$	7.6	0.087	3.948E-05
NO_x	10	0.117	5.195E-05
CO_2	120000	1371	0.623

[a] heating value of natural gas = 1,050 Btu/scf, power generation heat rate = 12,000 Btu/kW-hr

Overall, 31%, 30% and 29% reduction was obtained on using hybrid technology for NOx, CO_2 and $PM_{2.5}$, respectively. Similar to previous study, major benefits of using hybrid technology was obtained during Transit mode as the large main propulsion engines are not operating for the hybrid. Table 7-18 and 7-19 shows modal and overall benefits in gaseous and particulate emissions due to the conversion to the hybrid technology. This study expects about 30% of fuel savings, which is similar to 25-28% fuel savings reported by the previous study.[4]

Table 7-18: Modal and Overall Emission Reductions for Campbell Foss with Hybrid Technology

Operating Modes	Weighing factors		NOx (g/hr)		% Reduction	CO_2 (kg/hr)		% Reduction	$PM_{2.5}$ (g/hr)		% Reduction
	Conv.	Hybrid	Conv.	Hybrid		Conv.	Hybrid		Conv.	Hybrid	
SHORE POWER	0.13	0.13	0.0002	0.0002	0%	0.002	0.002	0%	0.00013	0.00013	0%
STOP	0.38	0.38	94	42	55%	8.1	4.8	40%	3.3	1.5	54%
IDLE	0.02	0.02	78	6	93%	3.0	0.7	78%	0.5	0.2	70%
TRANSIT	0.14	0.14	1126	310	72%	71.0	31.2	56%	10.0	6.0	40%
ASSIST	0.33	0.33	2481	2243	10%	152.6	128.2	16%	23.2	18.6	20%
Overall	1.00	1.00	3780	2601	**31%**	235	165	**30%**	36.9	26.2	**29%**

Table 7-19: Modal and Overall Emission Reductions for Campbell Foss with Hybrid Technology

Operating Modes	Weighing factors		CO (g/hr)		%	THC (g/hr)		%	EC (g/hr)		%	OC (g/hr)		%
	Conv.	Hybrid	Conv.	Hybrid	Reduction	Conv.	Hybrid	Reduction	Conv.	Hybrid	Reduction	Conv.	Hybrid	Reductio
SHORE POWER	0.13	0.13	–	–	0%	–	–	0%	–	–	0%	–	–	0%
STOP	0.38	0.38	16	6.0	63%	3.6	2.9	20%	0.3	0.8	-160%	1.8	0.6	64%
IDLE	0.02	0.02	6.7	0.9	87%	2.3	0.5	78%	0.1	0.1	-5%	0.2	0.1	70%
TRANSIT	0.14	0.14	168	53	68%	28	16	41%	4.1	3.3	20%	3.8	3.1	17%
ASSIST	0.33	0.33	411	320	22%	61	58	5%	8.7	7.2	17%	9.1	7.2	21%
Overall	1.00	1.00	602	380	**37%**	95	78	**18%**	13.2	11.4	**13%**	14.9	11.1	**26%**

7.10. Summary

The primary goal of this project was to determine the emission benefits of a hybrid retrofit system on an existing tugboat. For this purpose, a conventional tugboat of "Dolphin" class was chosen and retrofitted with a new auxiliary engine and the hybrid components.

Emissions measurements were made from the main and auxiliary engine of the conventional *Campbell Foss* tug prior to retrofit. These engines were tested according to ISO 8178 E3/D2 test cycle to ensure that their emissions are within certification limits and EPA Tier 1 standards. Additional measurements were made at low loads where tug has been reported to spend most of the time during its operation and data are not available. This phase of the study concluded that the engines tested are well maintained and representative of engines in their emission class. Overall weighted emission factors for NO_x, CO, and $PM_{2.5}$ are within standards values. Emissions of CO_2 from both engines are typical of diesel engine of their category and are in agreement with manufacturer expectations.

The second phase of this project was to develop the activity of the hybrid *Campbell Foss* and emissions testing of the new retrofit AE engine according to ISO 8178 D2 and in-use test cycle based on activity data. A data-logging system, capable of simultaneously monitoring and reporting the status of the power sources was installed for a period of over one month. Four gigabytes of data were analyzed to determine the weighting factors, i.e., the fraction of time spent by the tug in the six discrete operating modes shore power, stop, idle, transit 1,

transit 2 and assist. Further engine histograms for all four engines on the tug at these operating modes were established.

The final analysis combined engine histogram and emission profile data to determine in-use emissions at each tug operating mode for both conventional and the hybrid *Campbell Foss*. These figures were coupled with the weighing factors for the operating modes to get the overall in-use emissions in g/hr for each tug. Significant emission benefits were observed for the hybrid technology.

The major findings of this project include:

The average weighting factors for the operating modes of the hybrid tugboat were 0.53 for Stop, 0.02 for Idle, 0.14 for Transit and 0.33 for Assist.

A significant difference in the Assist weighting factor was found in comparison to previous study. This was mainly due to the fact that the *Campbell Foss* is spending more time in moving barges because of the new travel restrictions at the Port of Long Beach.

Overall in-use emission reductions with the hybrid technology were found to be 29% for $PM_{2.5}$, 31% for NO_x and 30% for CO_2.

Emissions factors for the CAT 3512C MEs were within the Tier 1 standards. Similarly, for both AEs; JD 6081 and MTU/Detroit Series 60, emissions were within the Tier 1 and 2 standards, respectively.

The diesel electric drive train on the hybrid tug that allows the use of auxiliary power for propulsion was the primary cause for the overall in-use emission reductions as opposed to the energy storage device (batteries).

Like before, the transit operating mode was the most significant contributor to the overall emission reductions. In this mode the hybrid tug was powered by one or two auxiliary engines and batteries while the conventional tug used one auxiliary and two main engines.

7.11. Acknowledgements

This project would have not been possible without the financial support from Foss Maritime Company. The authors acknowledge the support from Foss crew members during emissions testing. A special thanks to US Environmental Protection Agency (USEPA), Mobile Source Division in the preparation of the test plan for this project. The authors also thanks to Ms. Kathalena Cocker, Mr. Jesus Sahagun for preparation and analysis of filter sample media.

7.12. Literature Cited

1. Society of Automotive Engineers, Recommended Practices for Measuring Exhaust Emissions and Fuel Economy of Hybrid Electric Vehicles. 1999, SAE J1711.
2. California Air Resources Board. California Exhaust Emission Standards and Test Procedures for 2009 and Subsequent Model Zero-Emission Vehicles, and Hybrid Electric Vehicles, In the Passenger Car, Light Duty Truck and Medium-Duty Vehicle Classes, 2009.

3. International Organization for Standardization. ISO 8178-1 Reciprocating internal combustion engines-Exhaust emission measurement. Part 1: Test bed measurement of gaseous and particulate exhaust emissions. 1996. First Edition 1996-08-15.
4. CARB. Evaluating Emission Benefits of a Hybrid Tug Boat. Final Report. October 2010.
5. International Organization for Standardization (ISO). ISO 8178-4, Reciprocating internal combustion engine-Exhaust emission measurement-Part 4: Test cycles for different engine applications, 1996.
6. Environ International Corporation. Cold Ironing Cost Effectiveness Study. 2004. *Prepared for Port of Long Beach*.
7. U.S. Environmental Protection Agency. AP-42 Compilation of Air Pollutant Emission Factors. **2004**, *Fifth Edition Vol 1*.

Chapter Eight: Conclusions

The main objective of this research was to characterize emissions measurement technologies for determining accurate emission rates and to evaluate control strategies such as switching to cleaner fuels, alternative fuels, hybridization of vessels and reducing OGVs speed in scope of reducing emissions from port-related activities and dependency on fossil fuels.

Chapter 2 investigates the performance of four Particulate Matter-Portable Emission Measurement Systems (PM-PEMS) for in-use emissions measurement by comparing them against gravimetric reference method. This study showed that the current PM-PEMS typically underreport the PM emissions compared to the reference method, with the exception of photo-acoustic based PEMS which also incorporated a gravimetric filter. PM-PEMS equipped with quartz crystal microbalance and photo-acoustic technology showed very similar unit-to-unit performance with photo-acoustic being precise. The large variability between newer and older versions of the same PM-PEMS for some PEMS was observed. All PM-PEMS had difficulty in quantifying PM during regeneration of DPF. This study also uncovered some issues with firmware, hardware, and post processing upgrades that can have a significant impact on the reported emissions. The implications from this study suggest that not all PM-PEMS are at the same level of development maturity with respect to correlations with gravimetric filter mass and that new PM-PEMS need to be carefully evaluated before they are widely adopted for emission inventory or regulatory purposes.

Chapter 3 compares international and U.S. federal methods for measuring in-use gaseous emissions from OGVs. IMO's SMM and USEPA's on-road certified PEMS were compared during three different trips on in-use container OGVs. Excellent correlation was observed for CO_2 measurements. PEMS measurements for NO_x were 6.5% higher on average than SMM which was could be attributed to some sensitivity of the NDUV wavelength light absorption to SO_2. This measurement error would become insignificant when lower sulfur fuel is burned in C3 marine engines. The PEMS, as currently configured, was unable to measure the typically low concentrations of CO in slow speed marine diesel engine exhaust. However, since IMO only regulates NO_x and sulfur content in fuel, PEMS can provide a simpler and more convenient method to perform on-board emission certification. The emission factors from two different trips from the same OGV were reproducible. Modal and weighted emission factors are provided for criteria pollutants (NO_x, CO, SO_2 and $PM_{2.5}$) and CO_2. Hydrated sulfate dominates the composition of PM and the fuel sulfur conversion to sulfate was consistent with the few studies available on emissions from OGVs.

Chapter 4 provides in-use emission rates for a marine vessel operating on hydrotreated algae biofuel. Emission measurements were made on a four-stroke marine diesel engine from a Stalwart class vessel to compare the emission profile burning ultra low sulfur diesel (ULSD) to a 50:50 blend of ULSD and algae biofuel (A50). Switching fuel from ULSD to A50 resulted in overall reduction of ~18 and ~25% in CO and $PM_{2.5}$, respectively. These reductions can be explained by the difference in CI and aromatic content of both fuels tested. Higher CI promotes shorter ignition delays, providing more time for the fuel consumption process to be completed and, hence, reducing the formation of CO and PM.

The lower density of A50 (804 kg m^{-3}) with respect to ULSD (829 kg m^{-3}) coupled with the higher CI likely contributed to the ~10% reduction in NO_x emission factors. A 4.5% reduction in overall weighted fuel consumption was also found. A slightly better fuel economy upon consuming A50 can be partially explained by the higher calorific value of A50. Overall, chapter 4 demonstrated that algae biofuel derived through the hydrotreated process has the potential to substantially reduce criteria pollutants without modifying the engine or infrastructure in the vessel.

The results in chapter 5 provide emission benefits from the two mitigation strategies (cleaner engines and cleaner fuels) for the modern container vessel. The actual in-use emission factors of NO_x was 5% and 14% lower than the Tier I certification value and Lloyds service data commonly used in the development of emission inventories, respectively. The overall in-use emission factors of EC and OC were 33% and 20% lower than the comparative post-Panamax container vessel in previous study, reflecting the benefits of newest engine technologies. Unimodal (~30 nm) and bimodal (~35 nm; ~75 nm) particle size distributions were observed when the vessel operated on MGO and HFO, respectively. First time emission measurements during fuel switching showed that concentrations of SO2 and particle NSD took ~55 min to reach steady-state when switching from MGO to HFO and ~84 nm in the opposite direction. Therefore, if OGVs commence fuel change at the regulated boundary, then vessel can travel up to 90% of the distance to the port before stead-state values are re-established. Hence, to achieve the maximum benefits from a fuel change regulation, fuel switch boundary should be further increased to provide the intended benefits for the people living near the ports.

In chapter 6, greenhouse gas and criteria pollutants benefits were quantified for container vessels when there vessel speed was reduced from cruise to 15 knots or below. VSR to 12 knots yielded CO_2 and NO_x emissions reductions (in kg/nmi) of approximately 61% and 56%, respectively, as compared to cruise speed. The mass emission rate (kg/nmi) of PM2.5 was reduced by 69% with VSR to 12 knots alone and by ~97% when coupled with the use of the MGO with 0.00065% sulfur content. Measurements from this research also demonstrated that the tidal current is a significant parameter affecting emission factors at lower engine loads. Emission factors at ≤20% loads calculated by methodology adopted by regulatory agencies were found to underestimate $PM_{2.5}$ and NO_x by 72% and 51%, respectively, when compared to emission factors measured in this study. Total pollutant emitted (TPE) in the ECA was calculated, and emission benefits were estimated as the VSR zone increased from 24 to 200 nautical miles. This analysis suggested that reducing the speed of large container and Suexmax class tankers to 12 knots would result in emission benefits, whereas small and medium container vessels may give emission benefits at 15 knots similar to those at 12 knots.

Chapter 7 evaluates hybrid retrofit system for a tugboat. Overall in-use emission reductions with the hybrid technology were found to be 29% for $PM_{2.5}$, 31% for NO_x and 30% for CO_2. The diesel electric drive train on the hybrid tug that allows the use of auxiliary power for propulsion was the primary cause for the overall in-use emission reductions as opposed to the energy storage device (batteries). The average weighting factors for the operating modes of the hybrid tugboat were 0.53 for Stop, 0.02 for Idle, 0.14 for Transit and 0.33 for Assist. A significant difference in the Assist weighting factor was found in comparison to previous

study. This was mainly due to the fact that the *Campbell Foss* is spending more time in moving barges because of the new travel restrictions at the Port of Long Beach. Like before, the transit operating mode was the most significant contributor to the overall emission reductions. In this mode the hybrid tug was powered by one or two auxiliary engines and batteries while the conventional tug used one auxiliary and two main engines.

Appendix A

Model Derivation

V_{DT} is the volume of the fuel in the day tank and is assumed to be constant (t≥0). *E, R* and *f* are fuel flow rate in L min^{-1} for feed line, return line and net fuel consumption, respectively. Delay time (T) for return line was assumed to be small.

$$f = E - R, but\ E \gg R$$

$$\therefore f = E \quad (1)$$

At time t = 0, Fuel 1 (F_1) valve is shut off and Fuel 2 (F_2) valve is turned on. Then, the change in amount of F_1 at any time t (t>0) is

$$\frac{dF_1}{dt} = -\left(\frac{F_1(t)}{V_{DT}}\right)E + \left(\frac{F_1(t-T)}{V_{DT}}\right)R \quad (2)$$

But from (1) and t ≈ t-T, (2) becomes

$$\frac{dF_1}{dt} = -\left(\frac{F_1(t)}{V_{DT}}\right)f \quad (3)$$

Correspondingly, the change in amount of F_2at any time t (t>0) is

$$\frac{dF_2}{dt} = f - \left(\frac{F_2(t)}{V_{DT}}\right)E + \left(\frac{F_2(t-T)}{V_{DT}}\right)R \quad (4)$$

Using above assumptions, (4) becomes

$$\frac{dF_2}{dt} = f - \left(\frac{F_2(t)}{V_{DT}}\right)f \quad (5)$$

Equation (3) or (5) can be used to calculate time required for changing fuel in the day tank. For 95% change in fuel, Eqn. (3) or (5) gives:

$$t_{95} = \frac{V_{DT}}{f} ln\ 20$$

Based on the equation, change in sulfur content is calculated and subsequently SO_2 concentrations every minute. The changes in calculated and measured SO^2 concentrations are observed with time as shown in Figure S1. The linear regression correlation for equation SO_2 showed an $R^2 = 0.99$, a slope of 0.97, and a positive intercept of 26 ppm for MGO to HFO. The HFO to MGO correlation showed an $R^2 = 0.98$, a slope of 0.95, and a negative intercept of 15 ppm.

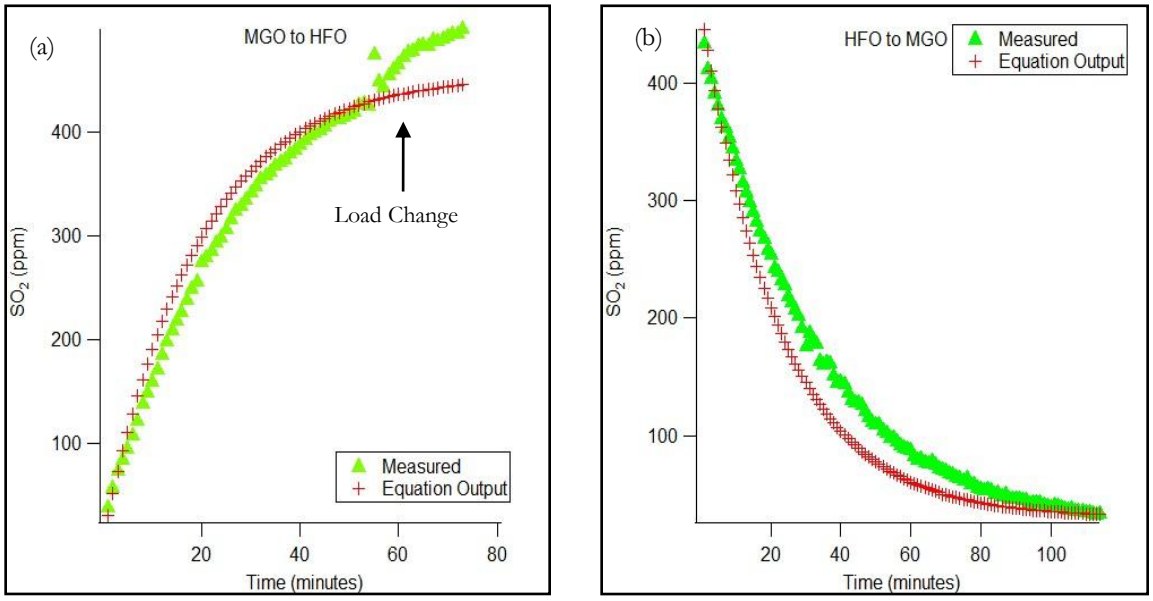

Figure A-1: Comparison of measured and calculated SO_2 concentrations based on the equation output for (a) MGO to HFO and (b) HFO to MGO.

Appendix B

Total number of vessels and average main engine power in each container class in presented in Table S5. Category A includes all container classes and category B includes container-6000 to container-9000. Table S1, S2 and S3 represent gaseous emissions in kg/hr, kg/nmi and g/kW-hr from all trips. Table S4 compares measured and calculated EFs (g/kW-hr) for vessels running at low loads (2-20%). Table S5, S6, S7 and S8 represents percent reduction in TPE_{CO2}, TPE_{NOx}, $TPE_{PM2.5}$ and TPE_{CO} in categories A, B and from Suezmax class tankers.

Table B-1: Comparison of emissions measured (kg/hr) at cruise and reduced speed from three trips

Trip 1 (Out of Long Beach Port)					
Gases	Emissions (kg/hr)			% Reduction with Reduced Speed	
	Cruise speed (24 Knots)	15 Knots	11 Knots	15 Knots	11 Knots
CO_2	17102	4855	3067	72	82
NO_x	567	150	98	74	83
CO	10	16	8	-57	20
Trip 2 (Out of Long Beach Port)					
Gases	Emissions (kg/hr)			% Reduction with Reduced Speed	
	Cruise speed (24 Knots)	14 Knots	13 Knots	14 Knots	13 Knots
CO_2	17513	4752	2733	73	84
NO_x	575	147	84	74	85
CO	10.6	10.0	6.9	5	35
Trip 3 (Into Oakland Port)					
Gases	Emissions (kg/hr)			% Reduction with Reduced Speed	
	Cruise speed (25 Knots)	15 Knots	12 Knots	15 Knots	12 Knots
CO_2	30524	10406	6194	66	80
NO_x	874	260	218	70	75
CO	17.0	29.3	3.3	-72	81

Table B-2: Comparison of emissions measured (kg/nmi) at cruise and reduced speed from three trips

Trip 1 (Out of Long Beach Port)					
Gases	Emissions (kg/nmi)			% Reduction with Reduced Speed	
	Cruise speed (24 Knots)	15 Knots	11 Knots	15 Knots	11 Knots
CO_2	744	324	279	56	63
NO_x	24.7	10.0	8.9	59	64
CO	0.45	1.08	0.75	-141	-66
Trip 2 (Out of Long Beach Port)					
Gases	Emissions (kg/nmi)			% Reduction with Reduced Speed	
	Cruise speed (24 Knots)	14 Knots	13 Knots	14 Knots	13 Knots
CO_2	761	339	210	55	72
NO_x	25.0	10.5	6.5	58	74
CO	0.46	0.72	0.53	-56	-16
Trip 3 (Into Oakland Port)					
Gases	Emissions (kg/nmi)			% Reduction with Reduced Speed	
	Cruise speed (25 Knots)	15 Knots	12 Knots	15 Knots	12 Knots
CO_2	1221	694	516	43	58
NO_x	35.0	17.3	18.2	50	48
CO	0.7	2.0	0.3	-187	60

Table B-3: Comparison of emissions measured (g/kW-hr) at cruise and reduced speed from three trips

Trip 1 (Out of Long Beach Port)					
Gases	Emissions (g/kW-hr)			% Reduction with Reduced Speed	
	Cruise speed (24 Knots)	15 Knots	11 Knots	15 Knots	11 Knots
CO_2	574	704	777	-23	-35
NO_x	19.0	21.7	24.9	-14	-31
CO	0.3	2.3	2.1	-579	-501
Trip 2 (Out of Long Beach Port)					
Gases	Emissions (g/kW-hr)			% Reduction with Reduced Speed	
	Cruise speed (24 Knots)	14 Knots	13 Knots	14 Knots	13 Knots
CO_2	579	709	828	-23	-43
NO_x	19.0	21.9	25.5	-15	-34
CO	0.4	1.5	2.1	-328	-500
Trip 3 (Into Oakland Port)					
Gases	Emissions (g/kW-hr)			% Reduction with Reduced Speed	
	Cruise speed (25 Knots)	15 Knots	12 Knots	15 Knots	12 Knots
CO_2	590	672	749	-14	-27
NO_x	16.9	16.8	26.4	1	-56
CO	0.3	1.9	0.4	-476	-20

Table B-4: Comparison of measured and calculated EFs (g/kW-hr) for vessels running at low loads (2-20%) on MGO and HFO. [a]US EPA methodology, [b]CARB methodology

Trip/Vessel		1/1	1/1	2/1	2/1	2/1	3/2	3/2
Fuel		MGO	HFO	MGO	MGO	MGO	MGO	MGO
Sulfur Content (%)		0.00065	3.14	0.00942	0.00942	0.00942	0.1657	0.1657
Speed (Knots)		11	12	13	14	14	12	12
Max. Speed (Knots)		24.3	24.3	24.3	24.3	24.3	26.7	26.7
Fractional Load		0.09	0.12	0.15	0.19	0.19	0.09	0.09
NO_x (g/kW-hr)	Calculated[a]	14.0	13.5	11.8	11.2	11.2	14.1	14.1
	Measured	24.5	32.1	25.5	21.9	22.5	32.5	26.4
	% Error[a]	-43%	-58%	-54%	-49%	-50%	-57%	-47%
CO_2 (g/kW-hr)	Calculated[a]	1014	1015	845	793	793	1024	1024
	Calculated[b]	620	620	620	620	620	620	620
	Measured	764	869	828	709	720	811	749
	% Error[a]	33%	17%	2%	12%	10%	26%	37%
	% Error[b]	-19%	-29%	-25%	-13%	-14%	-24%	-17%
CO (g/kW-hr)	Calculated[a]	9.2	7.1	5.6	4.5	4.5	9.4	9.4
	Measured	2.0	1.4	2.1	0.8	1.4	1.0	0.4
	% Error[a]	350%	407%	168%	449%	230%	805%	2273%
$PM_{2.5}$ (g/kW-hr)	Calculated[a]	0.05	0.40	–	0.03	–	–	0.08
	Measured	0.25	2.66	–	0.17	–	–	0.14
	% Error[a]	-81%	-85%	–	-81%	–	–	-41%

Table B-5: Total number of container ships in each class arrived at port of Los Angeles and Long Beach in 2009 (POLA 2009, POLB 2009)

Container Class	Port of Los Angeles		Port of Long Beach	
	No. of Vessels Arrived	Average Power (kW)	No. of Vessels Arrived	Average Power (kW)
Container-1000	115	13263	225	14043
Container-2000	165	22454	176	22897
Container-3000	89	32943	130	30432
Container-4000	295	40961	155	39824
Container-5000	359	51270	182	52441
Container-6000	138	60151	46	65527
Container-7000	106	61182	65	68732
Container-8000	78	68017	153	67975
Container-9000	10	68693		

Table B-6: Potential CO_2 emissions reduction within ECA when vessel speed is reduced to 15 and 12 knots and VSR range is extended to 24, 40, 100, 150 and 200 nautical miles. Emissions are calculated for all container ships, large container ships and Suezmax class tankers arrived at port of Los Angeles and Long Beach in 2009

All Container Ships (Category A)					
VSR zone (nautical miles)	CO_2 Emissions (tpy)			% Reduction	
	Cruise Speed	15 knots	12 knots	15 knots	12 knots
24	725333	674287	672423	7	7
40	725333	633891	637150	13	12
100	725333	508664	504875	30	30
150	725333	404309	394646	44	46
200	725333	299953	284416	59	61
Large Container Ships (Category B)					
VSR zone (nautical miles)	CO_2 Emissions (tpy)			% Reduction	
	Cruise Speed	15 knots	12 knots	15 knots	12 knots
24	291081	275997	270919	5	7
40	291081	265941	257478	9	12
100	291081	228231	207072	22	29
150	291081	196806	165068	32	43
200	291081	165381	123064	43	58
Suezmax Tankers					
VSR zone (nautical miles)	CO_2 Emissions (tpy)			% Reduction	
	Cruise Speed	15 knots	12 knots	15 knots	12 knots
24	16622	-	16049	-	3
40	16622	-	15666	-	6
100	16622	-	14232	-	14
150	16622	-	13036	-	22
200	16622	-	11841	-	29

Table B-7: Potential NO_x emissions reduction within ECA when vessel speed is reduced to 15 and 12 knots and VSR range is extended to 24, 40, 100, 150 and 200 nautical miles. Emissions are calculated for all container ships, large container ships and Suezmax class tankers arrived at port of Los Angeles and Long Beach in 2009

All Container Ships (Category A)					
VSR zone (nautical miles)	NO_x Emissions (tpy)			% Reduction	
	Cruise Speed	15 knots	12 knots	15 knots	12 knots
24	21624	20144	20114	7	7
40	21624	19157	19107	11	12
100	21624	15455	15330	29	29
150	21624	12281	12183	43	44
200	21624	9166	9036	58	58
Large Container Ships (Category B)					
VSR zone (nautical miles)	NO_x Emissions (tpy)			% Reduction	
	Cruise Speed	15 knots	12 knots	15 knots	12 knots
24	7834	7410	7414	5	5
40	7834	7093	7134	9	9
100	7834	5981	6084	24	22
150	7834	5055	5208	35	34
200	7834	4128	4333	47	45
Suezmax Tankers					
VSR zone (nautical miles)	NO_x Emissions (tpy)			% Reduction	
	Cruise Speed	15 knots	12 knots	15 knots	12 knots
24	492	-	473	-	4
40	492	-	460	-	6
100	492	-	412	-	16
150	492	-	372	-	24
200	492	-	333	-	32

Table B-8: Potential $PM_{2.5}$ emissions reduction within ECA when vessel speed is reduced to 15 and 12 knots and VSR range is extended to 24, 40, 100, 150 and 200 nautical miles. Emissions are calculated for all container ships, large container ships and Suezmax class tankers arrived at port of Los Angeles and Long Beach in 2009

All Container Ships (Category A)					
VSR zone (nautical miles)	$PM_{2.5}$ Emissions (tpy)			% Reduction	
	Cruise Speed	15 knots	12 knots	15 knots	12 knots
24	567	509	510	10	10
40	567	470	471	17	17
100	567	325	327	43	42
150	567	203	207	64	64
200	567	82	87	86	85
Large Container Ships (Category B)					
VSR zone (nautical miles)	$PM_{2.5}$ Emissions (tpy)			% Reduction	
	Cruise Speed	15 knots	12 knots	15 knots	12 knots
24	118	112	107	5	9
40	118	109	100	8	15
100	118	96	75	19	36
150	118	84	53	28	55
200	118	73	32	38	73
Suezmax Tankers					
VSR zone (nautical miles)	$PM_{2.5}$ Emissions (tpy)			% Reduction	
	Cruise Speed	15 knots	12 knots	15 knots	12 knots
24	9.4	-	8.9	-	6
40	9.4	-	8.5	-	10
100	9.4	-	7.2	-	24
150	9.4	-	6.0	-	36
200	9.4	-	4.9	-	48

Table B-9: Potential CO emissions reduction within ECA when vessel speed is reduced to 15 and 12 knots and VSR range is extended to 24, 40, 100, 150 and 200 nautical miles. Emissions are calculated for all container ships, large container ships and Suezmax class tankers arrived at port of Los Angeles and Long Beach in 2009

All Container Ships (Category A)					
VSR zone	CO Emissions (tpy)			% Reduction	
(nautical miles)	Cruise Speed	15 knots	12 knots	15 knots	12 knots
24	850	868	846	-2	0
40	850	880	844	-4	1
100	850	924	835	-9	2
150	850	962	827	-13	3
200	850	999	820	-18	4
Large Container Ships (Category B)					
VSR zone	CO Emissions (tpy)			% Reduction	
(nautical miles)	Cruise Speed	15 knots	12 knots	15 knots	12 knots
24	162	198	150	-22	7
40	162	223	143	-37	12
100	162	314	113	-94	30
150	162	389	89	-140	45
200	162	465	65	-187	60
Suezmax Tankers					
VSR zone	CO Emissions (tpy)			% Reduction	
(nautical miles)	Cruise Speed	15 knots	12 knots	15 knots	12 knots
24	10.1	-	10.3	-	-2
40	10.1	-	10.5	-	-3
100	10.1	-	11.0	-	-8
150	10.1	-	11.4	-	-13
200	10.1	-	11.8	-	-17

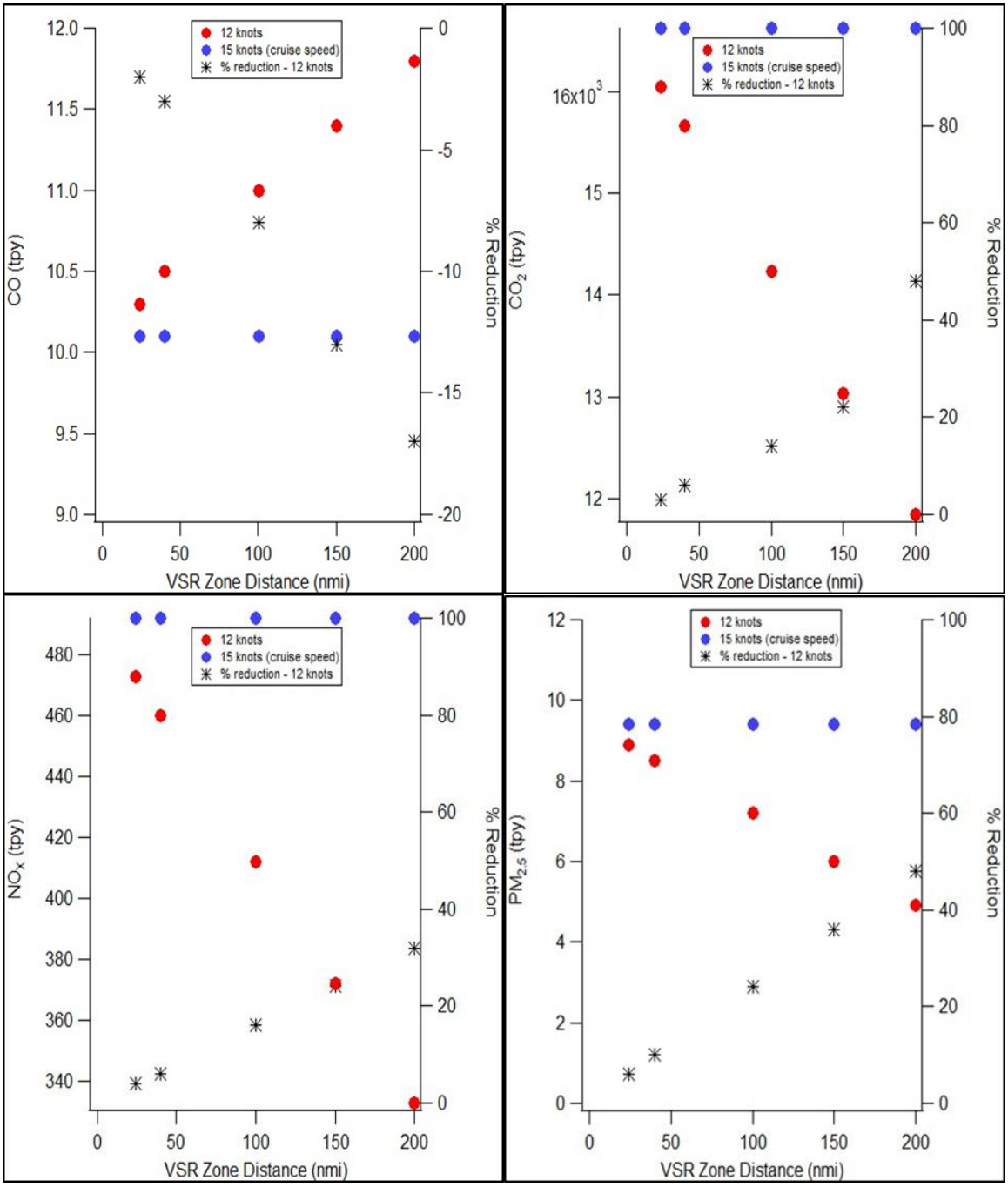

Figure B-1: The estimated emission scenarios for Tanker vessels consuming MGO and running at reduced speed of 12 knots. (a) CO_2, (b) NO_X, (c) $PM_{2.5}$, (d) CO are *TPE* (tpy) when VSR boundary is extended to 24, 40, 100, 150 and 200 nautical miles from coastline. Note: Total number of Suezmax class tanker arrived at port of Los Angeles and Long Beach in 2009 are used to calculate *TPE*. The percent reductions are calculated for both reduced speeds from the baseline (cruise speed)